JAEA-Research
2025-001
DOI:10.11484/jaea-research-2025-001

Detailed Computational Models for Nuclear Criticality Analyses on the First Startup Cores of NSRR: A TRIGA Annular Core Pulse Reactor

Hiroshi YANAGISAWA and Yuiko MOTOME

Nuclear Science Research Institute

June 2025
Japan Atomic Energy Agency
日本原子力研究開発機構

JAEA-Rearch

国立研究開発法人日本原子力研究開発機構　研究開発推進部　科学技術情報課
〒 319-1112　茨城県那珂郡東海村大字村松 4 番地 49
E-mail: ird-support@jaea.go.jp

4-49 Muramatsu, Tokai-mura, Naka-gun, Ibaraki-ken 319-1112, Japan
E-mail: ird-support@jaea.go.jp

JAEA-Research 2025-001

Detailed Computational Models for Nuclear Criticality Analyses on the First Startup Cores of NSRR: A TRIGA Annular Core Pulse Reactor

Hiroshi YANAGISAWA and Yuiko MOTOME

Nuclear Science Research Institute
Japan Atomic Energy Agency
Tokai-mura, Naka-gun, Ibaraki-ken

(Received January 16, 2025)

The detailed computational models for nuclear criticality analyses on the first startup cores of NSRR (Nuclear Safety Research Reactor), which is categorized as a TRIGA-ACPR (Annular Core Pulse Reactor), were created for the purposes of deeper understandings of safety inspection data on the neutron absorber rod worths of reactivity and improvement of determination technique of the reactivity worths. The uncertainties in effective neutron multiplication factor (k_{eff}) propagated from errors in the geometry, material, and operation data for the present models were evaluated in detail by using the MVP version 3 code with the latest Japanese nuclear data library, JENDL-5, and the previous versions of JENDL libraries. As a result, the overall uncertainties in k_{eff} for the present models were evaluated to be in the range of 0.0027 to 0.0029 Δk_{eff}. It is expected that the present models will be utilized as the benchmark on k_{eff} for TRIGA-ACPR. Moreover, it is confirmed that the overall uncertainties were sufficiently smaller than the values of absorber rod worths determined in NSRR. Thus, it is also considered that the present models are applicable to further analyses on the absorber rod worths in NSRR.

Keywords: Computational Model, Nuclear Criticality Analysis, Benchmark, NSRR, TRIGA-ACPR, Neutron Absorber Rod, Reactivity Worth, Effective Neutron Multiplication Factor, MVP, JENDL-5

TRIGA 環状炉心パルス炉 NSRR の初回起動炉心の臨界解析用詳細計算モデル

日本原子力研究開発機構
原子力科学研究所

柳澤　宏司、求　惟子

（2025 年 1 月 16 日受理）

中性子吸収棒の反応度価値に関する安全検査データのより深い理解と反応度価値の測定技術の向上のために、TRIGA-ACPR（環状炉心パルス炉）に分類される NSRR（原子炉安全性研究炉）の初回起動炉心の臨界解析用詳細計算モデルを作成した。本モデルの形状、材料、運転データの誤差から伝播する中性子実効増倍率（k_{eff}）の不確かさを、最新の核データライブラリ JENDL-5 及び旧版の JENDL ライブラリと MVP 第 3 版コードを用いて詳細に評価した。その結果、本モデルにおける k_{eff} の全体的な不確かさは、0.0027 から 0.0029 Δk_{eff} の範囲と評価した。本モデルは、TRIGA-ACPR の k_{eff} のベンチマークとして利用されることが期待される。さらに、全体的な不確かさは、NSRR で測定された吸収棒価値よりも十分小さいことを確認した。よって、本モデルは NSRR における吸収棒反応度価値に関する今後の解析にも適用できる。

原子力科学研究所：〒319-1195 茨城県那珂郡東海村大字白方 2-4

Contents

目　　次

1. Introduction

NSRR (Nuclear Safety Research Reactor) [1] operated and managed by the Nuclear Science Research Institute of the Japan Atomic Energy Agency is a versatile test and research nuclear reactor TRIGA (Training, Research, Isotopes, General Atomics) [2]. In general, the TRIGA reactor has excellent inherent safety, in which the rapid and large negative feedback reactivity is brought by uranium-zirconium hydride fuel during nuclear excursions due to the shift of thermal neutron spectra towards its higher energy. For this feature, NSRR is utilized for irradiation tests on nuclear fuel and materials of nuclear power reactors under the condition that the reactivity is added exceeding prompt criticality, i.e., reactivity-initiated accident conditions. The TRIGA reactor like NSRR in which a vertical irradiation hole at the center of the core is equipped and pulse operations are enabled is further categorized as the TRIGA-ACPR (Annular Core Pulse Reactor).

NSRR generates extremely large thermal power up to 23,000 MW during the irradiation tests, however, its duration is so short because of the inherent safety as mentioned above. Hence, integrated thermal power during operation is small in NSRR. This means that the decay heat from fission products and minor actinide nuclides are quite small due to so small burnup. Therefore, the Japanese safety regulation requires the safety function of reactor shutdown with neutron absorber rods for NSRR as one of the important safety issues more than the reactor cooling function.

In NSRR, eleven neutron absorber rods controlling reactivity are equipped for operations, i.e., six control rods, two safety rods, and three transient rods. Reactivity worths of those rods are periodically determined and inspected once per fiscal year to confirm the compliance with safety criteria. From the former studies [3,4] on the other TRIGA reactors with multiple absorber rods, it is foreseen that the reactivity worth of a particular neutron absorber rod is strongly affected by the vertical position of each rod inserted into the core as well as the horizontal positional relationship of the other rods. However, those data on the reactivity worths in NSRR have not been examined with three-dimensional models accurately simulating core structures and positions of the absorber rods using precise analyses codes and the latest nuclear data libraries so far. It is considered that the detailed examination assisted by precise computational analyses is effective for deeper understandings of the inspected data on the reactivity worth and improvement of the determination technique of the worths in NSRR.

For this purpose, the authors tried to create detailed criticality analyses models for NSRR. Those models represent the detailed layout of the core structures and positional relationship of the control, safety, and transient rods accurately. Although a small burnup is expected, the models are subjected to the first startup cores of NSRR in 1975 since uncertainties from changes in fuel compositions are to be reduced as much as possible. To create detailed models as much as possible, the data in the present models were closely examined by referring to not only the published literatures [1,5] but also dimensional and material inspection records at the construction of NSRR in 1973, operation records during the first startup in 1975, and so on.

For the present models, analyses of effective neutron multiplication factor (k_{eff}), were performed using the continuous-energy Monte Carlo code MVP version 3 [6] with the latest Japanese nuclear data library, JENDL-5 [7], and the previous versions of JENDL libraries [8,9] to confirm the accuracy of the combination of the analyses code and libraries. Uncertainties in k_{eff} propagated from errors in dimensional, material, and operation data for the present models were also evaluated in detail with the code and libraries mentioned above.

This report summarizes the detailed criticality analyses models for the first startup cores of NSRR with the uncertainties in k_{eff}. It is expected that the present models will be used as the benchmarks on k_{eff} under delayed critical conditions with various positions of the neutron absorber rods in NSRR as a TRIGA-ACPR. For the reactivity worths of the neutron absorber rods of NSRR, it is necessary to examine the data determined at the first startup in detail. The comparison of the determined data on the reactivity worths and calculations using the present models will be conducted in future.

2. Geometry Data

For the definition of dimensions and shapes of the detailed models, the geometry data are described below with their data sources. The uranium-zirconium hydride fuel rods, and the neutron absorber rods for reactivity control, i.e., six control rods, two safety rods, three transient rods, are loaded in the NSRR core [1)]. The transient rods consist of one adjustable transient rod and two fast transient rods. The detailed models are categorized into three sorts of cores which were composed during the first startup, namely,

- Minimum core: a core in which the minimum number of fuel rods were loaded to reach the first criticality,
- Standard core: a core in routine uses for pulse operations having 8.52 $ of excess reactivity,
- Intermediate core: thirty-five cores composed by the one-by-one fuel rod addition step from the minimum to standard core.

2.1 Fuel rod

Figure 2.1.1 shows the geometry model for the fuel rod. The fuel meat is approximately 20 wt% enriched uranium-zirconium hydride with a vertical hole in the center of the fuel meat for hydriding process at the manufacturing. In the center hole, zirconium rods are vertically inserted. Axial graphite reflectors are installed at both top and bottom of the fuel rod. A thin molybdenum disc as burnable poison is also installed between the uranium-zirconium hydride and the bottom axial graphite reflector. The austenitic stainless-steel type SUS304 fuel cladding and top/bottom plugs are used in the fuel rod.

The actual top/bottom plugs are shaped like arrow feathers and have slightly complicated structures. Figure 2.1.2 shows photographs of the top/bottom plugs in a replica of the fuel rod. For simplicity, the top/bottom plugs in the geometry model are shaped with surfaces of cylinders and a truncated cone which are enveloping their real shapes, as shown in Fig. 2.1.1. For this reason, the mass and volume of the plug materials in the model is larger than the real ones.

The fuel rod is supported in the core by top/bottom grid plates made from aluminum alloy type A6061. In the bottom grid, counter sinks are machined in each grid hole to support the fuel rods.

For dimensions found in the dimensional inspection records at the construction in 1973, the dimensions and their errors were obtained by using the inspection records. The other dimension data referred to nominal values from design drawings. The numerical values underlined in Fig. 2.1.1 imply the dimensions based on the dimensional inspection records at the construction in 1973.

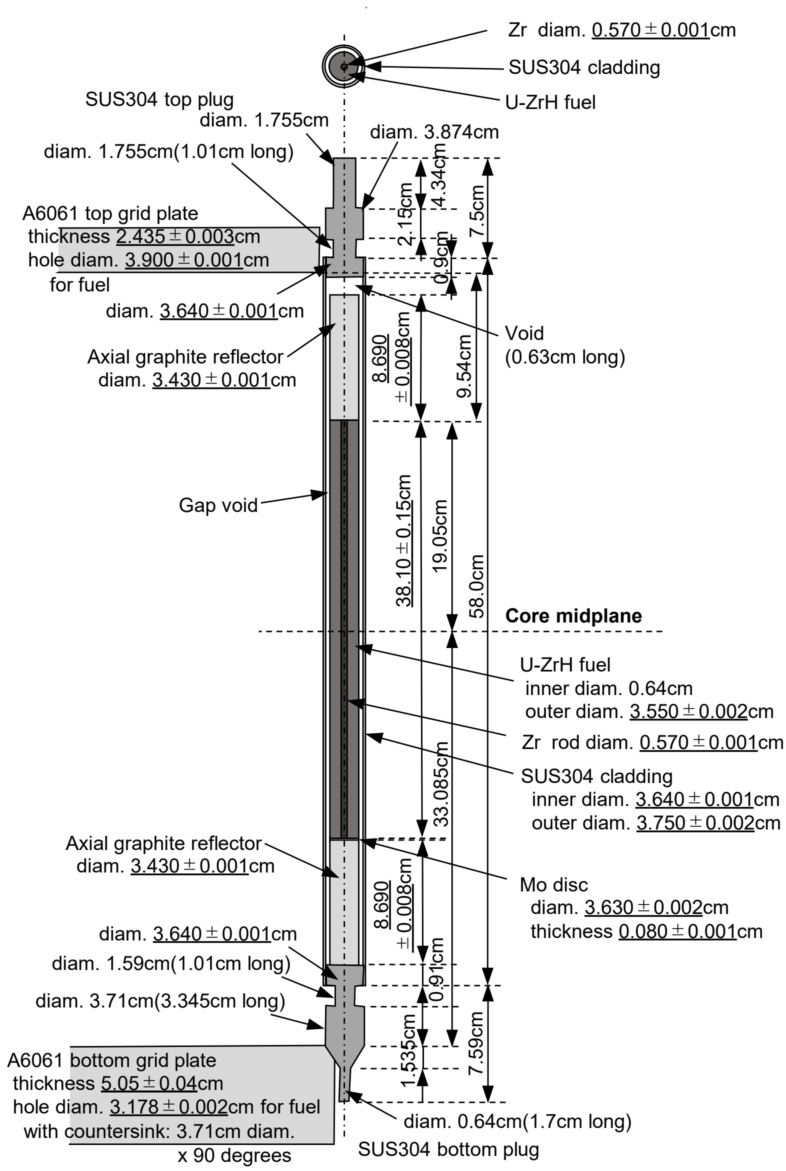

Fig. 2.1.1 Geometry model for the fuel rod.

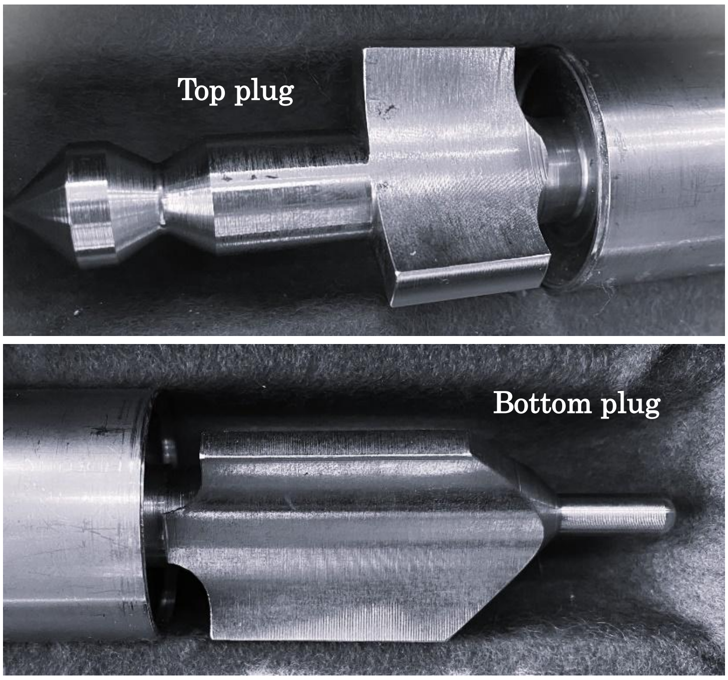

Fig. 2.1.2 Photographs of the top/bottom plugs in a replica of the fuel rod.

2.2 Control and safety rods with fuel followers

Figure 2.2.1 shows the geometry model for the control and safety rods. Six control and two safety rods with natural boron carbide absorber are installed in the core. The control and safety rods have uranium-zirconium hydride fuel followers of which composition is same as the fuel rod. The austenitic stainless-steel type SUS304 cladding, spacer, and top/bottom plugs are used in the control and safety rods. The aluminum alloy type A6061 spacer tube is used inside the bottom of the control and safety rods.

The control and safety rods are driven by an electric motor individually. In addition, six control rods can be simultaneously driven, as ‘bank mode’ [1]. The driving mechanisms for the control and safety rods are ignored in the geometry model since those are sufficiently far away from the core. The vertical position of the control and safety rods is expressed as ‘unit.’ The position of 100 units means full insertion of the rod, meanwhile that of 900 units does full withdrawal. The value of one unit is identical to 0.0476 cm (38.1 cm per 800 unit).

The dimensional inspection records on the control and safety rods at the construction in 1973 are not found at present. Thus, the dimension data referred to nominal values from design drawings.

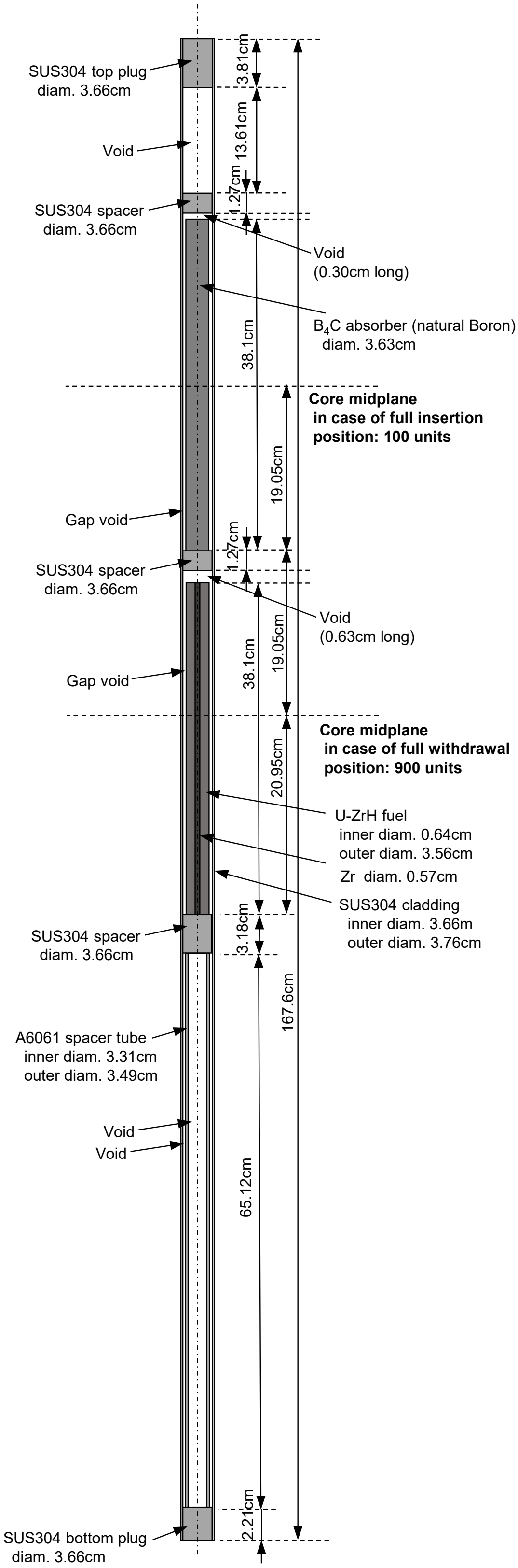

Fig. 2.2.1 Geometry model for the control and safety rods.

2.3 Adjustable transient rod

Figure 2.3.1 shows the geometry model for the adjustable transient rod. One adjustable transient rod with enriched boron carbide absorber is installed in the core. The aluminum alloy type A6061 cladding, spacer, air follower and spacer tubes, and top/bottom plugs are used.

The adjustable transient rod is driven by either an electric motor or compressed air. The driving mechanisms for the adjustable transient rod are ignored in the geometry model since those are sufficiently far away from the core. The vertical position of the adjustable transient rod is expressed as 'unit' for the motor driving, similar to the control and safety rods. The position of 100 units means full insertion of the rod, meanwhile that of 900 units does full withdrawal. The value of one unit is 0.0476 cm like the control and safety rods.

The dimensional inspection records on the adjustable transient rod at the construction in 1973 are not found at present. Thus, the dimension data referred to nominal values from design drawings.

2.4 Fast transient rod

Figure 2.4.1 shows the geometry model for the fast transient rod. Two fast transient rods with enriched boron carbide absorber are installed in the core. The aluminum alloy type A6061 cladding, spacer, air follower and spacer tubes, and top/bottom plugs are used like the adjustable transient rod.

The fast transient rods are driven only by compressed air individually. The driving mechanisms for the fast transient rods are ignored in the geometry model since those are sufficiently far away from the core.

The dimensional inspection records on the fast transient rods at the construction in 1973 are not found at present. Thus, the dimension data referred to nominal values from design drawings.

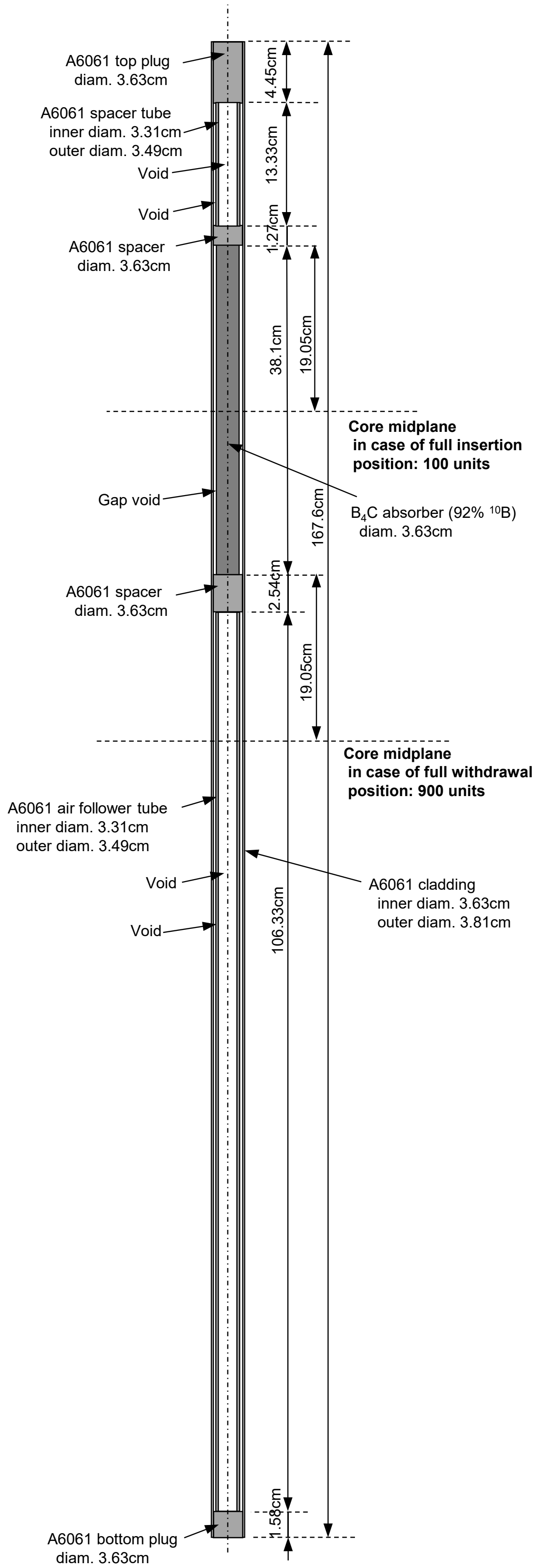

Fig. 2.3.1 Geometry model for the adjustable transient rod.

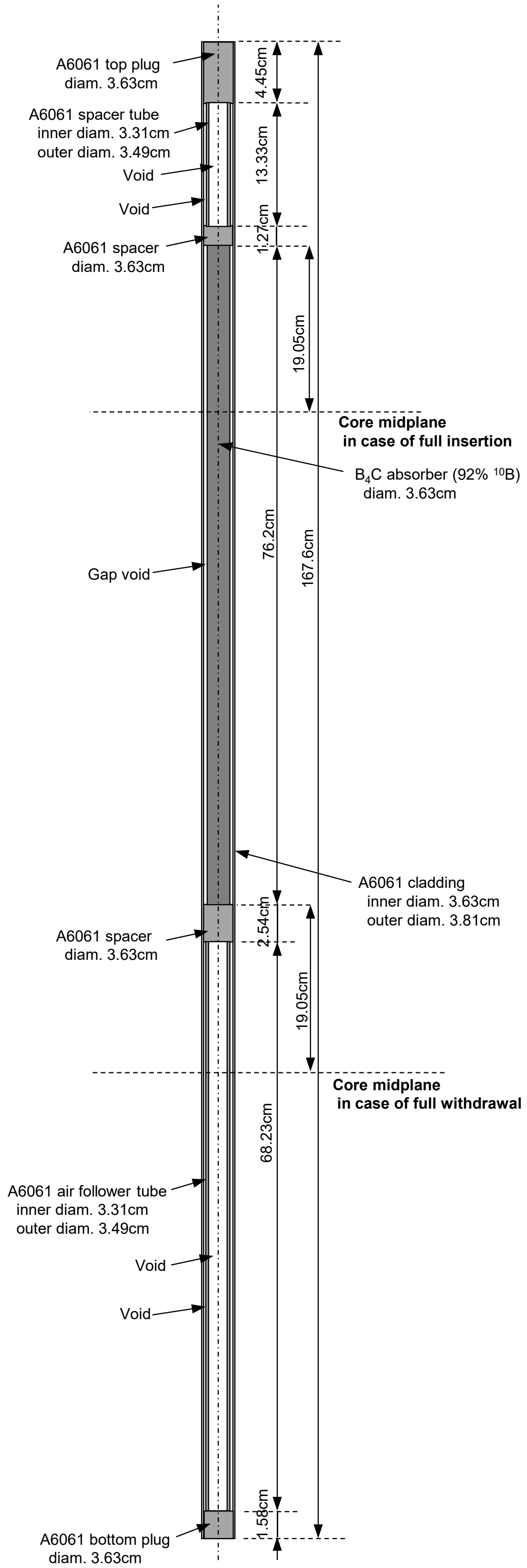

Fig. 2.4.1 Geometry model for the fast transient rod.

2.5 Horizontal layout of cores

2.5.1 Minimum core

The core of the minimum number of fuel rods was reached at delayed criticality during the first startup of NSRR in 1975 [1]. Figure 2.5.1.1 shows its horizontal layout. The minimum core was composed of one hundred and thirteen fuel rods, six control rods, and two safety rods. One adjustable transient rod and two fast transient rods were also installed in the core. The fuel rods, control and safety rods, and transient rods were configured in the hexagonal lattice using the aluminum alloy type A6061 top/bottom grid plates. The water to fuel volume ratio of a hexagonal fuel cell was about 0.423.

The cylindrical shaped aluminum alloy type A6061 shroud was installed surrounding the core. The A6061 experimental tube was installed in the center of core, which made a hexagonal shaped void region for an irradiation capsule.

For the grid plates, shroud, and experimental tube, the dimensions and their errors were obtained by using the dimensional inspection records at the construction in 1973. The numerical values underlined in Fig. 2.5.1.1 imply the dimensions based on the dimensional inspection records.

2.5.2 Standard core

Figure 2.5.2.1 shows the horizontal layout of the standard core. The standard core for pulse operations in NSRR was configured in 1975 [1] by adding thirty-six fuel rods in the minimum core.

The standard core was composed of one hundred and forty-nine fuel rods, six control rods, and two safety rods. The horizontal layout of the standard core was same as the minimum core excepting the difference in the number of fuel rods loaded in both cores.

The numerical values underlined in Fig. 2.5.2.1 imply the dimensions based on the inspection records at the construction in 1973, similar to the minimum core.

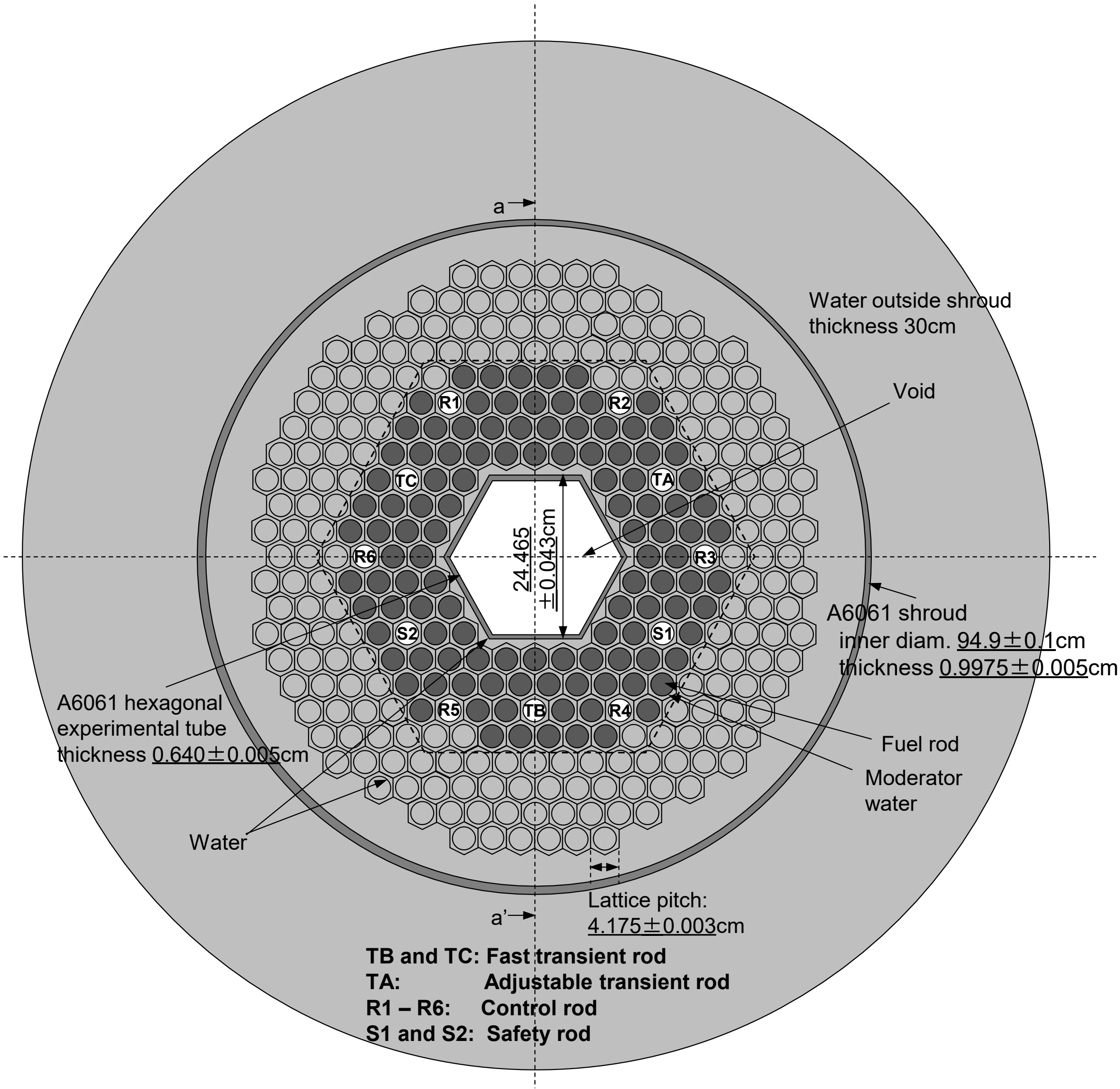

Fig. 2.5.1.1 Horizontal layout of the minimum core.

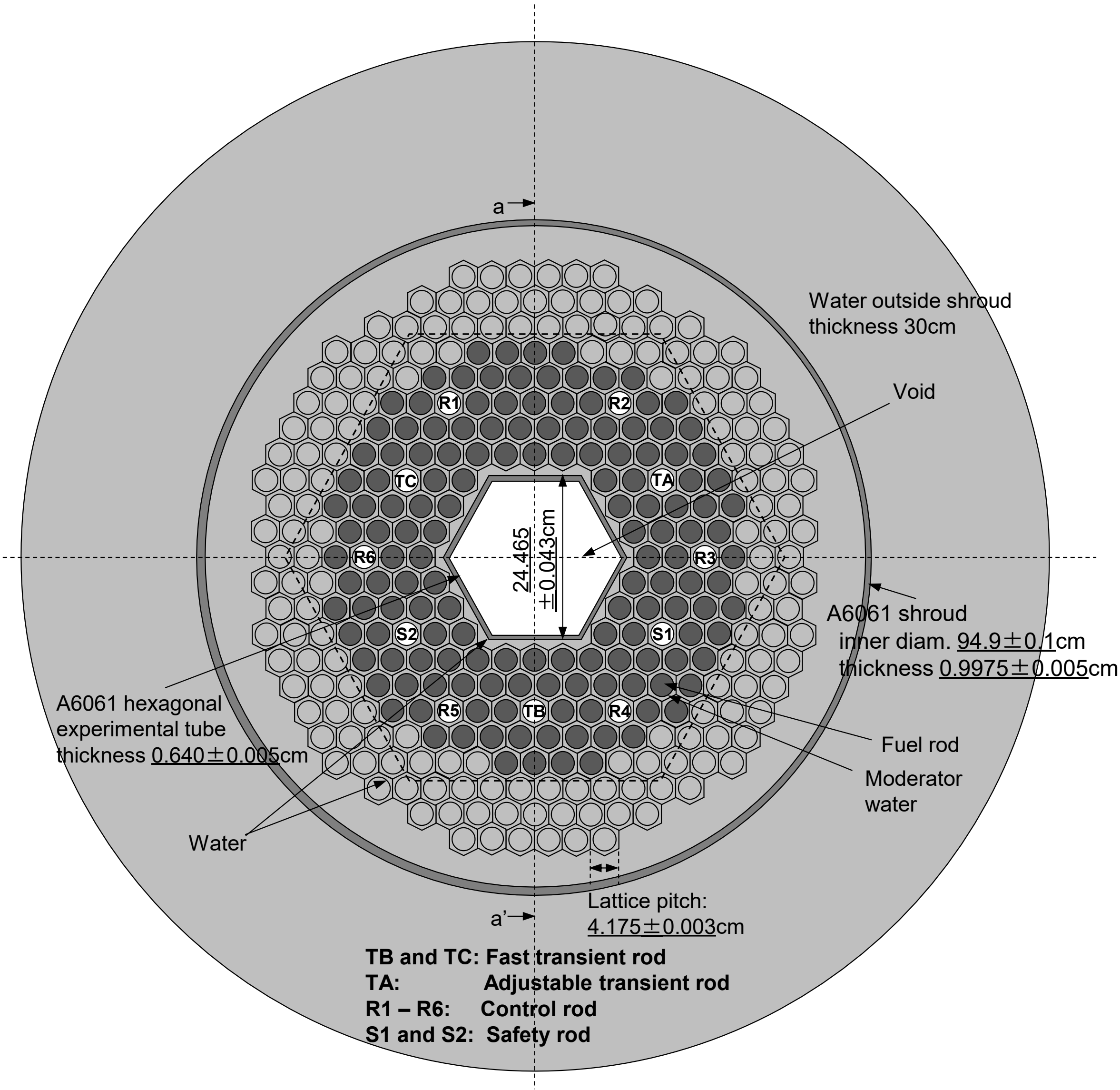

Fig. 2.5.2.1 Horizontal layout of the standard core.

2.5.3 Intermediate cores in fuel addition steps

Thirty-six fuel rods in total were added in the core using one-by-one step from the minimum to standard core during the first startup of NSRR in 1975 [1]. Thus, thirty-five intermediate cores were configured for each fuel addition step to determine reactivities inserted by the fuel addition. The last step, i.e., the 36th fuel addition step, made the standard core.

Figure 2.5.3.1 shows the position of the fuel addition. The positions of the fuel addition in Fig. 2.5.3.1 are shown with the symbols of 'D-xx' or 'E-yy,' in which 'xx' or 'yy' is numerical values for identification.

The horizontal layout of the intermediate cores was same as the minimum or standard core excepting the difference in the number of fuel rods.

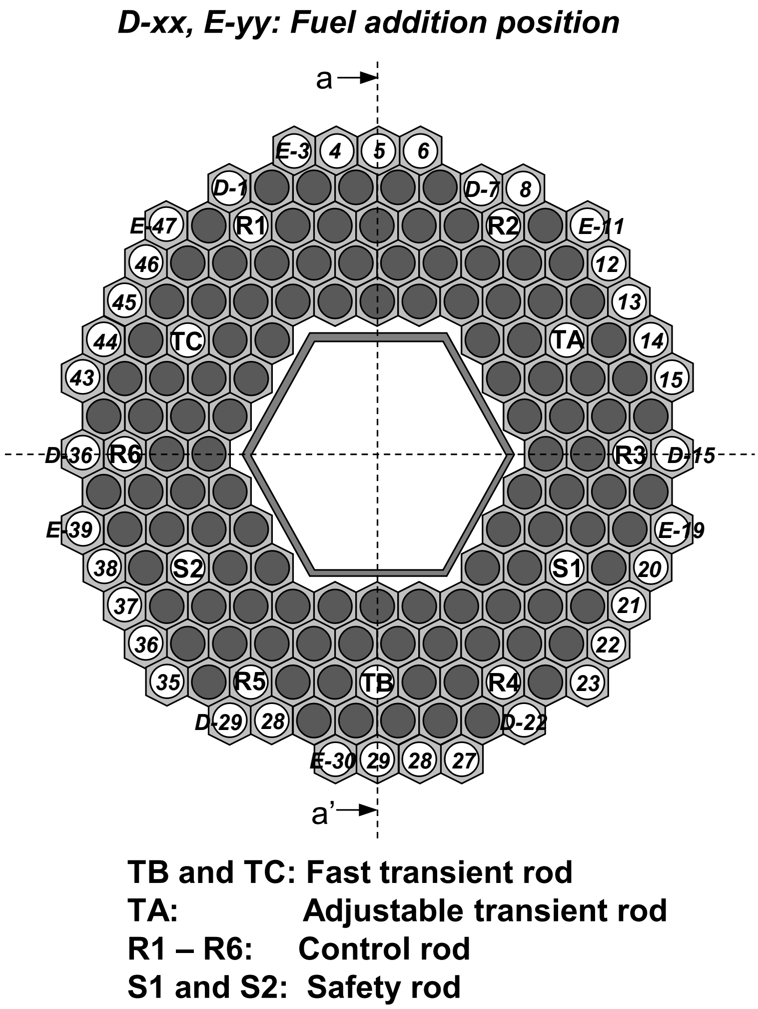

Fig. 2.5.3.1 Fuel addition position from the minimum to standard core.

2.6 Vertical layout of cores

Figure 2.6.1 shows the vertical layout of the core. The aluminum alloy type A6061 experimental tube had two sorts of shapes. As mentioned in Sec. 2.5, it has a hexagonal shaped void region below the vicinity of the top of the fuel rods. The cylindrical shaped experimental tube is placed on the top of hexagonal one.

The vertical positions of the control, safety, and transient rods were confirmed by using operation records during the first startup in 1975. Details of the position data of those rods for each core are summarized in Chap. 4.

The data source of the dimensions for the grid plates, shroud, and experimental tube is mentioned in Sec. 2.5.1. For the austenitic stainless-steel type SUS304 guide tubes for the transient rods, the dimensional inspection records at the construction in 1973 are not found at present. Thus, those dimensions referred to nominal values from design drawings. The numerical values underlined in Fig. 2.6.1 imply the dimensions based on the inspection records at the construction in 1973.

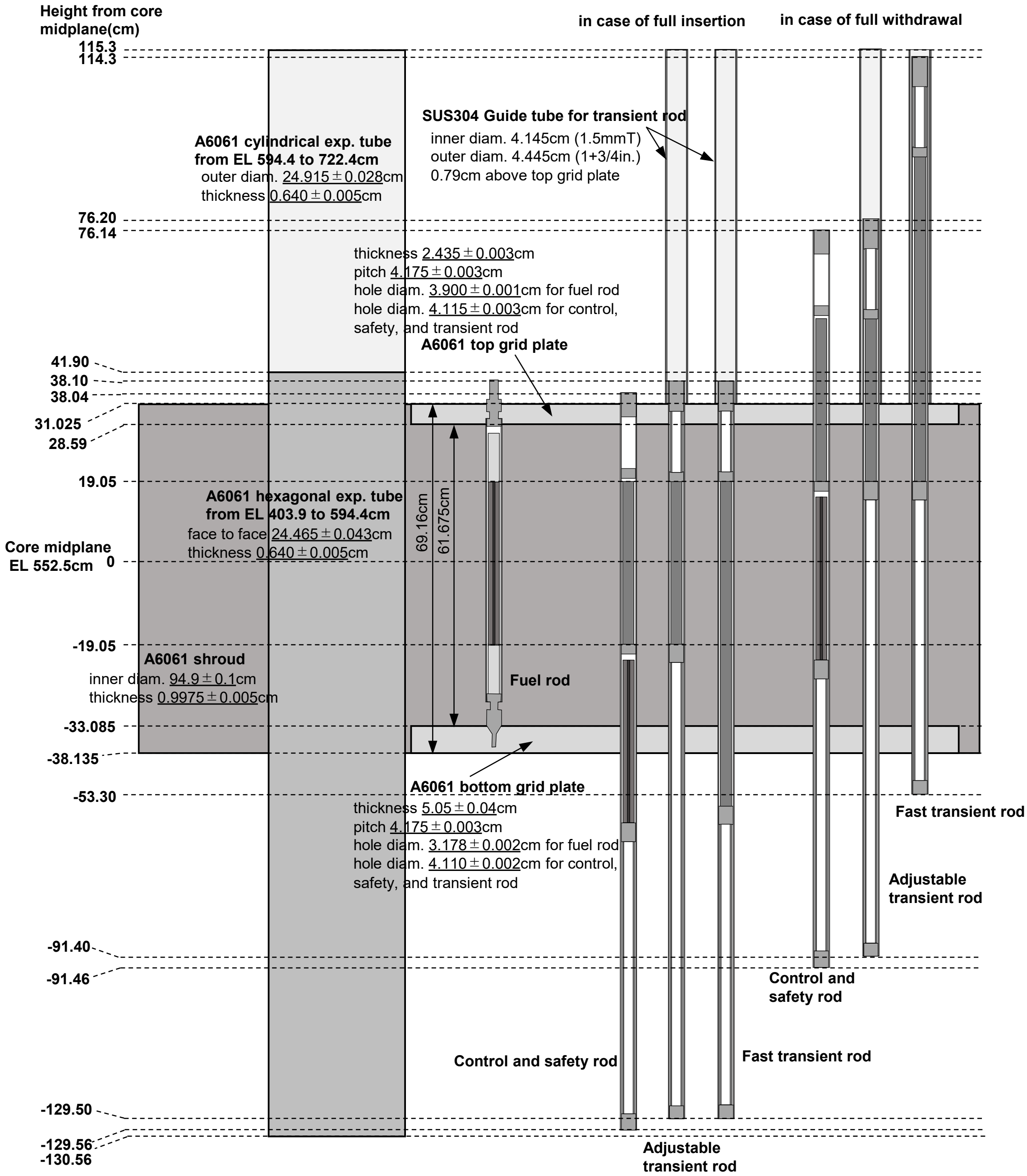

Fig. 2.6.1 Vertical layout of the core.

3. Material Data

The atomic number densities for the materials used in the present models are described below with their data sources. Nuclear constants, i.e., Avogadro's Number, atomic weight, and isotopic abundance, are based on the International Criticality Safety Benchmark Evaluation Project (ICSBEP) handbook [10].

3.1 Uranium-zirconium hydride in fuel, control, and safety rods

The density of uranium-235 was obtained by the mass inventory of uranium-235 in the whole core and the total volume of the uranium-zirconium hydride of the core. The mass inventory is consistent with nuclear material accountability data for safeguards. The total volume of the uranium-zirconium hydride was calculated by nominal dimensions in design drawings. The volume error was evaluated to be 0.41 % in relative by using both the design drawings and dimensional inspection records at the construction in 1973.

The atomic number ratio of hydrogen to uranium-235 was cited from the literature [5], as 152.76. The atomic number ratio of hydrogen to zirconium and its error were obtained by using records of material inspection for the hydriding process of uranium and zirconium mixture. The enrichment of uranium-235 and its error were also obtained by using records of material inspection on the uranium metal as raw materials. Those material inspection records were logged at the construction in 1973.

The uranium metal was composed of three heats, GUNFC (Gulf United Nuclear Fuels Corp., US.), AI (Atomic International Inc., US.) J-04, and AI J-06. For the heats, AI J-04 and AI J-06, uranium-234 and uranium-236 compositions are available in the material inspection records, but those nuclides are not found in the GUNFC record. Since the weight of the GUNFC uranium occupied 60% of the total uranium weight, only two sorts of uranium nuclide, uranium-235 and 238, were considered.

The impurities of uranium and zirconium were obtained by using records of material inspection for the uranium metal and zirconium sponge at the construction in 1973.

The parameters and impurities, which are necessary to obtain atomic number densities, are listed in Table 3.1.1 and Table 3.1.2, respectively.

Table 3.1.1 Parameters of the uranium-zirconium hydride
in the fuel, control, and safety rods.

Item	Value ± 1σ	Relative error (%)
Volume of U-ZrH (cm^3) *1	$(5.7483 \pm 0.024) \times 10^4$	0.41
Atomic ratio: H/Zr*2	1.62 ± 0.02	1.51
U-235 enrichment (wt%) *2	19.85 ± 0.11	0.55
Density of H (g/cm^3)	0.0930 ± 0.0004	0.41
Density of U-235 (g/cm^3)	0.1420 ± 0.0006	0.41
Density of U-238 (g/cm^3)	0.5734 ± 0.0046	0.80
Density of Zr (g/cm^3)	5.2050 ± 0.0813	1.56
Density of U-ZrH (g/cm^3)	6.0134 ± 0.0814	1.35

*1 Calculated by using the design drawings and dimensional inspection records.
*2 Obtained by using the material inspection records.

Table 3.1.2(1) Impurities in the uranium.

Element	Fraction (ppm)
Magnesium	12
Aluminum	30
Silicon	175
Chromium	28
Iron	158
Nickel	52

Table 3.1.2(2) Impurities in the zirconium.

Element	Fraction (ppm)
Carbon	140
Nitrogen	22
Oxygen	800
Magnesium	55
Aluminum	45
Chlorine	100
Chromium	46
Iron	315
Hafnium	28

The atomic number densities of nuclides for the uranium-zirconium hydride in the fuel, control, and safety rods are listed in Table 3.1.3.

Table 3.1.3 Atomic number densities of nuclides for the uranium-zirconium hydride in the fuel, control, and safety rods.

Nuclide	Atomic Number Density (1/barn cm)
H-1*1	5.5586×10^{-2}
Zr-90*1	1.7678×10^{-2}
Zr-91*1	3.8552×10^{-3}
Zr-92*1	5.8928×10^{-3}
Zr-94*1	5.9718×10^{-3}
Zr-96*1	9.6209×10^{-4}
U-235	3.6389×10^{-4}
U-238	1.4505×10^{-3}
C-12*2	3.6133×10^{-5}
C-13*2	4.0189×10^{-7}
N-14*2	4.9050×10^{-6}
N-15*2	1.8216×10^{-8}
O-16*2	1.5673×10^{-4}
Mg-24*2	5.7755×10^{-6}
Mg-25*2	7.3116×10^{-7}
Mg-26*2	8.0501×10^{-7}
Al-27*2	5.7067×10^{-6}
Si-28*2	2.4758×10^{-6}
Si-29*2	1.2536×10^{-7}
Si-30*2	8.3215×10^{-8}
Cl-35*2	6.6990×10^{-6}
Cl-37*2	2.1422×10^{-6}
Cr-50*2	1.3069×10^{-7}
Cr-52*2	2.5202×10^{-6}
Cr-53*2	2.8574×10^{-7}
Cr-54*2	7.1134×10^{-8}
Fe-54*2	1.1152×10^{-6}
Fe-56*2	1.7337×10^{-5}
Fe-57*2	3.9695×10^{-7}
Fe-58*2	5.2926×10^{-8}
Ni-58*2	2.5893×10^{-7}
Ni-60*2	9.8989×10^{-8}
Ni-61*2	4.2858×10^{-9}
Ni-62*2	1.3616×10^{-8}
Ni-64*2	3.4514×10^{-9}
Hf-174*2	7.9659×10^{-10}
Hf-176*2	2.5599×10^{-8}
Hf-177*2	9.1490×10^{-8}
Hf-178*2	1.3422×10^{-7}
Hf-179*2	6.7017×10^{-8}
Hf-180*2	1.7259×10^{-7}

*1 Thermal scattering law (TSL) data used as zirconium hydride.
*2 Impurities.

3.2 Zirconium rod in fuel, control, and safety rods

The density of zirconium was cited from the literature [11], as 6.52 g/cm^3. The difference in the density between the above value and that of the other TRIGA benchmarks, i.e., IEU-COMP-THERM-013 (ICT-013) [12] and IEU-COMP-THERM -003 (ICT-003) [13] in the ICSBEP handbook [10], is 0.03 g/cm^3 in maximum. Thus, the error in the zirconium density was estimated to be 0.03 g/cm^3 (0.46 %).

The impurities of zirconium were obtained by using material inspection records at the construction in 1973. The impurities, which are necessary to obtain atomic number densities, are listed in Table 3.2.1.

Table 3.2.1 Impurities in the zirconium rod.

Element	Fraction (ppm)
Boron	0.2
Carbon	115
Nitrogen	40
Chromium	71.5
Iron	560.5
Copper	12
Hafnium	32.5

The atomic number densities of nuclides for the zirconium rod in the fuel, control, and safety rods are listed in Table 3.2.2.

Table 3.2.2 Atomic number densities of nuclides for the zirconium rod in the fuel, control, and safety rods.

Nuclide	Atomic Number Density (1/barn cm)
Zr-90	2.2145×10^{-2}
Zr-91	4.8293×10^{-3}
Zr-92	7.3816×10^{-3}
Zr-94	7.4806×10^{-3}
Zr-96	1.2052×10^{-3}
B-10*1	1.4455×10^{-8}
B-11*1	5.8182×10^{-8}
C-12*1	3.7180×10^{-5}
C-13*1	4.1353×10^{-7}
N-14*1	1.1171×10^{-5}
N-15*1	4.1488×10^{-8}

*1 Impurities.

Table 3.2.2 (contd.) Atomic number densities of nuclides for the zirconium rod in the fuel, control, and safety rods.

Nuclide	Atomic Number Density (1/barn cm)
Cr-50*1	2.3460×10^{-7}
Cr-52*1	4.5240×10^{-6}
Cr-53*1	5.1293×10^{-7}
Cr-54*1	1.2769×10^{-7}
Fe-54*1	2.3251×10^{-6}
Fe-56*1	3.6146×10^{-5}
Fe-57*1	8.2759×10^{-7}
Fe-58*1	1.1035×10^{-7}
Cu-63*1	5.1287×10^{-7}
Cu-65*1	2.2859×10^{-7}
Hf-174*1	1.1582×10^{-9}
Hf-176*1	3.7220×10^{-8}
Hf-177*1	1.3302×10^{-7}
Hf-178*1	1.9516×10^{-7}
Hf-179*1	9.7440×10^{-8}
Hf-180*1	2.5095×10^{-7}

*1 Impurities.

3.3 Stainless-steel type SUS304 of cladding in fuel rod

The density of SUS304 was cited from the literature [14], as 7.93 g/cm^3. The difference in the density between the above value and that of the other TRIGA benchmarks, i.e., ICT-013 [12] and ICT-003 [13], is 0.07 g/cm^3 in maximum. Thus, the error in the density was estimated to be 0.07 g/cm^3 (0.88 %).

The composition of the cladding in the fuel rod based on the ASTM A213-66 [15] standard was obtained by using material inspection records at the construction in 1973. The elemental composition, which is necessary to obtain atomic number densities, is listed in Table 3.3.1.

Table 3.3.1 Elemental composition of the cladding in the fuel rod.

Element	Fraction (wt%)
Boron	0.0017
Carbon	0.0533
Silicon	0.5367
Phosphorus	0.021
Sulfur	0.0137
Chromium	18.4833
Manganese	1.3667
Iron	70.3569
Nickel	9.1667

The atomic number densities of nuclides for the cladding in the fuel rod are listed in Table 3.3.2.

Table 3.3.2 Atomic number densities of nuclides for the cladding in the fuel rod.

Nuclide	Atomic Number Density (1/barn cm)
B-10	1.4944×10^{-6}
B-11	6.0150×10^{-6}
C-12	2.0959×10^{-4}
C-13	2.3311×10^{-6}
Si-28	8.4167×10^{-4}
Si-29	4.2617×10^{-5}
Si-30	2.8290×10^{-5}
P-31	3.2378×10^{-5}
S-32	1.9388×10^{-5}
S-33	1.5303×10^{-7}
S-34	8.5901×10^{-7}
S-36	4.0808×10^{-9}
Cr-50	7.3760×10^{-4}
Cr-52	1.4224×10^{-2}
Cr-53	1.6127×10^{-3}
Cr-54	4.0148×10^{-4}
Mn-55	1.1880×10^{-3}
Fe-54	3.5498×10^{-3}
Fe-56	5.5184×10^{-2}
Fe-57	1.2635×10^{-3}
Fe-58	1.6847×10^{-4}
Ni-58	5.0923×10^{-3}
Ni-60	1.9468×10^{-3}
Ni-61	8.4288×10^{-5}
Ni-62	2.6778×10^{-4}
Ni-64	6.7878×10^{-5}

3.4 Stainless-steel type SUS304 of top/bottom plugs in fuel rod

The density of SUS304 was cited from the literature [14], as 7.93 g/cm^3, same as the cladding in the fuel rod. The error in the density was also estimated to be 0.07 g/cm^3 (0.88 %), same as the cladding in the fuel rod.

The composition of the top/bottom plugs in the fuel rod based on the AMS 5370[16] standard was obtained by using material inspection records at the construction in 1973. The elemental composition, which is necessary to obtain atomic number densities, is listed in Table 3.4.1.

Table 3.4.1 Elemental composition of the top/bottom plugs in the fuel rod.

Element	Fraction (wt%)
Carbon	0.027
Silicon	0.55
Phosphorus	0.016
Sulfur	0.02
Chromium	18.6
Manganese	1.28
Iron	70.557
Nickel	8.95

The atomic number densities of nuclides for the top/bottom plugs in the fuel rod are listed in Table 3.4.2.

Table 3.4.2 Atomic number densities of nuclides for the top/bottom plugs in the fuel rod.

Nuclide	Atomic Number Density (1/barn cm)
C-12	1.0617×10^{-4}
C-13	1.1809×10^{-6}
Si-28	8.6253×10^{-4}
Si-29	4.3674×10^{-5}
Si-30	2.8991×10^{-5}
P-31	2.4669×10^{-5}
S-32	2.8304×10^{-5}
S-33	2.2340×10^{-7}
S-34	1.2540×10^{-6}
S-36	5.9574×10^{-9}
Cr-50	7.4225×10^{-4}
Cr-52	1.4314×10^{-2}
Cr-53	1.6229×10^{-3}
Cr-54	4.0401×10^{-4}
Mn-55	1.1126×10^{-3}
Fe-54	3.5599×10^{-3}
Fe-56	5.5341×10^{-2}
Fe-57	1.2671×10^{-3}
Fe-58	1.6894×10^{-4}
Ni-58	4.9719×10^{-3}
Ni-60	1.9008×10^{-3}
Ni-61	8.2295×10^{-5}
Ni-62	2.6145×10^{-4}
Ni-64	6.6273×10^{-5}

3.5 Molybdenum disc in fuel rod

The density of molybdenum was cited from the literature [11], as 10.28 g/cm^3. The difference in the density between the above value and that of the other TRIGA benchmarks, i.e., ICT-013 [12] and ICT-003 [13], is 0.08 g/cm^3 in maximum. Thus, the error in the molybdenum density was estimated to be 0.08 g/cm^3 (0.78 %).

The impurities of the molybdenum disc were obtained by using material inspection records at the construction in 1973. The impurities, which are necessary to obtain atomic number densities, are listed in Table 3.5.1.

Table 3.5.1 Impurities in the molybdenum disc.

Element	Fraction (ppm)
Hydrogen	2
Nitrogen	5
Oxygen	25
Sodium	8
Aluminum	10
Silicon	17
Phosphorus	3
Calcium	30
Chromium	10
Manganese	10
Iron	40
Nickel	10
Copper	12
Tungsten	90

The atomic number densities of nuclides for the molybdenum disc in the fuel rod are listed in Table 3.5.2.

Table 3.5.2 Atomic number densities of nuclides for the molybdenum disc in the fuel rod.

Nuclide	Atomic Number Density (1/barn cm)
Mo-92	9.5767×10^{-3}
Mo-94	5.9693×10^{-3}
Mo-95	1.0274×10^{-2}
Mo-96	1.0764×10^{-2}
Mo-97	6.1629×10^{-3}
Mo-98	1.5572×10^{-2}
Mo-100	6.2145×10^{-3}

Table 3.5.2 (contd.) Atomic number densities of nuclides for the molybdenum disc in the fuel rod.

Nuclide	Atomic Number Density (1/barn cm)
H-1[*1]	1.2284×10^{-5}
N-14[*1]	2.2017×10^{-6}
N-15[*1]	8.1766×10^{-9}
O-16[*1]	9.6734×10^{-6}
Na-23[*1]	2.1542×10^{-6}
Al-27[*1]	3.5532×10^{-6}
Si-28[*1]	5.3522×10^{-6}
Si-29[*1]	2.7100×10^{-7}
Si-30[*1]	1.7990×10^{-7}
P-31[*1]	5.9961×10^{-7}
Ca-40[1]	3.1479×10^{-8}
Ca-42[*1]	6.4050×10^{-9}
Ca-43[*1]	9.8908×10^{-8}
Ca-44[*1]	1.9379×10^{-10}
Ca-46[*1]	9.0425×10^{-9}
Ca-48[*1]	8.6656×10^{-9}
Cr-50[*1]	5.1732×10^{-8}
Cr-52[*1]	9.9761×10^{-7}
Cr-53[*1]	1.1311×10^{-7}
Cr-54[*1]	2.8158×10^{-8}
Mn-55[*1]	1.1269×10^{-6}
Fe-54[*1]	2.6162×10^{-7}
Fe-56[*1]	4.0672×10^{-6}
Fe-57[*1]	9.3121×10^{-8}
Fe-58[*1]	1.2416×10^{-8}
Ni-58[*1]	7.2015×10^{-7}
Ni-60[*1]	2.7532×10^{-7}
Ni-61[*1]	1.1920×10^{-8}
Ni-62[*1]	3.7869×10^{-8}
Ni-64[*1]	9.5992×10^{-9}
Cu-63[*1]	8.0864×10^{-7}
Cu-65[*1]	3.6042×10^{-7}
W-180[*1]	3.6367×10^{-9}
W-182[*1]	7.9703×10^{-7}
W-183[*1]	4.3276×10^{-7}
W-184[*1]	9.3038×10^{-7}
W-186[*1]	8.6674×10^{-7}

*1 Impurities.

3.6 Axial graphite reflector in fuel rod

The density of graphite was cited from the ICT-013 [12)] benchmark referring to the General Atomic TRIGA model, as 1.73 g/cm^3. The error in the density is evaluated as 0.01 g/cm^3 in the ICT-013, however, the discrepancy in the density is

0.13 g/cm^3 between the ICT-013 and another TRIGA benchmark, ICT-003 [13]. For this reason, the error in the graphite density was estimated to be 0.13 g/cm^3 (7.51 %) conservatively.

The content of boron as an impurity in the axial graphite reflectors is mentioned in material inspection records at the construction in 1973. The boron content was smaller than 0.5 ppm of the lower limit of detection. Thus, no impurity was considered for the composition of the graphite.

The atomic number densities of nuclides for the axial graphite reflectors in the fuel rod are listed in Table 3.6.1.

Table 3.6.1 Atomic number densities of nuclides for the axial graphite reflectors in the fuel rod.

Nuclide	Atomic Number Density (1/barn cm)
C-12*1	8.5785×10^{-2}
C-13*1	9.5413×10^{-4}

*1 Thermal scattering law (TSL) data used as graphite.

3.7 Natural boron carbide absorber in control and safety rods

The material inspection records on the natural boron carbide in the control and safety rods at the construction in 1973 are not found at present. The composition of the natural boron carbide and its error were estimated by using data at the renewal of control and safety rods in 1995. The parameters, which are necessary to obtain atomic number densities, are listed in Table 3.7.1.

Table 3.7.1 Parameters of the natural boron carbide absorber in the control and safety rods.

Item	Value ± 1σ	Relative error (%)
Density of B_4C (g/cm^3) *1	2.5000 ± 0.0059	0.23
B content of B_4C (wt%) *1	78.263 ± 0.103	0.13

*1 Estimated by the material inspection records in 1995.

The atomic number densities of nuclides for the natural boron carbide absorber in the control and safety rods are listed in Table 3.7.2.

Table 3.7.2 Atomic number densities of nuclides for the natural boron carbide absorber in the control and safety rods.

Nuclide	Atomic Number Density (1/barn cm)
B-10	2.1688×10^{-2}
B-11	8.7299×10^{-2}
C-12	2.6947×10^{-2}
C-13	2.9971×10^{-4}

3.8 Stainless-steel type SUS304 of cladding, spacer, and top/bottom plugs in control and safety rods

The density of SUS304 was cited from the literature [14], as 7.93 g/cm^3, same as the cladding in the fuel rod. The error in the density was also estimated to be 0.07 g/cm^3 (0.88 %), same as the cladding in the fuel rod.

The material inspection records on stainless steel type SUS304 of the cladding, spacer, and top/bottom plugs in the control and safety rods at the construction in 1973 are not found at present. Thus, the composition of those was estimated by using the standard of SUS304. The ASTM A213-66 [15] standard was adopted for the estimation since the difference in the compositions between ASTM A213-66 and ASM 5370 [16] is quite small. The average of upper and lower limits was adopted as estimated fraction values for the elements of which fraction is specified with the range in the standard, e.g., chromium, manganese, and nickel. The fraction value of the upper limits was adopted as estimated fraction values for the other elements, e.g., carbon, silicon, phosphorus, and sulfur.

The elemental composition, which is necessary to obtain atomic number densities, is listed in Table 3.8.1.

Table 3.8.1 Elemental composition of the cladding, spacer, and top/bottom plugs in the control and safety rods.

Element	Fraction (wt%)
Carbon	0.08
Silicon	0.75
Phosphorus	0.04
Sulfur	0.03
Chromium	19
Manganese	2
Iron	68.6
Nickel	9.5

The atomic number densities of nuclides for the cladding, spacer, and top/bottom plugs in the control and safety rods are listed in Table 3.8.2.

Table 3.8.2 Atomic number densities of nuclides for the cladding, spacer, and top/bottom plugs in the control and safety rods.

Nuclide	Atomic Number Density (1/barn cm)
C-12	3.1458×10^{-4}
C-13	3.4988×10^{-6}
Si-28	1.1762×10^{-3}
Si-29	5.9555×10^{-5}
Si-30	3.9533×10^{-5}
P-31	6.1672×10^{-5}
S-32	4.2456×10^{-5}
S-33	3.3510×10^{-7}
S-34	1.8811×10^{-6}
S-36	8.9361×10^{-9}
Cr-50	7.5822×10^{-4}
Cr-52	1.4622×10^{-2}
Cr-53	1.6578×10^{-3}
Cr-54	4.1270×10^{-4}
Mn-55	1.7385×10^{-3}
Fe-54	3.4612×10^{-3}
Fe-56	5.3806×10^{-2}
Fe-57	1.2319×10^{-3}
Fe-58	1.6426×10^{-4}
Ni-58	5.2775×10^{-3}
Ni-60	2.0176×10^{-3}
Ni-61	8.7352×10^{-5}
Ni-62	2.7752×10^{-4}
Ni-64	7.0346×10^{-5}

3.9 Aluminum alloy type A6061 of spacer tube in control and safety rods, and of cladding, spacer, air follower/spacer tubes, and top/bottom plugs in adjustable and fast transient rods

The density of A6061 was cited from the literature [17], as 2.7 g/cm^3. There is no difference in the density between the above value and that of the other TRIGA benchmarks, i.e., ICT-013 [12] and ICT-003 [13]. Thus, the error in the density was assumed not to be taken into account.

The material inspection records on aluminum alloy type A6061 for the control and safety rods, and the adjustable and fast transient rods at the construction in

1973 are not found at present. Thus, the composition of those was estimated by using the ASTM B210-12 [18] standard of A6061. The average of upper and lower limits was adopted as estimated fraction values for the elements of which fraction is specified with the range in the standard, e.g., magnesium, silicon, chromium, and copper. The fraction value of the upper limits was adopted as estimated fraction values for the other elements, e.g., titanium, manganese, iron, and zinc.

The elemental composition, which is necessary to obtain atomic number densities, is listed in Table 3.9.1.

Table 3.9.1 Elemental composition of the spacer tube in the control and safety rods, and of the cladding, spacer, air follower/spacer tubes, and top/bottom plugs in the adjustable and fast transient rods.

Element	Fraction (wt%)
Magnesium	1.0
Aluminum	96.68
Silicon	0.6
Titanium	0.15
Chromium	0.195
Manganese	0.15
Iron	0.7
Copper	0.275
Zinc	0.25

The atomic number densities of nuclides for the spacer tube in the control and safety rods, and for the cladding, spacer, air follower/spacer tubes, and top/bottom plugs in the adjustable and fast transient rods are listed in Table 3.9.2.

Table 3.9.2 Atomic number densities of nuclides for the spacer tube in the control and safety rods, and for the cladding, spacer, air follower/spacer tubes, and top/bottom plugs in the adjustable and fast transient rods.

Nuclide	Atomic Number Density (1/barn cm)
Mg-24	5.2843×10^{-4}
Mg-25	6.6998×10^{-5}
Mg-26	7.3655×10^{-5}
Al-27	5.8261×10^{-2}
Si-28	3.2037×10^{-4}
Si-29	1.6222×10^{-5}
Si-30	1.0768×10^{-5}

Table 3.9.2 (contd.) Atomic number densities of nuclides for the spacer tube in the control and safety rods, and for the cladding, spacer, air follower/spacer tubes, and top/bottom plugs in the adjustable and fast transient rods.

Nuclide	Atomic Number Density (1/barn cm)
Ti-46	4.0752×10^{-6}
Ti-47	3.7187×10^{-6}
Ti-48	3.7594×10^{-5}
Ti-49	2.8017×10^{-6}
Ti-50	2.7508×10^{-6}
Cr-50	2.6495×10^{-6}
Cr-52	5.1094×10^{-5}
Cr-53	5.7929×10^{-6}
Cr-54	1.4421×10^{-6}
Mn-55	4.4395×10^{-5}
Fe-54	1.2025×10^{-5}
Fe-56	1.8694×10^{-4}
Fe-57	4.2801×10^{-6}
Fe-58	5.7068×10^{-7}
Cu-63	4.8672×10^{-5}
Cu-65	2.1694×10^{-5}
Zn-64	3.0209×10^{-5}
Zn-66	1.7342×10^{-5}
Zn-67	2.5485×10^{-6}
Zn-68	1.1686×10^{-5}
Zn-70	3.7295×10^{-7}

3.10 Enriched boron carbide absorber in adjustable and fast transient rods

The material inspection records on the enriched boron carbide absorber in the adjustable and fast transient rods at the construction in 1973 are not found at present. The composition of the enriched boron carbide and its error were estimated by using data at the renewal of the adjustable transient rod in 1992 and the fast transient rod in 1995. The parameters, which are necessary to obtain atomic number densities, are listed in Table 3.10.1.

Table 3.10.1 Parameters of the enriched boron carbide absorber in the adjustable and fast transient rods.

Item	Value ± 1σ	Relative error (%)
Density of B_4C (g/cm^3) *1	2.3000 ± 0.0343	1.49
B content of B_4C (wt%) *1	77.0701 ± 0.4699	0.61
B-10 enrichment (wt%) *1	92.00 ± 0.47	0.51

*1 Estimated by the material inspection records in 1992 and 1995.

The atomic number densities of nuclides for the enriched boron carbide absorber in the adjustable and fast transient rods are listed in Table 3.10.2.

Table 3.10.2 Atomic number densities of nuclides for the enriched boron carbide absorber in the adjustable and fast transient rods.

Nuclide	Atomic Number Density (1/barn cm)
B-10	9.8082×10^{-2}
B-11	7.7570×10^{-3}
C-12	2.6151×10^{-2}
C-13	2.9086×10^{-4}

3.11 Water as moderator and reflector

The density of water was cited from the literature [19)]. The water densities in the range of 16 to 28 ^{o}C, which are necessary to obtain atomic number densities, are listed in Table 3.11.1.

Table 3.11.1 Density of water.

Temperature (^{o}C)	Density (g/cm^3)
16	0.99894
17	0.99877
18	0.99859
19	0.99840
20	0.99820
21	0.99799
22	0.99777
23	0.99754
24	0.99730
25	0.99704
26	0.99678
27	0.99651
28	0.99623

The atomic number densities of nuclides for the moderator and reflector water of typical temperature, 21 and 23 ^{o}C, are listed in Table 3.11.2.

Table 3.11.2 Atomic number densities of nuclides for the moderator and reflector water of typical temperature, 21 and 23 °C.

	Nuclide	Atomic Number Density (1/barn cm)
21 °C		
	H-1*1	6.6719×10^{-2}
	O-16*1	3.3361×10^{-2}
23 °C		
	H-1*1	6.6689×10^{-2}
	O-16*1	3.3346×10^{-2}

*1 Thermal scattering law (TSL) data used as light water. The TSL data of O-16 used in the case of JENDL-5 library only.

3.12 Other core structures

The material inspection records on the other core structures, i.e., the experimental tube, grid plates, shroud, and guide tubes for the transient rods, at the construction in 1973 are not found at present. Thus, it was assumed that the compositions of the experimental tube, grid plates, and shroud were based on the ASTM B210-12 [18] standard of A6061 described in Sec. 3.9, same as the spacer tube in the control and safety rods and so on. The composition of the guide tubes for the transient rods was also assumed to be based on the ASTM A213-66 [15] standard of SUS304 described in Sec. 3.8, same as the cladding in the control and safety rods.

4. Operation Data

The vertical positions of the control, safety, and transient rods are essential parameters to define delayed critical conditions. The position data were confirmed by using operation records during the first startup in 1975. In addition, the model temperature affecting criticality was obtained by using the operation records. These data are described below.

4.1 Minimum and standard cores

The first criticality of the minimum core was attained by the reactivity control with only the adjustable transient rod (TA) whilst all control (R1 to R6), safety (S1 and S2), and fast transient rods (TA and TB) were being fully withdrawn [1]. On the other hand, the first criticality of the standard core was attained by the reactivity control of 'bank mode' with all control rods whilst all safety and transient rods were being fully withdrawn [1].

In NSRR, the absorber rod position of 100 units means full insertion of the control, safety, and adjustable transient rod, meanwhile that of 900 units does full withdrawal of them. The stroke length from full insertion to full withdrawal is 38.1 cm. Thus, one unit is identical to 0.0476 cm (38.1 cm per 800 unit). The rod positions were confirmed by operation records logged for the first startup in 1975. The uncertainty in the rod position was estimated to be 5 units (about 2.4 mm) conservatively by the maintenance standard for the position indicator. The rod positions of both the minimum and standard cores are listed in Table 4.1.1.

The temperature of the models was also estimated to be 23 ^{o}C by using the pool water temperature logged in the operation records in 1975. The uncertainty in the temperature was assumed to be 5 ^{o}C conservatively considering the variation of the pool water temperature for each day of operations although the water temperature was measured by thermometers with ±0.43 ^{o}C of precision.

The operation power at criticality was 0.4 and 50 W for the minimum and standard cores, respectively. The heat capacity of the uranium-zirconium hydride totally loaded in the standard core is estimated to be 1.21×10^5 J/^{o}C at 25 ^{o}C, which is obtained by the mass heat capacity of the uranium-zirconium hydride[*1] and its mass inventory[*2]. Even if the operation time during the criticality at 50 W would

[*1] The mass heat capacity is estimated to be 0.350 J/g/^{o}C at 25^{o}C in the case of 11.9 wt% of uranium in the uranium-zirconium hydride [20].

[*2] The mass inventory is calculated to be 3.46×10^5 g from the data in Table 3.1.1.

be overestimated as one hour (= 3,600 s), the increase of the temperature of the uranium-zirconium hydride is estimated to be 1.5 °C without heat removal. This increase of temperature is within the above-mentioned uncertainty in the temperature.

4.2 Intermediate cores

The delayed criticality of the intermediate cores was attained by the reactivity control of 'bank mode' [1], similar to the standard core. The positions of the control, safety, and transient rods, and their uncertainties were obtained by the same method as those for the minimum and standard cores. The absorber rod positions of the intermediate cores are listed in Table 4.2.1. The core composed in the last step, i.e., ID=aj, is identical to the standard core.

The temperature of the cores was estimated to be 21 °C by using the pool water temperature logged in the operation records for the first startup in 1975. The uncertainty in temperature was assumed to be same as that of the minimum and standard cores.

The operation power at criticality was in the range of 1.5 to 50 W. Even if the operation time during the criticality at 50 W would be overestimated as one hour, the increase of temperature in the uranium-zirconium hydride during the operation is within the uncertainty in the temperature, as described in Sec. 4.1.

Table 4.1.1 Rod positions of the minimum and standard cores.

Date and time	The number of fuel rods	ID	Rod position (unit) for R1-R6, S1-S2, and TA, up: full withdrawal and dn: full insertion for TB and TC											BANK av. (unit)	Remarks
			R1	R2	R3	R4	R5	R6	S1	S2	TA	TB	TC		
1975/06/30 12:00	113	a	898	901	897	903	896	894	899	897	782	up	up	898.2	Minimum core
1975/07/03 20:02	149	a	218	211	216	211	209	213	899	897	895	up	up	213.0	Standard core

Table 4.2.1 Rod positions of the intermediate cores.

Date and time	The number of fuel rods	ID	Rod position (unit) for R1-R6, S1-S2, and TA, up: full withdrawal and dn: full insertion for TB and TC											BANK av. (unit)	Position of fuel addition
			R1	R2	R3	R4	R5	R6	S1	S2	TA	TB	TC		
1975/07/02 14:32	114	a	812	808	810	808	803	802	898	896	895	up	up	807.2	D-1
1975/07/02 15:35	115	b	780	776	779	776	771	771	898	896	894	up	up	775.5	D-36
1975/07/02 16:30	116	c	748	743	746	744	739	739	898	896	894	up	up	743.2	D-7
1975/07/02 16:57	117	d	723	717	721	718	714	713	897	899	894	up	up	717.7	D-28
1975/07/02 17:30	118	e	704	699	703	701	696	695	899	897	894	up	up	699.7	D-8
1975/07/02 17:45	119	f	688	682	686	684	679	678	899	897	894	up	up	682.8	D-29
1975/07/02 18:01	120	g	672	667	670	668	663	663	899	897	894	up	up	667.2	D-15
1975/07/02 18:25	121	h	656	651	655	652	647	647	899	897	895	up	up	651.3	D-22
1975/07/03 10:35	122	i	634	628	632	629	624	624	898	896	894	up	up	628.5	E-37
1975/07/03 10:50	123	j	615	609	614	611	606	606	898	896	894	up	up	610.2	E-13
1975/07/03 11:08	124	k	596	590	594	591	586	586	898	896	894	up	up	590.5	E-21
1975/07/03 11:23	125	l	580	573	577	574	570	570	898	896	894	up	up	574.0	E-45
1975/07/03 11:59	126	m	555	562	556	561	558	554	898	896	894	up	up	557.7	E-29
1975/07/03 11:55	127	n	546	540	544	541	538	543	898	896	895	up	up	542.0	E-5
1975/07/03 12:26	128	o	530	524	529	525	521	528	898	896	895	up	up	526.2	E-36
1975/07/03 13:50	129	p	518	511	517	514	509	516	898	896	895	up	up	514.2	E-12
1975/07/03 14:08	130	q	503	497	502	499	494	501	898	896	895	up	up	499.3	E-20
1975/07/03 14:26	131	r	491	484	490	486	482	489	899	897	895	up	up	487.0	E-44

Table 4.2.1 (contd.) Rod positions of the intermediate cores.

Date and time	The number of fuel rods	ID	Rod position (unit) for R1-R6, S1-S2, and TA, up: full withdrawal and dn: full insertion for TB and TC											BANK av. (unit)	Position of fuel addition
			R1	R2	R3	R4	R5	R6	S1	S2	TA	TB	TC		
1975/07/03 14:42	132	s	478	471	477	473	469	475	899	897	895	up	up	473.8	E-28
1975/07/03 14:58	133	t	464	457	462	460	455	461	899	897	895	up	up	459.8	E-4
1975/07/03 15:12	134	u	448	441	447	443	440	445	899	897	895	up	up	444.0	E-38
1975/07/03 15:27	135	v	434	428	433	430	425	432	899	897	895	up	up	430.3	E-14
1975/07/03 15:45	136	w	418	412	418	414	410	416	899	897	895	up	up	414.7	E-22
1975/07/03 16:02	137	x	406	399	405	401	397	403	899	897	895	up	up	401.8	E-46
1975/07/03 16:47	138	y	394	387	392	388	385	390	899	897	895	up	up	389.3	E-30
1975/07/03 17:13	139	z	378	371	377	373	369	375	899	897	895	up	up	373.8	E-6
1975/07/03 17:27	140	aa	364	357	362	358	355	360	899	897	895	up	up	359.3	E-35
1975/07/03 17:42	141	ab	352	345	350	346	343	348	899	897	895	up	up	347.3	E-11
1975/07/03 17:58	142	ac	338	331	336	332	329	333	899	897	895	up	up	333.2	E-19
1975/07/03 18:08	143	ad	326	319	324	320	316	320	899	897	895	up	up	320.8	E-43
1975/07/03 18:22	144	ae	311	305	311	306	303	307	899	897	895	up	up	307.2	E-27
1975/07/03 18:37	145	af	296	290	296	288	288	293	899	897	895	up	up	291.8	E-3
1975/07/03 19:17	146	ag	278	272	277	272	270	274	899	897	895	up	up	273.8	E-39
1975/07/03 19:32	147	ah	260	254	260	254	252	257	899	897	895	up	up	256.2	E-15
1975/07/03 19:45	148	ai	240	234	239	233	231	236	899	897	895	up	up	235.5	E-23
1975/07/03 20:02	149	aj	218	211	216	211	209	213	899	897	895	up	up	213.0	E-47 Same as std. core

5. Analyses of Effective Neutron Multiplication Factors

The results of criticality analyses using the present detailed models are described below for the confirmation of both the effective neutron multiplication factor (k_{eff}) calculated by the Monte Carlo method and differences in k_{eff} among the evaluated nuclear data libraries adopted in the present work.

5.1 Calculation method

The analyses of k_{eff} of the present detailed models for minimum, standard, and intermediate cores were performed by using the MVP version 3 code [6] with the evaluated nuclear data libraries JENDL-4.0 [8], JENDL-4.0u1 [9], and JENDL-5 [7]. Fifty million histories (100,000 particles per batch, 700 batches in total, 200 initial batches skipped) were set for the analyses.

5.2 Calculated results

The results of the analyses on minimum and standard cores are listed in Table 5.2.1 and Table 5.2.2, respectively. In Tables 5.2.1 and 5.2.2, the standard deviation (σ) is the statistical error only from Monte Carlo calculations. The differences in k_{eff} between JENDL-4.0 and JENDL-4.0u1 are within their σ's. The k_{eff}'s by JENDL-5 are 0.43 to 0.57 % larger than those by JENDL-4.0. The differences in k_{eff} between JENDL-5 and JENDL-4.0 are larger than three times their σ's.

Table 5.2.1 Calculated k_{eff} for the minimum core.

The number of fuel rods	ID	BANK av. (unit)	Library *	k_{eff} ± 1σ	k_{eff} difference ± 1σ J40-J40u1	k_{eff} difference ± 1σ J5-J40
113	a	898.2	J40	0.99969 ± 0.00013	-0.00015 ± 0.00018	
			J40u1	0.99984 ± 0.00013		
			J5	1.00535 ± 0.00013		0.00566 ± 0.00018

* J40: JENDL-4.0, J40u1: JENDL-4.0u1, J5: JENDL-5

Table 5.2.2 Calculated k_{eff} for the standard core.

The number of fuel rods	ID	BANK av. (unit)	Library *	k_{eff} ± 1σ	k_{eff} difference ± 1σ J40-J40u1	k_{eff} difference ± 1σ J5-J40
149	a	213.0	J40	1.00067 ± 0.00012	0.00002 ± 0.00018	
			J40u1	1.00065 ± 0.00013		
			J5	1.00492 ± 0.00012		0.00425 ± 0.00017

* J40: JENDL-4.0, J40u1: JENDL-4.0u1, J5: JENDL-5

The results of the analyses on the intermediate cores are listed in Table 5.2.3. In Table 5.2.3, σ is the statistical error only from Monte Carlo calculations, same as shown in the results from the minimum and standard cores. The differences in k_{eff} between JENDL-4.0 and JENDL-4.0u1 are within their σ's. The k_{eff}'s by JENDL-5 are 0.36 to 0.54 % larger than those by JENDL-4.0. The differences in k_{eff} between JENDL-5 and JENDL-4.0 are larger than three times their σ's, same as shown in the results from the minimum and standard cores.

Figure 5.2.1 shows the calculated k_{eff} and the averaged bank rod position as function of the number of fuel rods loaded in the minimum, standard, and intermediated cores. The k_{eff}'s by JENDL-4.0, JENDL-4.0u1, and JENDL-5 vary with the number of fuel rods in the range of 0.99966 to 1.00098, 0.99964 to 1.00086, and 1.00448 to 1.00535, respectively. The magnitude of the variation of k_{eff} for JENDL-5 is smaller than those for JENDL-4.0 and JENDL-4.0u1. The averaged values of k_{eff} by JENDL-4.0, JENDL-4.0u1, and JENDL-5 are 1.00042 ± 0.00035, 1.00042 ± 0.00034, and 1.00489 ± 0.00020, respectively.

Figure 5.2.2 shows the residual from the averaged k_{eff} as function of the number of fuel rods loaded in the cores. It is confirmed that the residual for JENDL-5 tends to decrease as the number of fuel rods increases, on the other hand the residuals for JENDL-4.0 and JENDL-4.0u1 tend to increase with the number of fuel rods.

The difference in k_{eff} varying with the number of fuel rods loaded in the cores and the difference in k_{eff} among the libraries are needed to be examined with consideration of uncertainties in k_{eff} involved in the present detailed models. Hence, the uncertainties in k_{eff}, which are propagated from errors in the geometry, material, and operation data, were evaluated by using the MVP version 3 code. The evaluated results are shown in Chap. 6.

Table 5.2.3 Calculated k_{eff} for the intermediate cores.

The number of fuel rods	ID	BANK av. (unit)	Library [*1]	k_{eff} ± 1σ			k_{eff} difference ± 1σ J40-J40u1			k_{eff} difference ± 1σ J5-J40		
114	a	807.2	J40	0.99986	±	0.00013	0.00018	±	0.00018			
			J40u1	0.99968	±	0.00013						
			J5	1.00495	±	0.00012				0.00509	±	0.00018
115	b	775.5	J40	0.99966	±	0.00013	0.00002	±	0.00019			
			J40u1	0.99964	±	0.00012						
			J5	1.00505	±	0.00013				0.00539	±	0.00018
116	c	743.2	J40	0.99993	±	0.00013	0.00015	±	0.00018			
			J40u1	0.99978	±	0.00012						
			J5	1.00503	±	0.00012				0.00511	±	0.00017
117	d	717.7	J40	1.00012	±	0.00012	-0.00001	±	0.00018			
			J40u1	1.00013	±	0.00013						
			J5	1.00486	±	0.00013				0.00474	±	0.00018
118	e	699.7	J40	0.99993	±	0.00012	-0.00015	±	0.00018			
			J40u1	1.00008	±	0.00013						
			J5	1.00504	±	0.00013				0.00511	±	0.00017
119	f	682.8	J40	1.00007	±	0.00012	-0.00015	±	0.00017			
			J40u1	1.00022	±	0.00012						
			J5	1.00517	±	0.00012				0.00510	±	0.00017
120	g	667.2	J40	1.00012	±	0.00013	-0.00006	±	0.00017			
			J40u1	1.00018	±	0.00012						
			J5	1.00503	±	0.00013				0.00491	±	0.00018
121	h	651.3	J40	1.00013	±	0.00013	0.00014	±	0.00018			
			J40u1	0.99999	±	0.00013						
			J5	1.00512	±	0.00012				0.00499	±	0.00017
122	i	628.5	J40	1.00009	±	0.00012	-0.00007	±	0.00017			
			J40u1	1.00016	±	0.00012						
			J5	1.00480	±	0.00012				0.00471	±	0.00017
123	j	610.2	J40	1.00003	±	0.00012	0.00006	±	0.00017			
			J40u1	0.99997	±	0.00012						
			J5	1.00483	±	0.00012				0.00480	±	0.00017
124	k	590.5	J40	1.00019	±	0.00012	0.00001	±	0.00018			
			J40u1	1.00018	±	0.00013						
			J5	1.00468	±	0.00013				0.00449	±	0.00018
125	l	574.0	J40	1.00041	±	0.00013	0.00007	±	0.00018			
			J40u1	1.00034	±	0.00013						
			J5	1.00475	±	0.00013				0.00434	±	0.00018
126	m	557.7	J40	1.00028	±	0.00012	-0.00015	±	0.00018			
			J40u1	1.00043	±	0.00013						
			J5	1.00490	±	0.00012				0.00462	±	0.00017
127	n	542.0	J40	1.00056	±	0.00013	0.00017	±	0.00018			
			J40u1	1.00039	±	0.00013						
			J5	1.00511	±	0.00012				0.00455	±	0.00018
128	o	526.2	J40	1.00029	±	0.00013	-0.00012	±	0.00018			
			J40u1	1.00041	±	0.00013						
			J5	1.00492	±	0.00012				0.00463	±	0.00018
129	p	514.2	J40	1.00060	±	0.00013	0.00016	±	0.00018			
			J40u1	1.00044	±	0.00013						
			J5	1.00506	±	0.00012				0.00446	±	0.00018

*1 J40: JENDL-4.0, J40u1: JENDL-4.0u1, J5: JENDL-5

Table 5.2.3 (contd.) Calculated k_{eff} for the intermediate cores.

The number of fuel rods	ID	BANK av. (unit)	Library *1	k_{eff} ± 1σ			k_{eff} difference ± 1σ J40-J40u1			J5-J40		
130	q	499.3	J40	1.00047	±	0.00012	-0.00009	±	0.00017			
			J40u1	1.00056	±	0.00012						
			J5	1.00488	±	0.00012				0.00441	±	0.00017
131	r	487.0	J40	1.00040	±	0.00012	-0.00002	±	0.00017			
			J40u1	1.00042	±	0.00012						
			J5	1.00498	±	0.00012				0.00458	±	0.00017
132	s	473.8	J40	1.00044	±	0.00013	0.00000	±	0.00019			
			J40u1	1.00044	±	0.00013						
			J5	1.00495	±	0.00013				0.00451	±	0.00018
133	t	459.8	J40	1.00057	±	0.00012	-0.00011	±	0.00017			
			J40u1	1.00068	±	0.00012						
			J5	1.00488	±	0.00013				0.00431	±	0.00018
134	u	444.0	J40	1.00045	±	0.00013	-0.00016	±	0.00018			
			J40u1	1.00061	±	0.00012						
			J5	1.00511	±	0.00012				0.00466	±	0.00018
135	v	430.3	J40	1.00043	±	0.00012	-0.00005	±	0.00018			
			J40u1	1.00048	±	0.00013						
			J5	1.00472	±	0.00012				0.00429	±	0.00017
136	w	414.7	J40	1.00038	±	0.00013	-0.00003	±	0.00018			
			J40u1	1.00041	±	0.00013						
			J5	1.00485	±	0.00012				0.00447	±	0.00017
137	x	401.8	J40	1.00083	±	0.00012	0.00005	±	0.00017			
			J40u1	1.00078	±	0.00012						
			J5	1.00478	±	0.00012				0.00395	±	0.00017
138	y	389.3	J40	1.00071	±	0.00012	0.00002	±	0.00017			
			J40u1	1.00069	±	0.00012						
			J5	1.00483	±	0.00012				0.00412	±	0.00017
139	z	373.8	J40	1.00084	±	0.00013	-0.00002	±	0.00017			
			J40u1	1.00086	±	0.00012						
			J5	1.00526	±	0.00012				0.00442	±	0.00018
140	aa	359.3	J40	1.00057	±	0.00012	-0.00013	±	0.00017			
			J40u1	1.00070	±	0.00013						
			J5	1.00481	±	0.00012				0.00424	±	0.00017
141	ab	347.3	J40	1.00098	±	0.00012	0.00017	±	0.00017			
			J40u1	1.00081	±	0.00012						
			J5	1.00460	±	0.00012				0.00362	±	0.00017
142	ac	333.2	J40	1.00090	±	0.00012	0.00007	±	0.00017			
			J40u1	1.00083	±	0.00013						
			J5	1.00503	±	0.00013				0.00413	±	0.00018
143	ad	320.8	J40	1.00086	±	0.00012	0.00009	±	0.00018			
			J40u1	1.00077	±	0.00013						
			J5	1.00465	±	0.00012				0.00379	±	0.00017
144	ae	307.2	J40	1.00088	±	0.00013	0.00010	±	0.00018			
			J40u1	1.00078	±	0.00012						
			J5	1.00483	±	0.00013				0.00395	±	0.00018
145	af	291.8	J40	1.00073	±	0.00012	0.00003	±	0.00017			
			J40u1	1.00070	±	0.00012						
			J5	1.00465	±	0.00013				0.00392	±	0.00017

*1 J40: JENDL-4.0, J40u1: JENDL-4.0u1, J5: JENDL-5

Table 5.2.3 (contd.) Calculated k_{eff} for the intermediate cores.

The number of fuel rods	ID	BANK av. (unit)	Library *1	$k_{eff} \pm 1\sigma$			k_{eff} difference ± 1σ J40-J40u1			J5-J40		
146	ag	273.8	J40	1.00083	±	0.00013	0.00008	±	0.00019			
			J40u1	1.00075	±	0.00013						
			J5	1.00471	±	0.00013				0.00388	±	0.00018
147	ah	256.2	J40	1.00067	±	0.00012	0.00000	±	0.00016			
			J40u1	1.00067	±	0.00011						
			J5	1.00448	±	0.00012				0.00381	±	0.00017
148	ai	235.5	J40	1.00060	±	0.00012	-0.00015	±	0.00017			
			J40u1	1.00075	±	0.00013						
			J5	1.00453	±	0.00012				0.00393	±	0.00017
149	aj *2	213.0	J40	1.00067	±	0.00012	0.00002	±	0.00018			
			J40u1	1.00065	±	0.00013						
			J5	1.00492	±	0.00012				0.00425	±	0.00017

*1 J40: JENDL-4.0, J40u1: JENDL-4.0u1, J5: JENDL-5

*2 Same as standard core

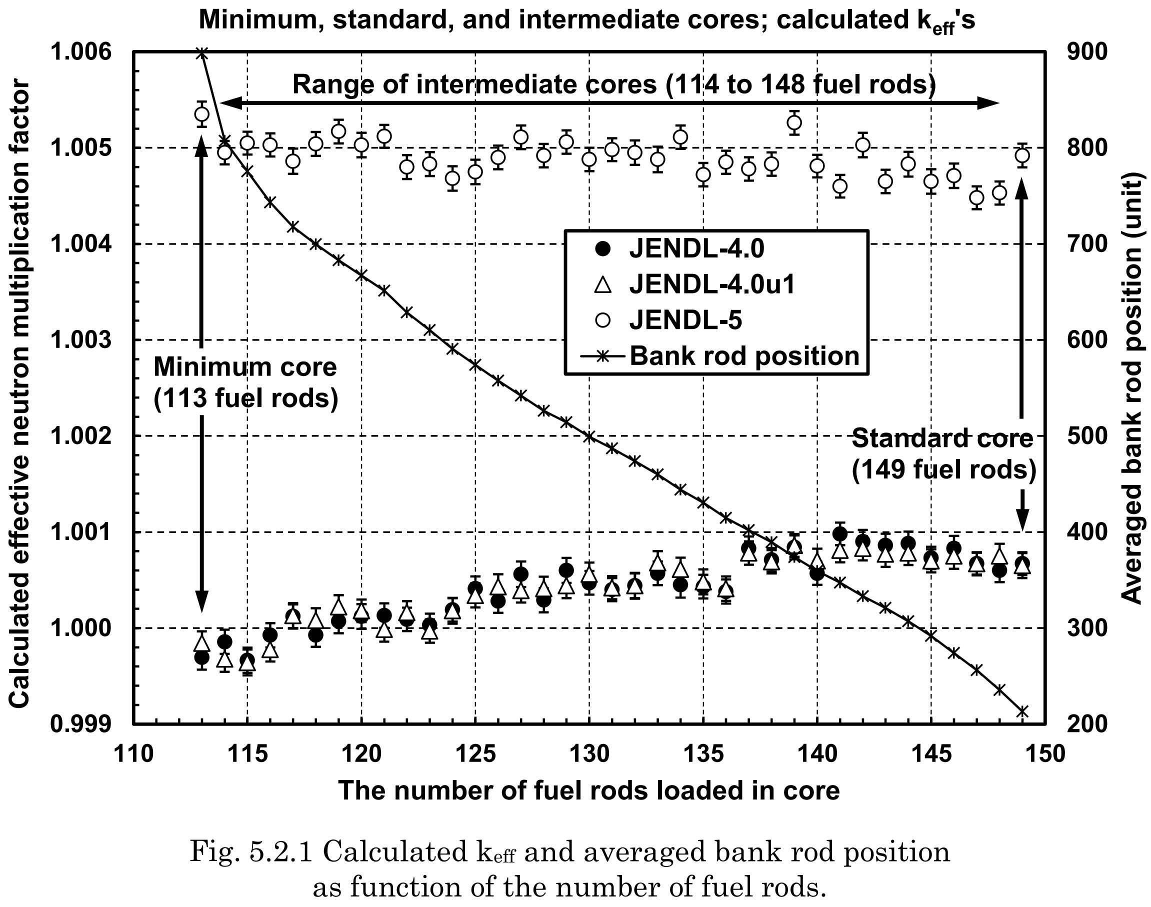

Fig. 5.2.1 Calculated k_{eff} and averaged bank rod position as function of the number of fuel rods.

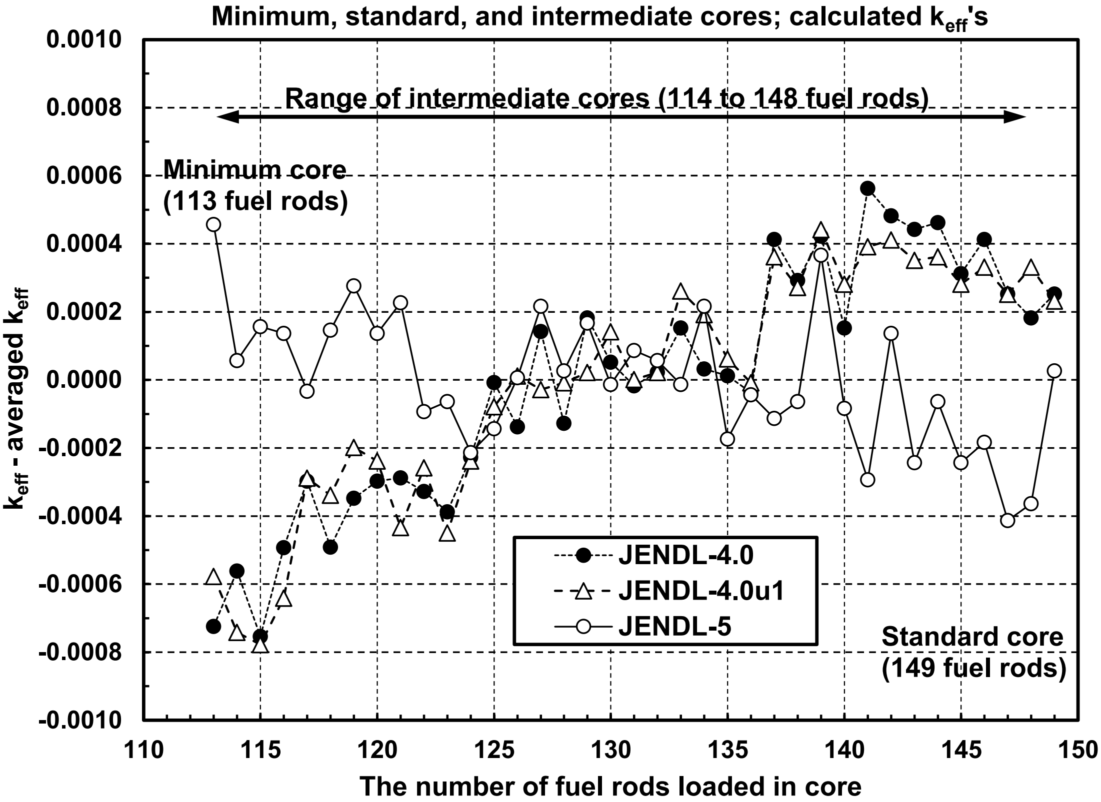

Fig. 5.2.2 Residual from averaged k_{eff} as function of the number of fuel rods.

6. Evaluation of Uncertainties for Detailed Models

The uncertainties in k_{eff} for the present detailed models, which are propagated from the errors in the geometry, material, and operation data as sources of the uncertainties, were evaluated by using the MVP version 3 code with the evaluated nuclear data libraries JENDL-4.0, JENDL-4.0u1, and JENDL-5. The uncertainties in k_{eff} were respectively evaluated for the minimum, standard, and intermediate cores. For the intermediate cores, three sorts of representative cores were selected, in which all control rods were being inserted to the vicinity of the core midplane. This means that those rod positions bring the largest amount of reactivity addition per unit of the control rod. The core ID's of the representative intermediate cores are p, q, and r listed in Table 4.2.1.

If both positive and negative values of errors were given as a source of the uncertainty, the bias of k_{eff} was evaluated as the mean of absolute value of the difference in k_{eff} due to the positive error, and of that due to the negative one. If either positive or negative value of an error was given as a source of the uncertainty, the bias of k_{eff} was evaluated as the positive or negative value of the difference in k_{eff} due to the error.

The bias of k_{eff} was calculated with the above JENDL libraries for each error as a source of the uncertainty in k_{eff}. The histories in the Monte Carlo calculations were set to be the same as described in Chap. 5. The averaged bias of k_{eff} was determined by using the mean of the biases calculated by the JENDL-4.0, JENDL-4.0u1, and JENDL-5 libraries. For the intermediate core, the averaged bias was determined further by using the mean of the bias for each representative core (ID = p, q, and r).

The uncertainty in k_{eff} propagated from the error was finally evaluated by the square root of the summation of the square values of the averaged bias and its standard deviation (σ). If the absolute value of the averaged bias was smaller than its σ, the uncertainty in k_{eff} was considered to be negligibly small and not taken into account for the evaluation of the uncertainties.

6.1 Uncertainties from errors in geometry data

The evaluated results of the uncertainties in k_{eff} propagated from the errors in the geometry data are summarized in Table 6.1. For each item listed in Table 6.1, details are described below.

Table 6.1 Summary of uncertainties in k_{eff} propagated from the errors in the geometry data.

Item	Source of uncertainty	Core	Averaged bias: B_{av} ($\Delta k_{eff} \pm 1\sigma$)	Max. difference in B_{av}: D	D/σ	Uncertainty in k_{eff} (Δk_{eff})	Aggregated uncertainty for item (Δk_{eff})
Fuel rod	0.06% of outer diameter of U-ZrH: ± 0.002 (cm)	Minimum	±0.00043 ± 0.00007	0.00005	0.71	0.0004	Minimum: 0.0016 Standard: 0.0016 Intermediate: 0.0016
		Standard	±0.00040 ± 0.00007			0.0004	
		Intermediate	±0.00045 ± 0.00007			0.0005	
	0.39% of height of U-ZrH: ± 0.15 (cm)	Minimum	±0.00062 ± 0.00007	0.00004	0.51	0.0006	
		Standard	±0.00064 ± 0.00007			0.0006	
		Intermediate	±0.00066 ± 0.00007			0.0007	
	0.31% of inner diameter of U-ZrH: ± 0.002 (cm)	Minimum	±0.00005 ± 0.00007	0.00001	0.18	negligible	
		Standard	±0.00006 ± 0.00007			negligible	
		Intermediate	±0.00007 ± 0.00007			negligible	
	0.18% of diameter of Zr rod: ± 0.001 (cm)	Minimum	±0.00004 ± 0.00007	0.00002	0.22	negligible	
		Standard	±0.00005 ± 0.00007			negligible	
		Intermediate	±0.00004 ± 0.00007			negligible	
	0.03% of inner diameter of cladding: ± 0.001 (cm)	Minimum	±0.00049 ± 0.00007	0.00003	0.37	0.0005	
		Standard	±0.00046 ± 0.00007			0.0005	
		Intermediate	±0.00046 ± 0.00007			0.0005	
	0.05% of outer diameter of cladding: ± 0.002 (cm)	Minimum	±0.00120 ± 0.00007	0.00005	0.64	0.0012	
		Standard	±0.00124 ± 0.00007			0.0012	
		Intermediate	±0.00125 ± 0.00007			0.0012	
	0.06% of diameter of Mo disc: ± 0.002 (cm)	Minimum	±0.00001 ± 0.00007	0.00002	0.23	negligible	
		Standard	±0.00002 ± 0.00007			negligible	
		Intermediate	±0.00000 ± 0.00007			negligible	
	1.25% of thickness of Mo disc: ± 0.001 (cm)	Minimum	±0.00002 ± 0.00007	0.00002	0.24	negligible	
		Standard	±0.00001 ± 0.00007			negligible	
		Intermediate	±0.00001 ± 0.00007			negligible	
	0.03% of diameter of axial graphite reflector: ± 0.001 (cm)	Minimum	±0.00004 ± 0.00007	0.00001	0.20	negligible	
		Standard	±0.00003 ± 0.00007			negligible	
		Intermediate	±0.00004 ± 0.00007			negligible	
	0.09% of height of axial graphite reflector: ± 0.008 (cm)	Minimum	±0.00000 ± 0.00007	0.00002	0.29	negligible	
		Standard	±0.00000 ± 0.00007			negligible	
		Intermediate	±0.00002 ± 0.00007			negligible	
	Replacement of the parts of top/bottom plugs with water	Minimum	+0.00047 ± 0.00007	0.00002	0.25	0.0005	
		Standard	+0.00047 ± 0.00007			0.0005	
		Intermediate	+0.00045 ± 0.00007			0.0005	
Control and safety rods	0.28% of outer diameter of U-ZrH: ± 0.01 (cm)	Minimum	±0.00010 ± 0.00007	0.00006	0.85	0.0001	Minimum: 0.0007 Standard: 0.0003 Intermediate: 0.0007
		Standard	±0.00003 ± 0.00007			negligible	
		Intermediate	±0.00004 ± 0.00007			negligible	
	0.31% of inner diameter of U-ZrH: ± 0.002 (cm)	Minimum	±0.00001 ± 0.00007	0.00004	0.50	negligible	
		Standard	±0.00003 ± 0.00007			negligible	
		Intermediate	±0.00004 ± 0.00007			negligible	
	0.39% of height of U-ZrH: ± 0.15 (cm)	Minimum	±0.00024 ± 0.00007	0.00040	5.49	0.0003	
		Standard	±0.00031 ± 0.00007			0.0003	
		Intermediate	±0.00064 ± 0.00007			0.0006	
	0.18% of diameter of Zr rod: ± 0.001 (cm)	Minimum	±0.00004 ± 0.00007	0.00004	0.59	negligible	
		Standard	±0.00006 ± 0.00007			negligible	
		Intermediate	±0.00002 ± 0.00007			negligible	
	0.55% of inner diameter of cladding: ± 0.02 (cm)	Minimum	±0.00054 ± 0.00007	0.00051	7.01	0.0005	
		Standard	±0.00003 ± 0.00007			negligible	
		Intermediate	±0.00028 ± 0.00007			0.0003	
	0.27% of outer diameter of cladding: ± 0.01 (cm)	Minimum	±0.00037 ± 0.00007	0.00028	3.86	0.0004	
		Standard	±0.00009 ± 0.00007			0.0001	
		Intermediate	±0.00024 ± 0.00007			0.0003	

Table 6.1 (contd.) Summary of uncertainties in k_{eff} propagated from the errors in the geometry data.

Item	Source of uncertainty	Core	Averaged bias: B_{av} ($\Delta k_{eff} \pm 1\sigma$)	Max. difference in B_{av}: D	D/σ	Uncertainty in k_{eff} (Δk_{eff})	Aggregated uncertainty for item (Δk_{eff})
Fast and adjustable transient rods	1.38% smaller diameter of B4C: - 0.05 (cm)	Minimum	+0.00002 ± 0.00007	0.00005	0.75	negligible	Minimum: negligible Standard: negligible Intermediate: negligible
		Standard	-0.00002 ± 0.00007			negligible	
		Intermediate	+0.00003 ± 0.00007			negligible	
	0.05% and 0.01% of height of B_4C in adjustable and fast transient rod: ± 0.02 and ± 0.01 (cm)	Minimum	±0.00006 ± 0.00007	0.00005	0.74	negligible	
		Standard	±0.00006 ± 0.00007			negligible	
		Intermediate	±0.00001 ± 0.00007			negligible	
	0.26% of outer diameter of cladding: ± 0.01 (cm)	Minimum	±0.00005 ± 0.00007	0.00002	0.23	negligible	
		Standard	±0.00006 ± 0.00007			negligible	
		Intermediate	±0.00005 ± 0.00007			negligible	
Grid plate	0.07% of hexagonal lattice pitch: ± 0.003 (cm)	Minimum	±0.00008 ± 0.00007	0.00011	1.46	0.0001	Minimum: 0.0001 Standard: 0.0002 Intermediate: 0.0002
		Standard	±0.00019 ± 0.00007			0.0002	
		Intermediate	±0.00014 ± 0.00007			0.0002	
	Replacement of grid plates with water	Minimum	-0.00006 ± 0.00007	0.00006	0.78	negligible	
		Standard	-0.00008 ± 0.00007			0.0001	
		Intermediate	-0.00002 ± 0.00007			negligible	
Experimental tube	0.18% of face-to-face distance of hexagonal experimental tube: ± 0.043 (cm)	Minimum	±0.00025 ± 0.00007	0.00004	0.51	0.0003	Minimum: 0.0003 Standard: 0.0003 Intermediate: 0.0003
		Standard	±0.00028 ± 0.00007			0.0003	
		Intermediate	±0.00027 ± 0.00007			0.0003	
	0.78% of thickness of hexagonal experimental tube: ± 0.005 (cm)	Minimum	±0.00004 ± 0.00007	0.00002	0.27	negligible	
		Standard	±0.00004 ± 0.00007			negligible	
		Intermediate	±0.00002 ± 0.00007			negligible	
	0.11% of outer diameter of cylindrical experimental tube: ± 0.028 (cm)	Minimum	±0.00006 ± 0.00007	0.00005	0.75	negligible	
		Standard	±0.00001 ± 0.00007			negligible	
		Intermediate	±0.00000 ± 0.00007			negligible	
	0.78% of thickness of cylindrical experimental tube: ± 0.005 (cm)	Minimum	±0.00006 ± 0.00007	0.00005	0.75	negligible	
		Standard	±0.00000 ± 0.00007			negligible	
		Intermediate	±0.00003 ± 0.00007			negligible	
Shroud	Replacement of shroud with water	Minimum	-0.00001 ± 0.00007	0.00009	1.20	negligible	-
		Standard	-0.00004 ± 0.00007			negligible	
		Intermediate	+0.00004 ± 0.00007			negligible	
Guide tube for transient rod	Replacement of guide tube with water	Minimum	-0.00001 ± 0.00007	0.00005	0.61	negligible	-
		Standard	-0.00002 ± 0.00007			negligible	
		Intermediate	+0.00003 ± 0.00007			negligible	

6.1.1 Fuel rod

Outer diameter and height of uranium-zirconium hydride

The relative errors in the outer diameter and height of the uranium-zirconium hydride in the fuel rod were evaluated as 0.06 % and 0.39 %, respectively, using the dimensional inspection records at the construction in 1973. The relative error in the height is more than six times larger than that in the outer diameter. This suggests that the effect to the volume and mass inventory of the uranium-zirconium hydride by the former may be greater than that by the latter.

The difference in the averaged bias among the minimum, standard, and intermediate cores for the error in the outer diameter of the uranium-zirconium hydride in the fuel rod is within 0.71 times its σ. It is confirmed that the uncertainties in k_{eff} propagated from the error in the outer diameter of the uranium-zirconium hydride in the fuel rod for the minimum, standard, and intermediate cores are of comparable magnitude.

The difference in the averaged bias among the minimum, standard, and intermediate cores for the error in the height of the uranium-zirconium hydride in the fuel rod is within 0.51 times its σ. It is also confirmed that the uncertainties in k_{eff} propagated from the error in the height of the uranium-zirconium hydride in the fuel rod for the minimum, standard, and intermediate cores are of comparable magnitude.

The uncertainties in k_{eff} propagated from the error in the height of the uranium-zirconium hydride are larger than those from the error in the outer diameter due to the greater effect to the volume and mass inventory of the uranium-zirconium hydride brought by the error in the height, as mentioned above. The error in the outer diameter of the uranium-zirconium hydride brings changes in the water to fuel volume ratio of the hexagonal fuel cell, which may affect k_{eff}, however, it is considered that the impact of changes in the volume and mass inventory of the uranium-zirconium hydride is dominant.

<u>Inner diameter of uranium-zirconium hydride</u>

The inner diameter of the uranium-zirconium hydride in the fuel rods was confirmed by design drawings since the dimensional inspection records at the construction in 1973 are not found at present. Thus, the dimension error in the inner diameter of the uranium-zirconium hydride was assumed to be same as the error in the outer diameter, which was estimated to be ±0.002 cm. The relative error in the inner diameter became to be 0.31 %.

The difference in the averaged bias among the minimum, standard, and intermediate cores is within 0.18 times its σ. It is confirmed that the uncertainties in k_{eff} propagated from the error in the inner diameter of the uranium-zirconium hydride in the fuel rod are negligibly small for all cores.

The relative error in the inner diameter is larger than that in the outer one, but the effect to the volume and mass inventory of uranium-zirconium hydride by the former may be smaller than that by the latter. For this reason, it is considered that the uncertainties in k_{eff} propagated from the error in the inner diameter of the uranium-zirconium hydride become smaller than those from the error in the outer diameter.

Diameter of zirconium rod

For the zirconium rod in the fuel rods, the relative error in the diameter was evaluated as 0.18 % using the dimensional inspection records at the construction in 1973.

The difference in the averaged bias among the minimum, standard, and intermediate cores is within 0.22 times its σ. It is confirmed that the uncertainties in k_{eff} propagated from the error in the diameter of the zirconium rod in the fuel rod are negligibly small for all cores.

Inner and outer diameter of cladding in fuel rod

For the cladding in the fuel rod, the relative errors in the inner and outer diameters were evaluated as 0.03 and 0.05 %, respectively, using the dimensional inspection records at the construction in 1973.

The difference in the averaged bias among the minimum, standard, and intermediate cores for the error in the inner diameter of the cladding in the fuel rod is within 0.37 times its σ. It is confirmed that there is almost no difference in the uncertainties in k_{eff} propagated from the error in the inner diameter of the cladding in the fuel rod among the minimum, standard, and intermediate cores.

The difference in the averaged bias among the minimum, standard, and intermediate cores for the error in the outer diameter of the cladding in the fuel rod is within 0.64 times its σ. It is also confirmed that there is almost no difference in the uncertainties in k_{eff} propagated from the error in the outer diameter of the cladding in the fuel rod among the minimum, standard, and intermediate cores.

Both the relative and absolute errors in the outer diameter of the cladding in the fuel rod are larger than those in the inner one. This means that the effect to k_{eff} by the former may be greater than that by the latter due to the stainless-steel cladding behaving as thermal neutron absorber. In addition, the error in the outer diameter of the cladding brings changes in the water to fuel volume ratio of the hexagonal fuel cell, which affects k_{eff}. For this reason, it is considered that the uncertainties in k_{eff} propagated from the error in the outer diameter of the cladding become larger than those from the error in inner one.

Diameter and thickness of molybdenum disc

For the molybdenum disc in the fuel rod, the relative errors in the diameter and thickness were evaluated as 0.06 and 1.25 %, respectively, using the dimensional inspection records at the construction in 1973.

The difference in the averaged bias among the minimum, standard, and intermediate cores for the error in the diameter of the molybdenum disc is within 0.23 times its σ. It is confirmed that the uncertainties in k_{eff} propagated from the error in the diameter of the molybdenum disc in the fuel rod are negligibly small for all cores.

The difference in the averaged bias among the minimum, standard, and intermediate cores for the error in the thickness of the molybdenum disc is within 0.24 times its σ. It is also confirmed that the uncertainties in k_{eff} propagated from the error in the thickness of the molybdenum disc in the fuel rod are negligibly small for all cores.

Diameter and height of axial graphite reflector

For the axial graphite reflector in the fuel rod, the relative errors in the diameter and height were evaluated as 0.03 % and 0.09 %, respectively, using the dimensional inspection records at the construction in 1973.

The difference in the averaged bias among the minimum, standard, and intermediate cores for the error in the diameter of the axial graphite reflector is within 0.20 times its σ. It is confirmed that the uncertainties in k_{eff} propagated from the error in the diameter of the axial graphite reflector in the fuel rod are negligibly small for all cores.

The difference in the averaged bias among the minimum, standard, and intermediate cores for the error in the height of the axial graphite reflector is within 0.29 times its σ. It is also confirmed that the uncertainties in k_{eff} propagated from the error in the height of the axial graphite reflector in the fuel rod are negligibly small for all cores.

Replacement of top/bottom plugs with water

The top/bottom plugs in the fuel rod were modeled using the enveloping surfaces of their real shapes. For simplicity, the uncertainties in k_{eff}'s propagated from the errors in the dimensions of the plugs were evaluated conservatively by the replacement of both the top plug over the cladding and the bottom plug under the cladding with water.

The difference in the averaged bias among the minimum, standard, and intermediate cores is within 0.25 times its σ. It is confirmed for all cores that the positive reactivity effect is brought by the replacement. It is also confirmed that there is almost no difference in the uncertainties in k_{eff} propagated from the replacement among the minimum, standard, and intermediate cores.

Aggregated uncertainty in k_{eff}

The aggregated uncertainties in k_{eff} propagated from the errors in the geometry data of the fuel rod were obtained as the square root of summation of square values of the respective uncertainties mentioned above. Hereinafter, the same method was adopted to obtain the aggregated uncertainties.

There is almost no difference in the aggregated uncertainties in k_{eff} propagated from the errors in the geometry data of the fuel rod among the minimum, standard, and intermediate cores, evaluated to be 0.0016 Δk_{eff} for all cores. The largest contribution to the uncertainties in k_{eff} is the error in the outer diameter of the cladding in the fuel rod. The second largest contribution is the error in the height of the uranium-zirconium hydride in the fuel rod.

6.1.2 Control and safety rods

Outer diameter of uranium-zirconium hydride

For the control and safety rods, all dimensions were confirmed by design drawings since the dimensional inspection records at the construction in 1973 are not found at present. Thus, the relative error in the outer diameter of the uranium-zirconium hydride in the control and safety rods was assumed to be 0.28 % using the difference in the dimensions from that in the fuel rod. On the other hand, the error in the outer diameter of the uranium-zirconium hydride in the fuel rod was 0.06 % as mentioned above, using the dimensional inspection records. It is considered that 0.28 % as the relative error in the outer diameter of the uranium-zirconium hydride in the control and safety rods is conservative assumption.

The difference in the averaged bias among the minimum, standard, and intermediate cores is within 0.85 times its σ. It is confirmed that the averaged bias for the minimum core is slightly larger than those for the standard and intermediate cores, but the uncertainty in k_{eff} propagated from the error in the outer diameter of the uranium-zirconium hydride in the control and safety rods is quite small for the minimum core. It is also confirmed that the uncertainties in

k_{eff} propagated from the error in the outer diameter of the uranium-zirconium hydride in the control and safety rods are negligibly small for the standard and intermediate cores.

The error in the outer diameter affects the volume and mass inventory of the uranium-zirconium hydride in the fuel followers, similar to the fuel rods. In the minimum core, all control and safety rods were being fully withdrawn. This means that all fuel followers were being fully inserted. Thus, it is considered for the minimum core that the volume and mass inventory of the uranium-zirconium hydride in the fuel followers affect k_{eff} more than for the standard and intermediate cores. For this reason, it is considered that the uncertainty for the minimum core is slightly larger than those for the standard and intermediate cores.

Inner diameter of uranium-zirconium hydride

For the inner diameter of the uranium-zirconium hydride in the control and safety rods, there is no difference in the dimension from that in the fuel rod. Thus, the relative error in the inner diameter was assumed to be 0.31 % as much as that for the fuel rod.

The difference in the averaged bias among the minimum, standard, and intermediate cores is within 0.50 times its σ. It is confirmed that the uncertainties in k_{eff} propagated from the error in the inner diameter of the uranium-zirconium hydride in the control and safety rods are negligibly small for all cores.

Height of uranium-zirconium hydride

For the height of the uranium-zirconium hydride in the control and safety rods, there is also no difference in the dimension from that in the fuel rod. Thus, the relative error in the height was assumed to be 0.39 % as much as that for the fuel rod.

The difference in the averaged bias among the minimum, standard, and intermediate cores is more than three times its σ. It is considered that the error in the height of the uranium-zirconium hydride in the control and safety rods affects the vertical position of the fuel followers rather than the volume and mass inventory of the uranium-zirconium hydride in the cores. In the representative intermediate cores, the top planes of the fuel followers in the control rods were positioned at the vicinity of the core midplane where changes in the positions of the fuel followers affect k_{eff} maximally, but on the other hand the top planes of the fuel followers for the minimum and standard cores were at the vicinities of the top and bottom edges of cores, respectively. For this reason, it is considered that the uncertainty in k_{eff} for the intermediate cores is larger than those for the minimum and standard cores.

Diameter of zirconium rod

For the diameter of the zirconium rod in the control and safety rods, there is also no difference in the dimension from that in the fuel rod. Thus, the relative error in the diameter was assumed to be 0.18 % as much as that for the fuel rod.

The difference in the averaged bias among the minimum, standard, and intermediate cores is within 0.59 times its σ. It is confirmed that the uncertainties in k_{eff} propagated from the error in the diameter of the zirconium rod in the control and safety rods are negligibly small for all cores.

Inner and outer diameter of cladding in control and safety rods

The errors in the inner and outer diameters of the cladding in the control and safety rods were assumed to be 0.55 and 0.27 %, respectively, using the difference in the dimensions from those of the cladding in the fuel rod. On the other hand, the errors in the inner and outer diameters of the cladding in the fuel rod were 0.03 and 0.05 %, respectively, as mentioned above. It is considered that both 0.55 and 0.27 % as the relative errors in the inner and outer diameters of the cladding in the control and safety rods are conservative assumption.

The difference in the averaged bias among the minimum, standard, and intermediate cores for the error in the inner diameter of the cladding in the control and safety rods is more than three times its σ. The difference in the averaged bias among the minimum, standard, and intermediate cores for the error in the outer diameter of the cladding in the control and safety rods is also more than three times its σ.

It is confirmed for the errors in both the inner and outer diameter that the averaged biases tend to become larger as the number of fuel rods loaded in the core decreases. In the minimum core, where the minimum number of fuel rods were loaded, all fuel followers were being fully inserted. Thus, it is considered for the minimum core that the errors in both the inner and outer diameter of the stainless-steel cladding behaving as thermal neutron absorber like the cladding in the fuel rod affect k_{eff} more than those for the standard and intermediate cores.

Diameter and height of natural boron carbide

For the natural boron carbide absorber in the control and safety rods, its diameter and height in the present detailed models were compared with the dimensional inspection records at the renewal of several control rods in 1995. There were no differences in values of the diameter and height of the absorber between the present model and the inspection records in 1995. In addition, it was confirmed that there were not any variations of multi-point measurement values for the diameter and height in the inspection records in 1995. For this reason, the errors in the diameter and height of the natural boron carbide absorber in the control and safety rods were assumed not to be taken into account.

Aggregated uncertainty in k_{eff}

The aggregated uncertainties in k_{eff} propagated from the errors in the geometry data of the control and safety rods are in the range of 0.0003 to 0.0007 Δk_{eff}. The largest contribution to the uncertainties in k_{eff} excepting the minimum core is the error in the height of the uranium-zirconium hydride in the control and safety rods. For the minimum core, the largest contribution to the uncertainties in k_{eff} is the error in the inner diameter of the cladding in the control and safety rods.

6.1.3 Adjustable and fast transient rods

Diameter of enriched boron carbide

The dimensions of the adjustable and fast transient rods were confirmed by design drawings since the dimensional inspection records at the construction in 1973 are not found at present. The adjustable and fast transient rods were renewed in 1993 and 1995, respectively, of which dimension inspection records are available.

For the enriched boron carbide absorber in the adjustable and fast transient rods, the diameter in the present detailed models was compared with the dimensional inspection records at the renewal in 1993 and 1995. The measured diameters of the enriched boron carbide absorber shown in the dimensional inspection records were maximally 1.38 % smaller than those of the present detailed models. Thus, the error in the diameters of the enriched boron carbide absorber in the adjustable and fast transient rods was estimated using the 1.38 % smaller dimensions of the diameters.

The difference in the averaged bias among the minimum, standard, and intermediate cores is within 0.75 times its σ. It is confirmed that the uncertainties in k_{eff} propagated from the error in the diameter of the enriched boron carbide absorber in the adjustable and fast transient rods are negligibly small for all cores.

Height of enriched boron carbide

The height of the enriched boron carbide absorber in the adjustable and fast transient rods in the present detailed models was compared with the dimensional inspection records at the renewal in 1993 and 1995, respectively. The inspection records in 1993 and 1995 showed ±0.02 cm (0.05% in relative) and ±0.01 cm (0.01% in relative) of errors in the height of the enriched boron carbide absorber for the adjustable and fast transient rods, respectively. Thus, the errors in the height of the enriched boron carbide absorber were estimated by assuming that the same errors existed in the present detailed models.

The difference in the averaged bias among the minimum, standard, and intermediate cores is within 0.74 times its σ. It is confirmed that the uncertainties in k_{eff} propagated from the error in the height of the enriched boron carbide absorber in the adjustable and fast transient rods are negligibly small for all cores.

Inner and outer diameter of cladding in adjustable and fast transient rods

For the cladding in the adjustable and fast transient rods, the inner and outer diameters of the present detailed models were also compared with dimensional inspection records at the renewal in 1993 and 1995. There was no difference in values of the inner diameters between the present detailed models and the inspection records. For this reason, the error in the inner diameters of the cladding in the adjustable and fast transient rods was assumed not to be taken into account. On the other hand, differences in the outer diameters between the present detailed models and the inspection records in 1993 and 1995 were confirmed as maximally 0.26 %. Thus, the relative error in the outer diameter of the claddings in the adjustable and fast transient rods was assumed to be 0.26 %.

The difference in the averaged bias among the minimum, standard, and intermediate cores for the error in the outer diameter of the claddings in the adjustable and fast transient rods is within 0.23 times its σ. It is confirmed that the uncertainties in k_{eff} propagated from the error in the outer diameter of the cladding in the adjustable and fast transient rods are negligibly small for all cores.

Aggregated uncertainty in k_{eff}

The aggregated uncertainties in k_{eff} propagated from the errors in the geometry data of the adjustable and fast transient rods are negligibly small for all cores. The adjustable and fast transient rods were being fully withdrawn for the standard and intermediate cores. For the minimum core, the adjustable transient rod was being inserted up to 15 % of full stroke whilst the fast transient rods were being fully withdrawn. In those cases, it is considered that the errors in the geometry data of the adjustable and fast transient rods may not significantly affect the uncertainties in k_{eff}. The effect of the transient rod positions on the uncertainties in k_{eff} is discussed in Appendix-1.

6.1.4 Grid plate

Hexagonal lattice pitch of grid plate

The relative error in the hexagonal lattice pitch of the top/bottom grid plates was evaluated as 0.07 % using the dimensional inspection records at the construction in 1973.

The difference in the averaged bias among the minimum, standard, and intermediate cores is within 1.46 times its σ. It is confirmed that the uncertainties in k_{eff} propagated from the error in the lattice pitch for the minimum core in which the minimum number of fuel rods is loaded is slightly smaller than the standard and intermediate cores.

Replacement of grid plates with water

The errors in the thickness of the grid plates, and in the diameter of the holes for the loading the fuel rods were confirmed in the dimensional inspection records at the construction in 1973. It is considered that the effects of those errors may be small since the grid plates are made from aluminum alloy and installed far away from the core midplane. Thus, the uncertainties in k_{eff} propagated from the errors in the dimensions of the grid plates other than the lattice pitch were evaluated conservatively by the replacement of the whole grid plates with water.

The difference in the averaged bias among the minimum, standard, and intermediate cores is within 0.78 times its σ. It is confirmed that the uncertainties in k_{eff} propagated from the replacement are negligibly small for the minimum and intermediate cores. It is also confirmed that the uncertainty in k_{eff} propagated from the replacement is quite small for the standard core.

Aggregated uncertainty in k_{eff}

The aggregated uncertainties in k_{eff} propagated from the errors in the geometry data of the grid plates are in the range of 0.0001 to 0.0002 Δk_{eff}. For all cores, the largest contribution to the uncertainties in k_{eff} is the errors in the lattice pitch, but they are quite small.

6.1.5 Experimental tube

Face-to-face distance and thickness of hexagonal experimental tube

The experimental tube is composed of two sorts of shapes as mentioned in Sec. 2.6. The relative errors in the face-to-face distance and thickness of the hexagonal experimental tube were evaluated as 0.18 and 0.78 %, respectively, using the dimensional inspection records at the construction in 1973.

The differences in the averaged bias among the minimum, standard, and intermediate cores for the errors in the face-to-face distance and thickness of the hexagonal experimental tube are 0.51 and 0.27 times their σ's, respectively. It is confirmed that there is almost no difference in the uncertainties in k_{eff} from the error in the face-to-face distance of the hexagonal experimental tube among the minimum, standard, and intermediate cores. It is also confirmed that the uncertainties in k_{eff} from the error in the thickness of the hexagonal experimental tube are negligibly small for all cores. It is considered that the former uncertainties become larger than the latter ones since the absolute error in the face-to-face distance is larger than that in the thickness.

Outer diameter and thickness of cylindrical experimental tube

The relative errors in the outer diameter and thickness of the cylindrical experimental tube were evaluated as 0.11 and 0.78 %, respectively, using the dimensional inspection records at the construction in 1973.

The differences in the averaged bias among the minimum, standard, and intermediate cores for the errors both in the outer diameter and thickness of the cylindrical experimental tube are 0.75 times their σ's. It is confirmed that the uncertainties in k_{eff} propagated from the errors both in the outer diameter and thickness of the cylindrical experimental tube are negligibly small for all cores. The cylindrical experimental tube was being installed at the horizontal center of the core, but vertically far away from the core. Thus, it is considered that the errors in the dimensions of the cylindrical experimental tube less affect k_{eff}.

Aggregated uncertainty in k_{eff}

There is almost no difference in the aggregated uncertainties in k_{eff} propagated from the errors in the geometry data of the experimental tubes among the minimum, standard, and intermediate cores. The aggregated uncertainties are 0.0003 Δk_{eff} for all cores. There is no contribution to the uncertainties in k_{eff} from the errors in the geometry data excepting the face-to-face distance of the hexagonal experimental tube for all cores.

For reference, evaluated results of the uncertainties in k_{eff} from the replacement of the experimental tube with water are shown in Appendix-2.

6.1.6 Shroud

The errors in the dimensions of the shroud were confirmed in the dimensional inspection records at the construction in 1973. but it is considered that the effects of those errors may be small since the shroud is made from aluminum alloy and installed far away from the core. Thus, the uncertainties in k_{eff} propagated from the errors in the dimensions of the shroud were evaluated conservatively by the replacement of the whole shroud with water.

The difference in the averaged bias among the minimum, standard, and intermediate cores is within 1.20 times its σ. It is confirmed that the uncertainties in k_{eff} propagated from the replacement are negligibly small for all cores.

6.1.7 Guide tube for transient rod

The dimensions of the guide tubes for transient rods were confirmed by design drawings since the dimensional inspection records at the construction in 1973 are not found at present. It is considered that the effects of the errors in the dimensions of the guide tubes may be small since those are installed far away from the core. Thus, the uncertainties in k_{eff} propagated from the errors in the dimensions of the guide tubes were evaluated conservatively by the replacement of all guide tubes with water like the evaluation for the shroud.

The difference in the averaged bias among the minimum, standard, and intermediate cores is within 0.61 times its σ. It is confirmed that the uncertainties in k_{eff} propagated from the replacement are negligibly small for all cores.

6.1.8 Summary for geometry data

The aggregated uncertainties in k_{eff} propagated from the errors in the geometry data are summarized in Table 6.1.8.1. The aggregated uncertainties are in the range of 0.0017 to 0.0018 Δk_{eff}.

Figure 6.1.8.1 shows the contribution of the geometry data to the uncertainties in k_{eff}. As shown in Fig. 6.1.8.1, it is confirmed that 80 to 91 % of the aggregated uncertainties are owing to the errors in the geometry data of the fuel rod. Figure 6.1.8.2 shows the contribution of the geometry data in the fuel rod to the uncertainties in k_{eff}. As shown in Fig. 6.1.8.2, it is confirmed that the error in the outer diameter of the cladding in the fuel rod contributes to 58 to 60 % of the aggregated uncertainties owing to the error in the fuel rod.

Table 6.1.8.1 Aggregated uncertainties in k_{eff} propagated from the errors in the geometry data.

Source of uncertainty	Core	Uncertainty in k_{eff} (Δk_{eff})
Aggregation of uncertainties in geometry data	Minimum	0.0018
	Standard	0.0017
	Intermediate	0.0018

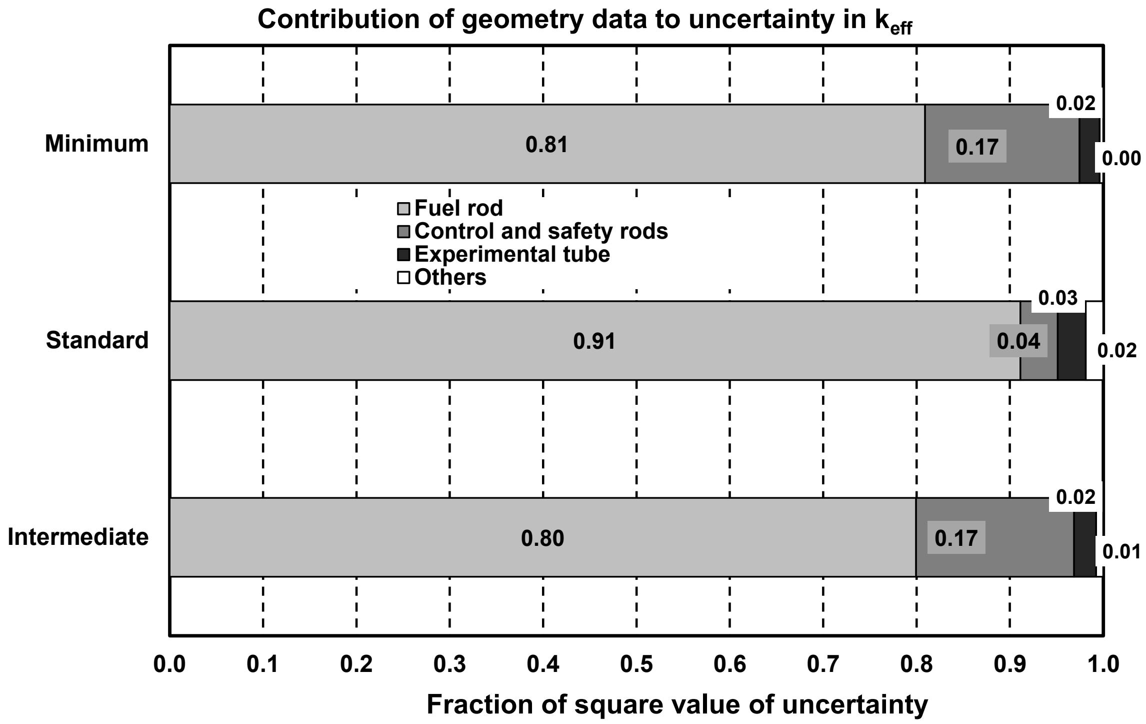

Fig. 6.1.8.1 Contribution of the geometry data to the uncertainty in k_{eff}.

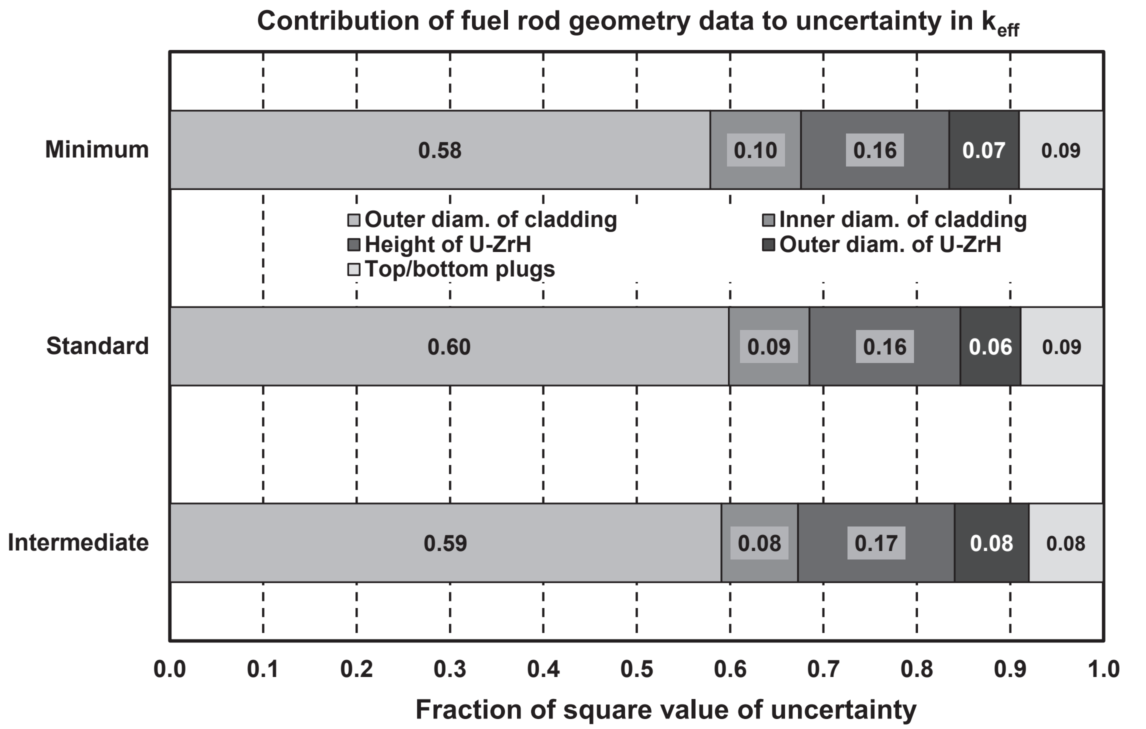

Fig. 6.1.8.2 Contribution of the geometry data in the fuel rod
to the uncertainty in k_{eff}.

6.2 Uncertainties from errors in material data

The evaluated results of the uncertainties in k_{eff} propagated from the errors in the material data are summarized in Table 6.2. For each item listed in Table 6.2, details are described below.

Table 6.2 Summary of uncertainties in k_{eff} propagated from the errors in the material data.

Item	Source of uncertainty	Core	Averaged bias: B_{av} ($\Delta k_{eff} \pm 1\sigma$)	Max. difference in B_{av}: D	D/σ	Uncertainty in k_{eff} (Δk_{eff})	Aggregated uncertainty for item (Δk_{eff})
U-ZrH in fuel, control, and safety rods	0.41% of U-ZrH volume: ± 0.024 ×10^4 (cm^3)	Minimum	±0.00169 ± 0.00007	0.00005	0.72	0.0017	Minimum: 0.0018 Standard: 0.0018 Intermediate: 0.0017
		Standard	±0.00168 ± 0.00007			0.0017	
		Intermediate	±0.00164 ± 0.00007			0.0016	
	1.51% of H/Zr atomic number ratio: ± 0.02	Minimum	±0.00042 ± 0.00007	0.00008	1.11	0.0004	
		Standard	±0.00035 ± 0.00007			0.0004	
		Intermediate	±0.00043 ± 0.00007			0.0004	
	0.55% of U-235 enrichment: ± 0.11 (wt%)	Minimum	±0.00020 ± 0.00007	0.00007	0.97	0.0002	
		Standard	±0.00021 ± 0.00007			0.0002	
		Intermediate	±0.00027 ± 0.00007			0.0003	
	Taking U-234 and U-236 into account as uranium composition	Minimum	-0.00021 ± 0.00007	0.00013	1.78	0.0002	
		Standard	-0.00032 ± 0.00007			0.0003	
		Intermediate	-0.00019 ± 0.00007			0.0002	
Zr rod in fuel, control, and safety rods	0.46% of Zr density: ± 0.03 (g/cm^3)	Minimum	±0.00006 ± 0.00007	0.00003	0.45	negligible	-
		Standard	±0.00002 ± 0.00007			negligible	
		Intermediate	±0.00003 ± 0.00007			negligible	
Stainless-steel in fuel, control, safety rods, and guide tube for transient rod	0.88% of stainless-steel density: ± 0.07 (g/cm3)	Minimum	±0.00047 ± 0.00007	0.00008	1.11	0.0005	Minimum: 0.0005 Standard: 0.0005 Intermediate: 0.0006
		Standard	±0.00045 ± 0.00007			0.0005	
		Intermediate	±0.00053 ± 0.00007			0.0005	
	Replacement of stainlees-steel composition in fuel rod with standard value	Minimum	-0.00012 ± 0.00007	0.00010	1.34	0.0001	
		Standard	-0.00021 ± 0.00007			0.0002	
		Intermediate	-0.00013 ± 0.00007			0.0001	
Mo disc in fuel rod	0.78% of Mo density: ± 0.08 (g/cm^3)	Minimum	±0.00002 ± 0.00007	0.00003	0.38	negligible	-
		Standard	±0.00005 ± 0.00007			negligible	
		Intermediate	±0.00002 ± 0.00007			negligible	
Axial graphite reflector in fuel rod	7.51% of graphite density: ± 0.13 (g/cm^3)	Minimum	±0.00092 ± 0.00007	0.00007	0.97	0.0009	Minimum: 0.0009 Standard: 0.0010 Intermediate: 0.0010
		Standard	±0.00098 ± 0.00007			0.0010	
		Intermediate	±0.00099 ± 0.00007			0.0010	
	Taking B-10 and B-11 into account as impurity	Minimum	+0.00008 ± 0.00007	0.00017	2.33	0.0001	
		Standard	-0.00008 ± 0.00007			0.0001	
		Intermediate	+0.00009 ± 0.00007			0.0001	
Al alloy in control, safety, transient rods, and other core structures	Replacement of aluminum alloy compositions with aluminum-27 only	Minimum	+0.00026 ± 0.00007	0.00003	0.45	0.0003	-
		Standard	+0.00025 ± 0.00007			0.0003	
		Intermediate	+0.00029 ± 0.00007			0.0003	

Table 6.2 (contd.) Summary of uncertainties in k_{eff} propagated from the errors in the material data.

Item	Source of uncertainty	Core	Averaged bias: B_{av} ($\Delta k_{eff} \pm 1\sigma$)	Max. difference in B_{av}: D	D/σ	Uncertainty in k_{eff} (Δk_{eff})	Aggregated uncertainty for item (Δk_{eff})
Natural B_4C absorber in control and safety rods	0.23% of natural B4C density: ± 0.0059 (g/cm^3)	Minimum	±0.00001 ± 0.00007	0.00006	0.88	negligible	Minimum: negligible Standard: 0.0001 Intermediate: negligible
		Standard	±0.00008 ± 0.00007			0.0001	
		Intermediate	±0.00002 ± 0.00007			negligible	
	0.13% of B content of natural B4C: ± 0.103 (wt%)	Minimum	±0.00004 ± 0.00007	0.00004	0.52	negligible	
		Standard	±0.00003 ± 0.00007			negligible	
		Intermediate	±0.00000 ± 0.00007			negligible	
Enriched B_4C absorber in transient rods	1.49% of enriched B4C density: ± 0.0343 (g/cm^3)	Minimum	±0.00001 ± 0.00007	0.00001	0.09	negligible	Minimum: negligible Standard: negligible Intermediate: negligible
		Standard	±0.00001 ± 0.00007			negligible	
		Intermediate	±0.00002 ± 0.00007			negligible	
	0.61% of B content of enriched B4C: ± 0.4694 (wt%)	Minimum	±0.00004 ± 0.00007	0.00004	0.55	negligible	
		Standard	±0.00005 ± 0.00007			negligible	
		Intermediate	±0.00001 ± 0.00007			negligible	
	0.51% of B-10 enrichment: ± 0.47 (wt%)	Minimum	±0.00002 ± 0.00007	0.00002	0.22	negligible	
		Standard	±0.00001 ± 0.00007			negligible	
		Intermediate	±0.00001 ± 0.00007			negligible	

6.2.1 Uranium-zirconium hydride in fuel, control, and safety rods

Total volume of uranium-zirconium hydride

The error in the total volume of the uranium-zirconium hydride in the core propagates to that of the density of the uranium-zirconium hydride. The relative error in the volume was evaluated as 0.41 % using both the design drawings and dimensional inspection records at the construction in 1973.

The difference in the averaged bias among the minimum, standard, and intermediate cores is within 0.72 times its σ. It is confirmed that the uncertainties in k_{eff} propagated from the error in the total volume of the uranium-zirconium hydride for the minimum, standard, and intermediate cores are of comparable magnitude.

Atomic number ratio of hydrogen to zirconium

The error in the atomic number ratio of hydrogen to zirconium propagates to that of the atomic number density of zirconium in the uranium-zirconium hydride. The relative error in the ratio was evaluated as 1.51 % using the material inspection records at the construction in 1973.

The difference in the averaged bias among the minimum, standard, and intermediate cores is within 1.11 times its σ. It is confirmed that there is almost no difference in the uncertainties in k_{eff} propagated from the error in the atomic number ratio of hydrogen to zirconium among the minimum, standard, and intermediate cores.

Uranium-235 enrichment

The error in the uranium-235 enrichment propagates to those of the atomic number densities of the uranium nuclides in the uranium-zirconium hydride. The relative error in the enrichment was evaluated as 0.55 % using the material inspection records at the construction in 1973.

The difference in the averaged bias among the minimum, standard, and intermediate cores is within 0.97 times its σ. It is confirmed that the uncertainties in k_{eff} propagated from the error in the uranium-235 enrichment for the minimum, standard, and intermediate cores are of comparable magnitude.

Effect of uranium-234 and uranium-236

The material inspection records at the construction in 1973 on two heats of the uranium metal supplied by AI showed that the uranium recovered by fuel reprocessing was used due to the presence of uranium-236. Thus, the effects of the uranium nuclides other than uranium-235 and uranium-238 were evaluated by using the composition of the AI J-04 and AI J-06 heats. The atomic number densities of the uranium including uranium-234 and uranium-236 are shown in Table 6.2.1.1.

Table 6.2.1.1 Atomic number densities of nuclides in the uranium including uranium-234 and uranium-236 based on the AI heats.

Nuclide	Atomic Number Density (1/barn cm)
U-234	1.8776×10^{-6}
U-235	3.6561×10^{-4}
U-236	2.5004×10^{-6}
U-238	1.4444×10^{-3}

The difference in the averaged bias among the minimum, standard, and intermediate cores is within 1.78 times its σ. It is confirmed for all cores that the negative reactivity effect is brought by taking uranium-234 and uranium-236 into account. It is also confirmed that the absolute value of the averaged bias for the standard core in which the largest amount of the uranium-zirconium hydride is loaded is slightly larger than those for the minimum and intermediate cores, but the uncertainty in k_{eff} propagated from taking uranium-234 and uranium-236 into account for the minimum, standard, and intermediate cores are of comparable magnitude.

Aggregated uncertainty in k_{eff}

The aggregated uncertainties are in the range of 0.0017 to 0.0018 Δk_{eff}. The largest contribution to the aggregated uncertainties is the error in the total volume of the uranium-zirconium hydride. The second largest contribution to the aggregated uncertainties is the error in the atomic number ratio of hydrogen to zirconium, but it is smaller than the contribution of the error in the total volume of the uranium-zirconium hydride.

For reference, evaluated results of the uncertainties in k_{eff} propagated from the ignoring the impurities in the uranium-zirconium hydride are shown in Appendix-3.

6.2.2 Zirconium rod in fuel, control, and safety rods

The relative error in the zirconium density was assumed to be 0.46 % in comparison with the other TRIGA benchmarks, ICT-013 [12] and ICT-003 [13]. The difference in the averaged bias among the minimum, standard, and intermediate cores is within 0.45 times its σ. It is confirmed that the uncertainties in k_{eff} propagated from the error in the zirconium density are negligibly small for all cores.

For reference, evaluated results of the uncertainties in k_{eff} propagated from the ignoring the impurities in the zirconium rod are shown in Appendix-3.

6.2.3 Stainless-steel in fuel, control, and safety rods, and in guide tube for transient rod

Density of stainless-steel

The relative error in the density of the stainless-steel was assumed to be 0.88 % in comparison with the other TRIGA benchmarks, ICT-013 [12] and ICT-003 [13]. The difference in the averaged bias among the minimum, standard, and intermediate cores is within 1.11 times its σ. It is confirmed that there is almost no difference in the uncertainties in k_{eff} propagated from the error in the density of the stainless-steel among the minimum, standard, and intermediate cores.

Composition of stainless-steel

The compositions of the stainless-steel in the fuel rods were evaluated by using the material inspection records at the construction in 1973, on the other hand those in the control and safety rods, and in the guide tubes for the transient rods were based on the standard values because of lack of the inspection records. It is considered that the difference in the compositions of the stainless-steel of the fuel rods affects k_{eff}'s more than those of the control and safety rods, and of the guide tubes since the total amount of the stainless-steel of the fuel rods is quite larger than the others. Thus, the uncertainties in k_{eff} from the difference in the compositions of the stainless-steel were evaluated by the replacement of the compositions of the stainless-steel in the fuel rods with those based on the standard values used in the control and safety rods, and in the guide tubes.

The difference in the averaged bias among the minimum, standard, and intermediate cores is within 1.34 times its σ. It is confirmed for all cores that the negative reactivity effect is brought by the replacement. It is also confirmed that the absolute value of the averaged bias for the standard core in which the largest number of fuel rods is loaded is slightly larger than those for the minimum and intermediate cores, but the uncertainty in k_{eff} propagated from the replacement for the minimum, standard, and intermediate cores are of comparable magnitude.

The total fraction of the elements of chromium, manganese, nickel, and iron is more than 98% of the atomic number density in the stainless-steel. The cross sections of (n, γ) capture reactions at 0.0253 eV (2,200 m/s) for the elements of chromium, manganese, and nickel are larger than that of the element of iron. For example. the capture cross sections at 0.0253 eV are evaluated in the JENDL-5 library [7] as 3.14, 13.27, 4.09, and 2.57 barns for the elements of chromium, manganese, nickel, and iron, respectively. The fraction of those elements other than iron in the stainless-steel based on the standard compositions is larger than those in the stainless-steel in the fuel rods, of which compositions are confirmed by the material inspection records. The reason for the negative reactivity effect is that the replacement with the standard compositions brings slightly larger cross sections for the thermal neutron capture of the stainless-steel more than those by the compositions in the fuel rods.

Aggregated uncertainty in k_{eff}

The aggregated uncertainties are in the range of 0.0005 to 0.0006 Δk_{eff}. The largest contribution to the uncertainties is the error in the density of the stainless-steel.

6.2.4 Molybdenum disc in fuel rod

The relative error in the molybdenum density was assumed to be 0.78 % in comparison with the other TRIGA benchmarks, ICT-013 [12] and ICT-003 [13]. The difference in the averaged bias among the minimum, standard, and intermediate cores is within 0.38 times its σ. It is confirmed that the uncertainties in k_{eff} propagated from the error in the molybdenum density are negligibly small for all cores.

For reference, evaluated results of the uncertainties in k_{eff} propagated from ignoring the impurities in the molybdenum disc are shown in Appendix-3.

6.2.5 Axial graphite reflector in fuel rod

Density of graphite

The relative error in the graphite density was conservatively assumed to be 7.51 % by the difference between the other TRIGA benchmarks, ICT-013 [12] and ICT-003 [13]. The difference in the averaged bias among the minimum, standard, and intermediate cores is within 0.97 times its σ. It is confirmed that the uncertainties in k_{eff} propagated from the error in the density of the graphite for the minimum, standard, and intermediate cores are of comparable magnitude.

Effect of impurities

The material inspection records at the construction in 1973 showed that the boron content in the graphite was smaller than 0.5 ppm of the lower limit of detection. Thus, the effects of the boron nuclides were evaluated by using the value of the lower limit. The atomic number densities of boron-10 and boron-11 are shown in Table 6.2.5.1.

Table 6.2.5.1 Atomic number densities of nuclides of boron in the axial graphite reflectors.

Nuclide	Atomic Number Density (1/barn cm)
B-10	9.5885×10^{-9}
B-11	3.8595×10^{-8}

The difference in the averaged bias among the minimum, standard, and intermediate cores is within 2.33 times its σ. It is confirmed that the uncertainties in k_{eff} propagated from the consideration of the boron nuclides are quite small for all cores.

Aggregated uncertainty in k_{eff}

The aggregated uncertainties are in the range of 0.0009 to 0.0010 Δk_{eff}, same as the uncertainties in k_{eff} propagated from the error in the density of the graphite.

6.2.6 Aluminum alloy in control, safety, and transient rods, and in other core structures

The compositions of the aluminum alloy were based on the standard values because of lack of the material inspection records at the construction in 1973. The nuclide of aluminum-27 is only considered in the other TRIGA benchmarks, ICT-013 [12] and ICT-003 [13]. Thus, the uncertainties in k_{eff} propagated from the difference in the compositions of the aluminum alloy were evaluated by the replacement of the compositions of the present models with the nuclide of aluminum-27 only.

The difference in the averaged bias among the minimum, standard, and intermediate cores is within 0.45 times its σ. It is confirmed for all cores that the positive reactivity effect is brought by the replacement. It is also confirmed that there is almost no difference in the uncertainties in k_{eff} propagated from the replacement of the aluminum alloy compositions among the minimum, standard, and intermediate cores.

The cross sections of (n, γ) capture reactions at 0.0253 eV (2,200 m/s) for the elements of titanium, chromium, manganese, iron, copper, and zinc are larger than that of the element of aluminum. For example, the capture cross sections at 0.0253 eV for the elements of titanium, chromium, manganese, iron, copper, and zinc are evaluated as 6.41, 3.14, 13.27, 2.57, 3.77, and 1.06 barns, respectively, in the JENDL-5 library [7]. On the other hand, the capture cross section for the element of aluminum is evaluated as 0.23 barns in the same library. The averaged capture cross section weighted by the atomic number densities for the aluminum alloy in the present models is calculated to be 0.26 barns. It is slightly larger than the value of the cross section for the element of aluminum only. The reason for the positive reactivity effect is that the replacement with the composition involving only aluminum-27 brings smaller cross sections for the thermal neutron capture of the aluminum alloy more than those by the composition in the present models.

6.2.7 Natural boron carbide absorber in control and safety rods

Density of natural boron carbide

The relative error in the density of the natural boron carbide was estimated to be 0.23 % using the material inspection records at the renewal of the control and safety rods in 1995. The difference in the averaged bias among the minimum, standard, and intermediate cores is within 0.88 times its σ. It is confirmed that the averaged bias for the standard core in which the largest amount of the natural boron carbide absorber in the control rods is inserted into the core is slightly larger than those for the minimum and intermediate cores, but the uncertainty in k_{eff} propagated from the error in the density of the natural boron carbide is quite small for the standard core. It is also confirmed that the uncertainties in k_{eff} propagated from the error in the density of the natural boron carbide are negligibly small for the minimum and intermediate cores.

Boron content in natural boron carbide

The relative error in the boron content in the natural boron carbide was also estimated to be 0.13 % using the material inspection records at the renewal of the control and safety rods in 1995. The difference in the averaged bias among the minimum, standard, and intermediate cores is within 0.52 times its σ. It is confirmed that the uncertainties in k_{eff} the error in the boron content are negligibly small for all cores.

Aggregated uncertainty in k_{eff}

The aggregated uncertainties in k_{eff} are same as the uncertainties propagated from the error in the density of the natural boron carbide since the uncertainties propagated from the error in the boron content are negligibly small for all cores.

6.2.8 Enriched boron carbide absorber in transient rod

Density of enriched boron carbide

The relative error in the density of the enriched boron carbide was estimated to be 1.49 % using the material inspection records at the renewal of transient rods in 1992 and 1995. The difference in the averaged bias among the minimum, standard, and intermediate cores is within 0.09 times its σ. It is confirmed that the uncertainties in k_{eff} propagated from the error in the density of the enriched boron carbide are negligibly small for all cores.

Boron content in enriched boron carbide

The relative error in the boron content in the enriched boron carbide was also estimated to be 0.61 % using the material inspection records at the renewal of transient rods in 1992 and 1995. The difference in the averaged bias among the minimum, standard, and intermediate cores is within 0.55 times its σ. It is confirmed that the uncertainties in k_{eff} propagated from the error in the boron content are negligibly small for all cores.

Boron-10 enrichment of enriched boron carbide

The relative error in the boron-10 enrichment of the enriched boron carbide was also estimated to be 0.51 % using the material inspection records at the renewal of transient rods in 1992 and 1995. The difference in the averaged bias among the minimum, standard, and intermediate cores is within 0.22 times its σ. It is confirmed that the uncertainties in k_{eff} propagated from the error in the boron-10 enrichment are negligibly small for all cores.

Aggregated uncertainty in k_{eff}

The aggregated uncertainties are negligibly small for all cores. This is considered to be due to the same reason as mentioned in Sec. 6.1.3. The effect of the transient rod positions on the uncertainties in k_{eff} is discussed in Appendix-1.

6.2.9 Summary for material data

The aggregated uncertainties in k_{eff} propagated from the errors in the material data are summarized in Table 6.2.9.1. The aggregated uncertainties are 0.0021 Δk_{eff} for all cores.

Figure 6.2.9.1 shows the contribution of the material data to the uncertainties in k_{eff}. As shown in Fig. 6.2.9.1, it is confirmed that 68 to 73% of the aggregated uncertainties are owing to the errors in the material data of the uranium-zirconium hydride.

Figure 6.2.9.2 shows the contribution of the material data of the uranium-zirconium hydride to the uncertainties in k_{eff}. As shown in Fig. 6.2.9.2, it is confirmed that the contribution of the error in the total volume of the uranium-zirconium hydride affecting its density becomes 90 to 91% of the aggregated uncertainties owing to the errors in the uranium-zirconium hydride.

Table 6.2.9.1 Aggregated uncertainties in k_{eff} propagated from the errors in the material data.

Source of uncertainty	Core	Uncertainty in k_{eff} (Δk_{eff})
Aggregation of uncertainties in material data	Minimum	0.0021
	Standard	0.0021
	Intermediate	0.0021

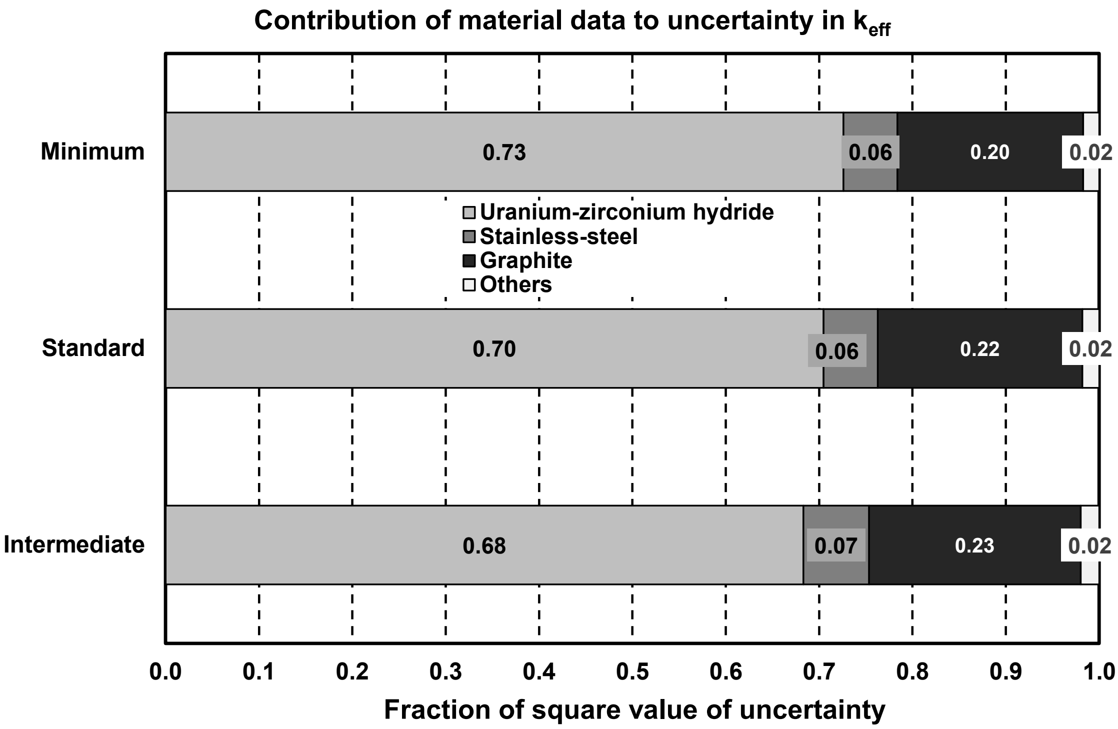

Fig. 6.2.9.1 Contribution of the material data to the uncertainty in k_{eff}.

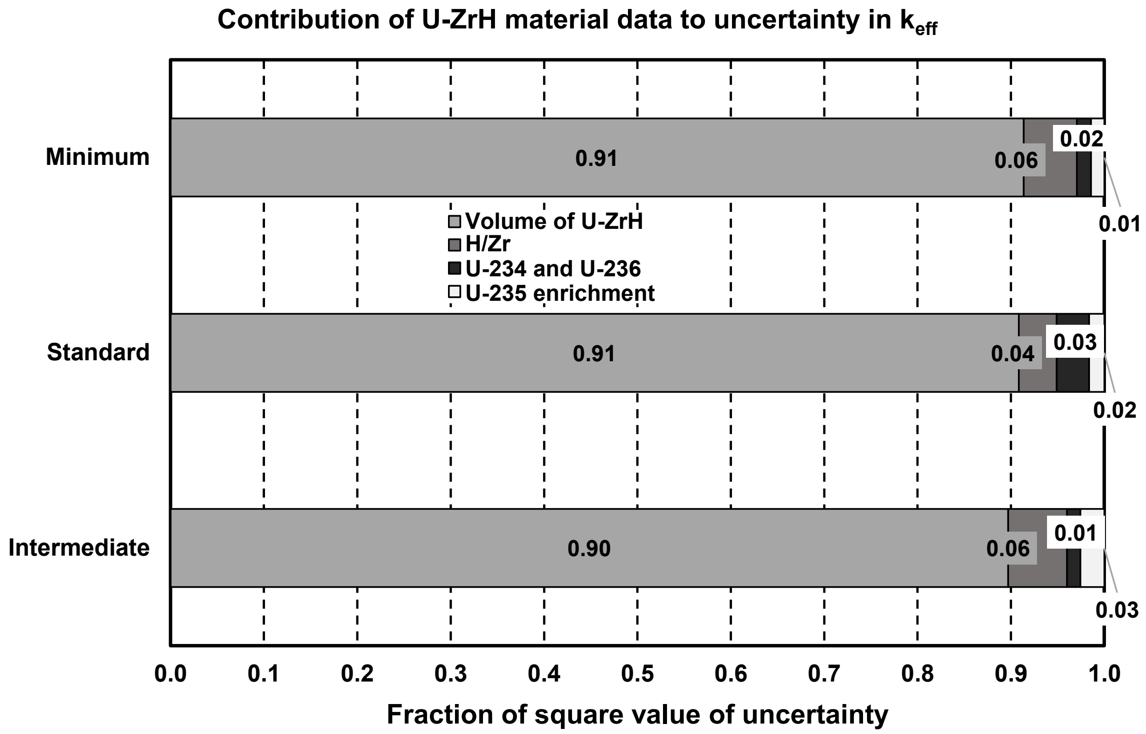

Fig. 6.2.9.2 Contribution of the material data of the uranium-zirconium hydride to the uncertainty in k_{eff}.

6.3 Uncertainties from errors in operation data

The evaluated results of the uncertainties in k_{eff} propagated from the errors in the operation data are summarized in Table 6.3. For each item listed in Table 6.3, details are described below.

Table 6.3 Summary of uncertainties in k_{eff} propagated from the errors in the operation data.

Source of uncertainty	Core	Averaged bias: B_{av} ($\Delta k_{eff} \pm 1\sigma$)	Max. difference in B_{av}: D	D/σ	Uncertainty in k_{eff} (Δk_{eff})
5 units of rod position: ± 0.24 (cm)	Minimum	±0.00029 ± 0.00007	0.00048	6.61	0.0003
	Standard	±0.00047 ± 0.00007			0.0005
	Intermediate	±0.00077 ± 0.00007			0.0008
Temperature changes: ± 5 (°C)	Minimum	±0.00066 ± 0.00007	0.00040	5.41	0.0007
	Standard	±0.00026 ± 0.00007			0.0003
	Intermediate	±0.00042 ± 0.00007			0.0004

6.3.1 Rod position for control, safety, and transient rods

The error in the absorber rod position was assumed to be 5 units (2.4 mm) conservatively by the maintenance standard. The difference in the averaged bias among the minimum, standard, and intermediate cores is more than three times of its σ. It is confirmed that the uncertainty in k_{eff} propagated from the error in the rod position for the representative intermediate cores is the largest one since all control rods were being inserted into the cores at the vicinity of the core midplane. It is also confirmed that the uncertainty in k_{eff} propagated from the error in the rod position for the minimum core is the smallest one since all control and safety rods were being fully withdrawn.

6.3.2 Temperature

The error in the temperature was assumed to be 5 °C, conservatively by the variation of the measured temperature in the operation records for the first startup in 1975. The difference in the averaged bias among the minimum, standard, and intermediate cores is more than three times of its σ. It is confirmed that the uncertainty in k_{eff} propagated from the error in the temperature tends to become larger as the number of fuel rods loaded in the core decreases.

It is considered that the neutron leakage along horizontal directions in the case of the smaller number of fuel rods loaded in the core is larger than that of the larger number of fuel rods since the smaller number of fuel rods may bring the larger horizontal geometrical buckling. In addition, it is considered that the neutron leakage from the core varies with both the changes in the water density, and the thermal neutron spectrum shift in the uranium-zirconium hydride and water, which are brought by temperature variation. For those reasons, it is considered that the larger uncertainty in k_{eff} is brought by the smaller number of fuel rods, i.e., larger horizontal geometrical buckling, which is sensitive to the changes in the neutron leakage.

6.3.3 Criticality judgement

The criticality judgement was done visually by NSRR operators with recorder chart of linear power channel detectors. In NSRR, the reactivity that the power increases by 25% in 5 minutes is evaluated to be 0.94 ¢ (= 0.000069 Δk_{eff})[*3]. It is considered that this degree of power variation can be easily found by the visual check of the operators. For this reason, the uncertainty in k_{eff} propagated from the criticality judgement is smaller than 0.00007 Δk_{eff}. Thus, the uncertainty in k_{eff} from the criticality judgement was assumed not to be taken into account.

6.3.4 Summary for operation data

The aggregated uncertainties in k_{eff} propagated from the errors in the operation data are summarized in Table 6.3.4.1. The aggregated uncertainties in k_{eff} are in the range of 0.0005 to 0.0009 Δk_{eff}.

Figure 6.3.4.1 shows the contribution of the operation data to the uncertainties in k_{eff}. As shown in Fig. 6.3.4.1, it is confirmed that the contribution of the error in the absorber rod position is 75 to 77 % of the aggregated uncertainties for the standard and intermediate cores. For the minimum core, the contribution of the error in the temperature is quite larger than the contribution of that in the rod positions and occupies 83 % of the aggregated uncertainties.

[*3] The value of effective delayed neutron fraction is set to be 0.0073 as shown in the literature [1)].

Table 6.3.4.1 Aggregated uncertainties in k_{eff} propagated from the errors in the operation data.

Source of uncertainty	Core	Uncertainty in k_{eff} (Δk_{eff})
Aggregation of uncertainties in operation data	Minimum	0.0007
	Standard	0.0005
	Intermediate	0.0009

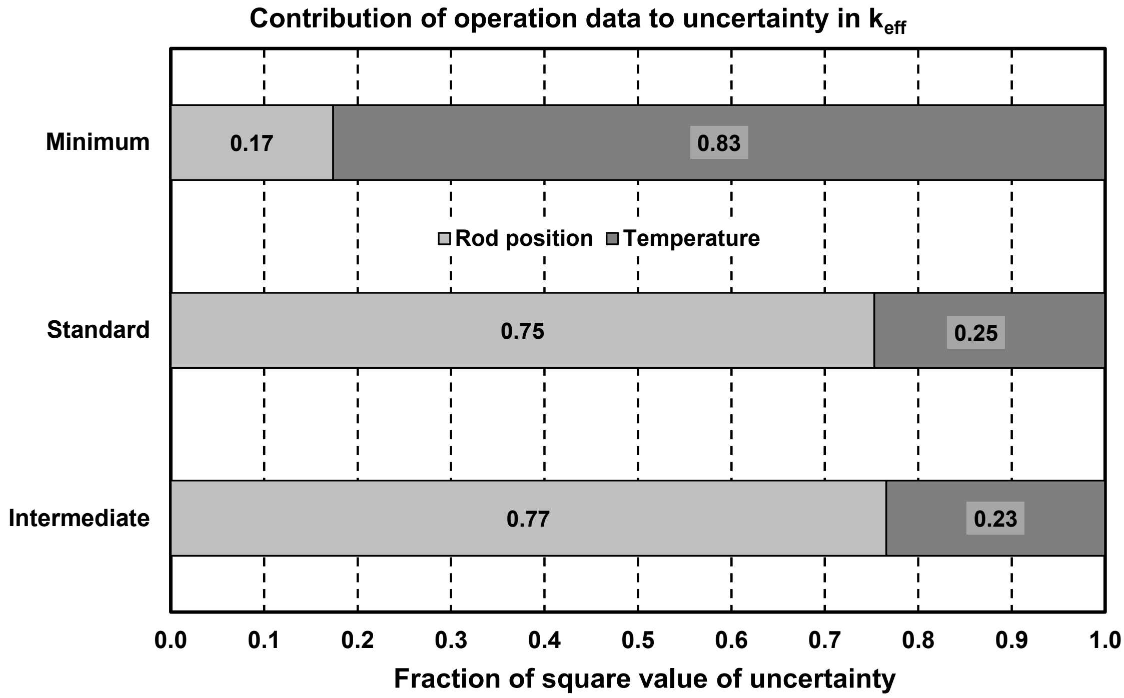

Fig. 6.3.4.1 Contribution of the operation data to the uncertainty in k_{eff}.

6.4 Overall uncertainties

As overall uncertainties in k_{eff}, the aggregated uncertainties in k_{eff} propagated from the errors in the geometry, material, and operation data are summarized in Table 6.4.1. The aggregated uncertainties in k_{eff} are evaluated to be in the range of 0.0027 to 0.0029 Δk_{eff}.

Figure 6.4.1 shows the contribution of the errors in the geometry, material, and operation data to the uncertainties in k_{eff}. As shown in Fig. 6.4.1, it is confirmed that the largest contribution to the uncertainties in k_{eff} is the errors in the material data. It is also confirmed that the second largest contribution is the errors in the geometry data.

Table 6.4.1 Aggregated uncertainties in k_{eff} propagated from the errors in the geometry, material, and operation data.

Source of uncertainty	Core	Uncertainty in k_{eff} (Δk_{eff})
Aggregation of uncertainties in geometry, material, and operation data	Minimum	0.0028
	Standard	0.0027
	Intermediate	0.0029

The evaluated overall uncertainties in k_{eff} are equivalent to about 40 ¢ [*4] as reactivity. It is shown in the literature [1] that the absorber rod worths were determined in the range of 162 to 225 ¢ for the individual rod (R1 to R6, S1, S2, TA, TB, and TC) of the standard core during the first startup in 1975. The uncertainty for the standard core is smaller than a quarter of those values of the absorber rod worths, thus it is considered that the evaluated overall uncertainty in k_{eff} may also be sufficiently applicable to the future analyses on the absorber rod worths.

In the cases of the other TRIGA benchmarks, ICT-003 [13] and ICT-013 [12], the overall uncertainties in k_{eff} are being evaluated to be 0.0056 and 0.0015 Δk_{eff}, respectively. The evaluated overall uncertainties in the present detailed models become about half the magnitude of that of ICT-003. On the other hand, the present evaluated uncertainties are about twice as large as that of ICT-013, but

[*4] The reactivity is obtained using the same value of effective delayed neutron fraction as described in the footnote *3.

it is suggested in the earlier studies [3,4] that an unknown bias might exist in the ICT-013 benchmark.

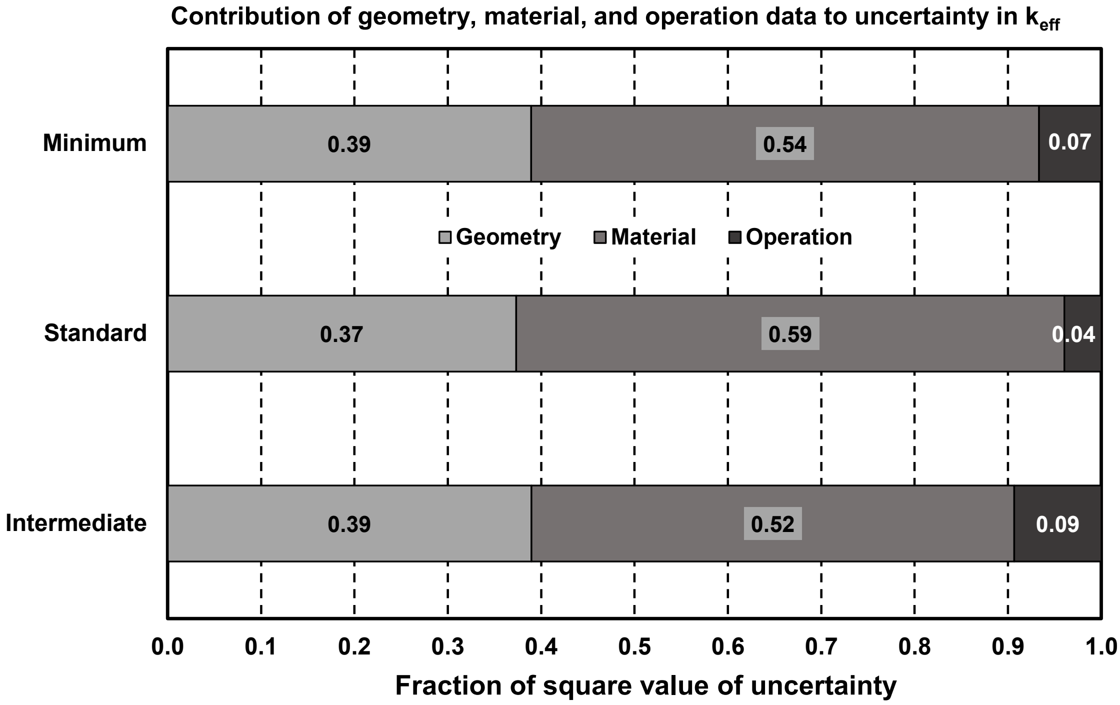

Fig. 6.4.1 Contribution of the geometry, material, and operation data to the uncertainty in k_{eff}.

From the results of the overall uncertainties in k_{eff} for the present detailed models mentioned above, it is concluded for the minimum, standard, and intermediate cores that the differences in the calculated k_{eff}'s by between JENDL-5 and JENDL-4.0, as confirmed in Tables 5.2.1, 5.2.2, and 5.2.3, are not significant in terms of the magnitude of the overall uncertainties in k_{eff} since the differences are within 2 times the overall uncertainties in k_{eff}. It is also concluded for the intermediate cores that the variations in the calculated k_{eff}'s, as shown in Fig. 5.2.1 and Fig. 5.2.2, are not significant in terms of the present overall uncertainties in k_{eff} since the variations are in the range of 0.30 to 0.45 times the overall uncertainties in k_{eff}.

7. Summary

The detailed models for the precise criticality analyses on the first startup cores of NSRR, i.e., the minimum, standard, and intermediate cores, were created for the purposes of deeper understandings of the safety inspection data on the absorber rod worths and improvement of the determination technique of the worth in NSRR. For the creation of detailed models as much as possible, the evaluation on model data was conducted using not only the published literature but also dimensional and material inspection records at the construction of NSRR in 1973, operation records during the first startup in 1975, and so on.

The uncertainties in k_{eff} propagated from the geometry, material, and operation data used in the present model were evaluated in detail by using the MVP version 3 code with the latest Japanese nuclear data library, JENDL-5, and the previous versions of JENDL. As a result, the overall uncertainties in k_{eff} for the present detailed models were evaluated to be in the range of 0.0027 to 0.0029 Δk_{eff}.

From the calculated results by using the MVP version 3 code, it is confirmed that the k_{eff}'s calculated by JENDL-5 were 0.36 to 0.57 % larger than those by JENDL-4.0, but the differences between them were within 2 times the overall uncertainties in k_{eff} for the present detailed models. In addition, it is confirmed for the intermediate cores that the variations in the calculated k_{eff}'s with the changes in the absorber rod position to attain delayed criticality by 'bank mode' were in the range of 0.30 to 0.45 times the overall uncertainties in k_{eff} for the present detailed models and there was no significancy in the variations.

It is considered that the present detailed models are expected to be utilized as the benchmark of k_{eff}'s for TRIGA-ACPR. Moreover, it is confirmed that the evaluated overall uncertainties were sufficiently smaller than the values of absorber rod worths determined in NSRR. Thus, it is also considered that the present models are applicable to future analyses on the absorber rod worths in NSRR.

Furthermore, the vertical positions of the control, safety, and transient rods were individually specified as 'symbolic parameters' [6)] in the MVP input data (refer to Appendix-4) for the analyses shown in this report. In the analyses, the positions of those absorber rods can be easily set like real operation in NSRR. It is considered that the present models implemented as the MVP input data are applicable to analyses prior to operations on the absorber rod worths with various rod positions. This function will be useful to examine further improvement of the determination technique of the absorber rod worths in NSRR.

Acknowledgements

The authors wish to express great thanks to Drs. T. Kugo and A. Endo, former Director Generals of the Nuclear Science Research Institute, for their encouragement to conduct the present work. Thanks are due Messrs. M. Yagi, Director of the Nuclear Facility Inspection Office, T. Kobayashi, General Manager of the NSRR Operation Section, M. Umeda, Deputy Director of the Department of Research Infrastructure Technology Development, and H. Murao, Director of the New Research Reactor Promotion Office, for their support to the work. The authors also greatly thank Dr. K. Suyama, Senior Principal Researcher of the Nuclear Safety Research Center, for his careful review of the manuscript and valuable comments on the work. The calculations using the MVP version 3 code, which are shown in this report, were executed with the supercomputer HPE SGI8600 in the Japan Atomic Energy Agency.

References

1) NSRR Operation Section and Reactivity Accident Laboratory, Start-up Tests of NSRR, JAERI-M 6791,1976, 268p [in Japanese].
2) General Atomics, TRIGA Nuclear Reactors, https://www.ga.com/triga/ (accessed 14th Jan. 2025).
3) Yanagisawa, H., Umeda, M., Motome, Y. and Murao, H., Nuclear Criticality Benchmark Analyses on TRIGA-type Reactor Systems by Using Continuous-energy Monte Carlo Code MVP with JENDL-5, JAEA-Technology 2022-030, 2023, 80p [in Japanese].
4) Yanagisawa, H., Umeda, M., Motome, Y. and Murao, H., Benchmark Analyses on Control Rod Worths of TRIGA Reactor Modeled in the ICSBEP Handbook Using Continuous-energy Monte Carlo Code MVP Version 3, Proc. of the 12th Intl. Conf. on Nuclear Criticality Safety (ICNC2023), Oct. 1-6, 2023, Sendai, Japan, JAEA-Conf 2024-001, P-19, Track 4, 2024 (CD-ROM).
5) Ise, T., Nakahara, Y., and Akimoto, M., Thermal Neutron Spectrum, Prompt Negative Temperature Coefficients, and Kinetics Parameters of the NSRR, JAERI-M 5730, 1974, 52p [in Japanese].
6) Nagaya, Y., Okumura, K., Sakurai, K., Mori, T., MVP/GMVP Version 3: General Purpose Monte Carlo Codes for Neutron and Photon Transport Calculations

Based on Continuous Energy and Multigroup Methods, JAEA-Data/Code 2016-018, 2017, 421p.
7) Iwamoto, O., Iwamoto, N., Kunieda, S., et al., Japanese evaluated nuclear data library version 5: JENDL-5, J. Nucl. Sci. Technol., vol.60, no.1, 2023, pp.1-60.
8) Shibata, K., Iwamoto, O., Nakagawa, T., et al., JENDL-4.0: A New Library for Nuclear Science and Engineering, J. Nucl. Sci. Technol., vol.48, no.1, 2011, pp.1-30.
9) Nuclear Data Centre, Japan Atomic Energy Agency, JENDL-4.0 Updated Files and JENDL-4.0 Plus Files, https://wwwndc.jaea.go.jp/jendl/j40/update/ (accessed 14th Jan. 2025).
10) Nuclear Energy Agency, Organization for Economic Co-operation and Development, International Handbook of Evaluated Criticality Safety Benchmark Experiments, NEA/NSC/DOC(95)03, May 2020.
11) National Astronomical Observatory of Japan, ed., Rika Nenpyo (Chronological Scientific Tables), Maruzen Publishing Co. Ltd., 2018, p.389 [in Japanese].
12) J. D. Bess, T. L. Maddock, M. A. Marshall, et al., Fresh-core Reload of the Neutron Radiography (NRAD) Reactor with Uranium(20)-Erbium-Zirconium-Hydride Fuel, IEU-COMP-THERM-013, NEA/NSC/DOC/(95)03/III, OECD/NEA, 2020, 1p.
13) R. Jeraj, M. Ravnik, et al., TRIGA Mark II Reactor: U(20) -Zirconium Hydride Fuel Rods in Water with Graphite Reflector, IEU-COMP-THERM-003, NEA/NSC/DOC/(95)03/III, OECD/NEA, 2020, 88p.
14) Japan Stainless Steel Association, ed., Sutenresu-ko Benran dai-3-han (Handbook for Stainless Steels, the 3rd ed.), The Nikkan Kogyo Shimbun Ltd., 1995, p.1428 [in Japanese].
15) American Society for Testing and Materials, Standard Specification for Seamless Ferric and Austenitic Alloy-steel Boiler, Superheater, and Heat-exchanger tubes, ASTM A213-66, 1969.
16) Aeronautical Material Specifications, Society of Automotive Engineers Inc., Steel Castings, Precision Investment, Corrosion and Heat Resistant 19.5Cr-10Ni (Low Carbon), AMS 5370, 1955.
17) Japan Light Metals Association, ed., Aruminiumu Gijutsu Benran (Handbook of Advanced Aluminum Technology), Kallos Publishing Co., Ltd., 1996, p.1276 [in Japanese].
18) American Society for Testing and Materials, Standard Specification for Aluminum and Aluminum-Alloy Drawn Seamless Tubes, ASTM B210-12, 2019.

19) National Astronomical Observatory of Japan, ed., Rika Nenpyo (Chronological Scientific Tables), Maruzen Publishing Co. Ltd., 2018, p.391 [in Japanese].
20) Fuketa, T., Ishijima, K., Tanzawa, S., et al., Analysis of Energy Deposition and Evaluation of Maximum Load of Irradiation Capsule for NSRR Experiment with Uranium-Zirconium Hydride Fuel, JAERI-Research 95-005, 1995, 53p [in Japanese].

Appendix-1 Effect of Transient Rod Positions on Uncertainties

The uncertainties in k_{eff} propagated from the errors in both the geometry data of the transient rods and the material data of the enriched boron carbide absorber in the transient rods were negligibly small for the minimum, standard, and intermediate cores, as described in Sec. 6.1.3 and Sec. 6.2.8, respectively. Those errors may not affect the uncertainties in k_{eff} because of the transient rods fully withdrawn or small amount of the insertion for those cores.

Hence, the effect of the transient rod positions on the uncertainties in k_{eff} was examined on the cores composed for the determination of absorber rod worths by the rod drop technique during the first startup in NSRR [1)]. Table A.1.1 lists the absorber rod positions of eleven sorts of cores (ID = tr1 to tr11) subjected to the present examination. Those cores were composed with various transient rod positions to confirm the operation power at delayed criticality before the absorber rod was dropped. The operation power at delayed criticality was in the range of 29 to 32 W. The number of fuel rods and their loaded pattern were the same as the standard core. The temperature of the cores was evaluated to be 23 ^{o}C by the operation records in 1975, which is the same as the standard core.

The results of the criticality analyses on those cores with the various transient rod positions are listed in Table A.1.2. In Table A.1.2, σ is the statistical error of Monte Carlo calculations. The differences in k_{eff} between JENDL-4.0 and JENDL-4.0u1 are within their σ's. The k_{eff}'s by JENDL-5 are 0.42 to 0.47 % larger than those by JENDL-4.0. The differences in k_{eff} between JENDL-5 and JENDL-4.0 are larger than three times their σ's, similar to the minimum, standard, and intermediate cores, as shown in Sec. 5.2.

As shown in Fig. A.1.1, the k_{eff} by JENDL-4.0, JENDL-4.0u1, and JENDL-5 varies with the transient rod positions in the range of 0.99743 to 1.00035, 0.99748 to 1.00037, and 1.00196 to 1.00502, respectively. The averaged values of k_{eff} by JENDL-4.0, JENDL-4.0u1, and JENDL-5 are 0.99932 ± 0.00104, 0.99937 ± 0.00095, and 1.00381 ± 0.00098, respectively. It is confirmed that the ranges of the above variations are larger than those for the intermediate cores shown in Sec. 5.2.

Table A.1.1 Critical cores with various transient rod positions.

Date and time	The number of fuel rods	ID	Rod position (unit) for R1-R6, S1-S2, and TA, up: full withdrawal and dn: full insertion for TB and TC											BANK av. (unit)	Safety rod	Transient rod	Remarks
			R1	R2	R3	R4	R5	R6	S1	S2	TA	TB	TC				
1975/07/03 20:02	149	a	218	211	216	211	209	213	899	897	895	up	up	213.0	All full withdrawal	All full withdrawal	Standard core
1975/07/07 17:35	149	tr1	905	106	104	103	103	102	587	588	589	up	up	237.2	All partial insertion	TA partial insertion	R1 worth measurement
1975/07/07 17:49	149	tr2	108	910	104	103	103	102	653	653	654	up	up	238.3	All partial insertion	TA partial insertion	R2 worth measurement
1975/07/07 18:02	149	tr3	108	106	907	103	103	102	664	664	665	up	up	238.2	All partial insertion	TA partial insertion	R3 worth measurement
1975/07/07 18:11	149	tr4	108	106	104	908	103	102	643	644	644	up	up	238.5	All partial insertion	TA partial insertion	R4 worth measurement
1975/07/07 18:24	149	tr5	108	106	104	103	900	102	657	657	658	up	up	237.2	All partial insertion	TA partial insertion	R5 worth measurement
1975/07/07 18:31	149	tr6	108	106	104	103	103	911	632	631	629	up	up	239.2	All partial insertion	TA partial insertion	R6 worth measurement
1975/07/07 19:07	149	tr7	906	106	104	103	103	102	672	672	894	dn	up	237.3	All partial insertion	TB full insertion	R1 worth measurement
1975/07/07 19:20	149	tr8	108	908	104	103	103	102	714	713	894	dn	up	238.0	All partial insertion	TB full insertion	R2 worth measurement
1975/07/07 20:18	149	tr9	908	526	526	102	103	526	899	896	100	up	dn	448.5	All full withdrawal	TA and TC full insertion	
1975/07/08 10:18	149	tr10	580	581	580	582	581	582	897	894	102	dn	dn	581.0	All full withdrawal	TA, TB, and TC full insertion	S1 worth measurement
1975/07/09 15:50	149	tr11	461	461	461	460	461	461	899	897	901	dn	dn	460.8	All full withdrawal	TB and TC full insertion	TA worth measurement

Table A.1.2 Calculated k_{eff} for the cores with various transient rod positions.

The number of fuel rods	ID	Library [*1]	$k_{eff} \pm 1\sigma$			k_{eff} difference ± 1σ J40-J40u1			k_{eff} difference ± 1σ J5-J40		
149	tr1	J40	0.99886	±	0.00013	-0.00008	±	0.00018			
		J40u1	0.99895	±	0.00012						
		J5	1.00349	±	0.00012				0.00463	±	0.00018
149	tr2	J40	0.99986	±	0.00012	0.00011	±	0.00018			
		J40u1	0.99975	±	0.00013						
		J5	1.00420	±	0.00012				0.00434	±	0.00017
149	tr3	J40	1.00035	±	0.00013	-0.00002	±	0.00019			
		J40u1	1.00037	±	0.00013						
		J5	1.00502	±	0.00013				0.00467	±	0.00018
149	tr4	J40	0.99988	±	0.00012	0.00001	±	0.00018			
		J40u1	0.99987	±	0.00012						
		J5	1.00430	±	0.00013				0.00442	±	0.00018
149	tr5	J40	0.99990	±	0.00013	0.00005	±	0.00018			
		J40u1	0.99985	±	0.00012						
		J5	1.00411	±	0.00013				0.00421	±	0.00018
149	tr6	J40	0.99957	±	0.00013	-0.00006	±	0.00018			
		J40u1	0.99963	±	0.00013						
		J5	1.00394	±	0.00013				0.00437	±	0.00018
149	tr7	J40	0.99748	±	0.00012	-0.00014	±	0.00018			
		J40u1	0.99761	±	0.00013						
		J5	1.00215	±	0.00013				0.00467	±	0.00017
149	tr8	J40	0.99743	±	0.00012	-0.00005	±	0.00018			
		J40u1	0.99748	±	0.00012						
		J5	1.00196	±	0.00012				0.00453	±	0.00017
149	tr9	J40	0.99966	±	0.00013	-0.00008	±	0.00018			
		J40u1	0.99974	±	0.00012						
		J5	1.00395	±	0.00012				0.00429	±	0.00018
149	tr10	J40	0.99962	±	0.00012	0.00006	±	0.00017			
		J40u1	0.99956	±	0.00012						
		J5	1.00427	±	0.00013				0.00465	±	0.00018
149	tr11	J40	1.00030	±	0.00013	0.00016	±	0.00018			
		J40u1	1.00014	±	0.00012						
		J5	1.00480	±	0.00013				0.00450	±	0.00018

*1 J40: JENDL-4.0, J40u1: JENDL-4.0u1, J5: JENDL-5

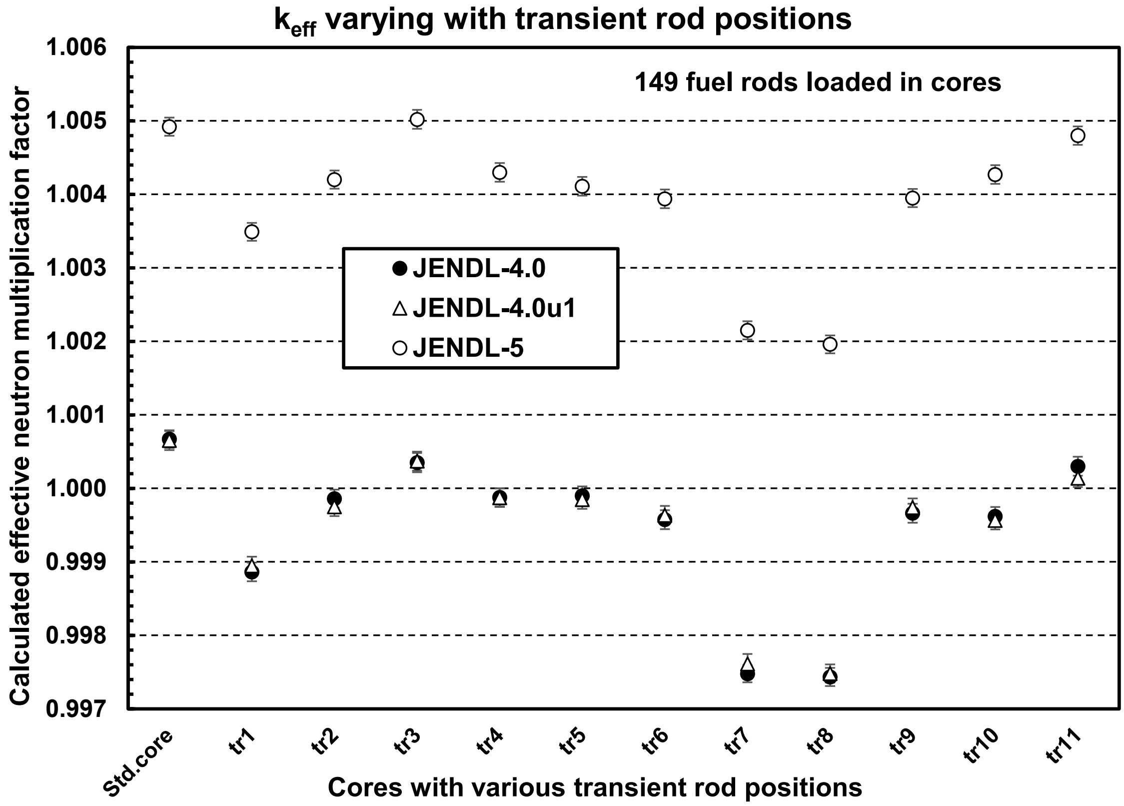

Fig. A.1.1 Calculated k_{eff} for the cores with various transient rod positions.

For the examination on significancy of those ranges of the variations in k_{eff}, the uncertainties in k_{eff} for six sorts of representative cores (ID = tr1, tr3, tr8, tr9, tr10, and tr11) were evaluated focusing on the errors in the data of the transient rods. The cores, ID = tr1 and tr3, give the minimum and maximum k_{eff}'s, respectively, among the cores, ID = tr1 to tr6, in which the adjustable transient rod (TA) was partially inserted. On the condition of the fast transient rod (TB) fully inserted, the core, ID = tr8, gives the smaller k_{eff} than that of the core, ID = tr7. For the cores, ID = tr9 to tr11, more than two transient rods were fully inserted. The evaluation method for the uncertainties was the same as described in Chap. 6.

(1) Uncertainties from geometry data of transient rods

The uncertainties in k_{eff} propagated from the errors in the diameter and height of the enriched boron carbide absorber, and the outer diameter of the cladding in the adjustable and fast transient rods were evaluated by using the method as described in Sec. 6.1.3. The evaluated results of the uncertainties in k_{eff}

propagated from those errors in the geometry data of the adjustable and fast transient rods are summarized in Table A.1.3. The aggregated uncertainties in k_{eff} propagated from those errors in the geometry data of the transient rods are summarized in Table A.1.4. The aggregated uncertainties in k_{eff} are in the range of 0.0001 to 0.0003 Δk_{eff} for the representative cores with various transient rod positions excepting the cores, ID = tr1 and tr3. The aggregated uncertainties in k_{eff} are negligibly small for the cores, ID = tr1 and tr3.

Table A.1.3 Summary of uncertainties in k_{eff} propagated from the errors in the geometry data of the adjustable and fast transient rods for the cores with various transient rod positions.

Source of uncertainty	Core	Averaged bias: B_{av} (Δk_{eff} ± 1σ)	Max. difference in B_{av}: D	D/σ	Uncertainty in k_{eff} (Δk_{eff})
1.38% smaller diameter of B_4C in adjustable and fast transient rods: - 0.05 (cm)	Standard	-0.00002 ± 0.00007	0.00029	3.96	negligible
	tr1	-0.00004 ± 0.00007			negligible
	tr3	+0.00007 ± 0.00007			negligible
	tr8	+0.00008 ± 0.00007			0.0001
	tr9	+0.00021 ± 0.00007			0.0002
	tr10	+0.00025 ± 0.00007			0.0003
	tr11	+0.00017 ± 0.00007			0.0002
0.05% and 0.01% of height of B_4C in adjustable and fast transient rod: ± 0.02 and 0.01 (cm)	Standard	±0.00006 ± 0.00007	0.00006	0.88	negligible
	tr1	±0.00000 ± 0.00007			negligible
	tr3	±0.00003 ± 0.00007			negligible
	tr8	±0.00001 ± 0.00007			negligible
	tr9	±0.00004 ± 0.00007			negligible
	tr10	±0.00000 ± 0.00007			negligible
	tr11	±0.00003 ± 0.00007			negligible
0.26% of outer diameter of adjustable and fast transient rods cladding: ± 0.01 (cm)	Standard	±0.00006 ± 0.00007	0.00005	0.71	negligible
	tr1	±0.00005 ± 0.00007			negligible
	tr3	±0.00003 ± 0.00007			negligible
	tr8	±0.00004 ± 0.00007			negligible
	tr9	±0.00005 ± 0.00007			negligible
	tr10	±0.00001 ± 0.00007			negligible
	tr11	±0.00004 ± 0.00007			negligible

Table A.1.4 Aggregated uncertainties in k_{eff} propagated from the errors in the geometry data of the adjustable and fast transient rods for the cores with various transient rod positions.

Source of uncertainty	Core	Uncertainty in k_{eff} (Δk_{eff})
Geometry data in adjustable and fast transient rods	Standard	negligible
	tr1	negligible
	tr3	negligible
	tr8	0.0001
	tr9	0.0002
	tr10	0.0003
	tr11	0.0002

(2) Uncertainties from material data of absorber in transient rods

The uncertainties in k_{eff} propagated from the errors in the density, boron content, and boron-10 enrichment of the enriched boron carbide absorber in the adjustable and fast transient rods were evaluated by using the method as described in Sec. 6.2.8. The evaluated results of the uncertainties in k_{eff} propagated from those errors in the material data of the adjustable and fast transient rods are summarized in Table A.1.5. The aggregated uncertainties in k_{eff} propagated from those errors in the material data of the transient rods are summarized in Table A.1.6. The aggregated uncertainties in k_{eff} are negligibly small for all cores.

Table A.1.5 Summary of uncertainties in k_{eff} propagated from the errors in the material data of the adjustable and fast transient rods for the cores with various transient rod positions.

Source of uncertainty	Core	Averaged bias: B_{av} ($\Delta k_{eff} \pm 1\sigma$)	Max. difference in B_{av}: D	D/σ	Uncertainty in k_{eff} (Δk_{eff})
1.49% of enriched B_4C density: ± 0.0343 (g/cm^3)	Standard	±0.00001 ± 0.00007	0.00006	0.83	negligible
	tr1	±0.00004 ± 0.00007			negligible
	tr3	±0.00000 ± 0.00007			negligible
	tr8	±0.00000 ± 0.00007			negligible
	tr9	±0.00006 ± 0.00007			negligible
	tr10	±0.00002 ± 0.00007			negligible
	tr11	±0.00005 ± 0.00007			negligible
0.61% of B content of enriched B_4C: ± 0.4694 (wt%)	Standard	±0.00005 ± 0.00007	0.00004	0.59	negligible
	tr1	±0.00003 ± 0.00007			negligible
	tr3	±0.00002 ± 0.00007			negligible
	tr8	±0.00002 ± 0.00007			negligible
	tr9	±0.00003 ± 0.00007			negligible
	tr10	±0.00005 ± 0.00007			negligible
	tr11	±0.00006 ± 0.00007			negligible
0.51% of B-10 enrichment: ± 0.47 (wt%)	Standard	±0.00001 ± 0.00007	0.00006	0.81	negligible
	tr1	±0.00002 ± 0.00007			negligible
	tr3	±0.00002 ± 0.00007			negligible
	tr8	±0.00004 ± 0.00007			negligible
	tr9	±0.00006 ± 0.00007			negligible
	tr10	±0.00000 ± 0.00007			negligible
	tr11	±0.00001 ± 0.00007			negligible

Table A.1.6 Aggregated uncertainties in k_{eff} propagated from the errors in the material data of the adjustable and fast transient rods for the cores with various transient rod positions.

Source of uncertainty	Core	Uncertainty in k_{eff} (Δk_{eff})
Material data in adjustable and fast transient rods	Standard	negligible
	tr1	negligible
	tr3	negligible
	tr8	negligible
	tr9	negligible
	tr10	negligible
	tr11	negligible

(3) Uncertainties from operation data of rod positions

For the cores examined here, the positions of the control and safety rods were also different from those in the minimum, standard, and intermediate cores. This means that there may be differences in the effect of the errors in the absorber rod positions to the uncertainties in k_{eff}. Hence, the uncertainties in k_{eff} propagated from the errors in the rod position were also evaluated by using the method as described in Sec. 6.3.1. The evaluated uncertainties in k_{eff} are listed in Table A.1.7. The uncertainties in k_{eff} are in the range of 0.0003 to 0.0007 Δk_{eff} for the representative cores with various transient rod positions.

Table A.1.7 Uncertainties in k_{eff} propagated from the error in the rod position of the control, safety, and transient rods for the cores with various transient rod positions.

Source of uncertainty	Core	Averaged bias: B_{av} ($\Delta k_{eff} \pm 1\sigma$)	Max. difference in B_{av}: D	D/σ	Uncertainty in k_{eff} (Δk_{eff})
5 units of rod position: ± 0.24 (cm)	Standard	±0.00047 ± 0.00007	0.00033	4.59	0.0005
	tr1	±0.00043 ± 0.00007			0.0004
	tr3	±0.00055 ± 0.00007			0.0006
	tr8	±0.00033 ± 0.00007			0.0003
	tr9	±0.00032 ± 0.00007			0.0003
	tr10	±0.00065 ± 0.00007			0.0007
	tr11	±0.00065 ± 0.00007			0.0007

(4) Overall uncertainties for cores with various transient rod positions

The aggregated uncertainties in k_{eff} were estimated as the overall uncertainties by assuming that the uncertainties other than the those in Tables A.1.4, A.1.6, and A.1.7 were the same magnitude as those for the standard cores. The aggregated uncertainties in k_{eff} propagated from the errors in the geometry, material, and operation data in total are summarized in Table A.1.8. The aggregated uncertainties in k_{eff} are in the range of 0.0027 to 0.0028 Δk_{eff} for the representative cores with various transient rod positions. It is confirmed that the differences in the overall uncertainties between the representative cores with various transient rod positions and standard core are quite small.

Table A.1.8 Aggregated uncertainties in k_{eff} propagated from the errors in the geometry, material, and operation data for the cores with various transient rod positions.

Source of uncertainty	Core	Uncertainty in k_{eff} (Δk_{eff})
Aggregation of uncertainties in geometry, material, and operation data	Standard	0.0027
	tr1	0.0027
	tr3	0.0028
	tr8	0.0027
	tr9	0.0027
	tr10	0.0028
	tr11	0.0028

From the results of the estimated overall uncertainties in k_{eff} mentioned above, it is considered that the variations in the calculated k_{eff}'s shown in Fig. A.1.1 are not significant in terms of the uncertainty of the calculation models since the variations are in the range of 1.03 to 1.13 times the overall uncertainties. It is also considered that the differences between k_{eff}'s by JENDL-5 and JENDL-4.0 are not significant in terms of the uncertainty of the calculation models since the differences are within 1.67 times the overall uncertainties.

Appendix-2 Effect of Replacement of Experimental Tube with Water on Uncertainties

For simplicity, the uncertainties in k_{eff} propagated from the geometry errors in the core structures, such as the grid plate, shroud, guide tube for the transient rod, were evaluated by the replacement of those with water, as described in Sec. 6.1. For reference, the uncertainties were evaluated by the same method as described in Chap. 6 in the case that the experimental tube is also replaced with water. The evaluated uncertainties are shown below.

(1) Uncertainties propagated from replacement of hexagonal shaped experimental tube with water

Table A.2.1 lists the uncertainties in k_{eff} propagated from the replacement of the hexagonal shaped experimental tube with water. The uncertainties in k_{eff} propagated from the replacement are evaluated to be in the range of 0.0032 to 0.0037 Δk_{eff} for the minimum, standard, and intermediate cores. The uncertainties in k_{eff} propagated from the replacement are larger than the overall uncertainties in k_{eff}, which were evaluated to be in the range of 0.0027 to 0.0029 Δk_{eff} in Table 6.4.1. It is confirmed that the replacement of the hexagonal shaped experimental tube with water affects the overall uncertainties in k_{eff}.

Table A.2.1 Uncertainties in k_{eff} propagated from the replacement of the hexagonal shaped experimental tube with water.

Source of uncertainty	Core	Averaged bias ($\Delta k_{eff} \pm 1\sigma$)	Uncertainty in k_{eff} (Δk_{eff})
Replacement of hexagonal shaped experimental tube with water	Minimum	+0.00372 ± 0.00007	0.0037
	Standard	+0.00318 ± 0.00007	0.0032
	Intermediate	+0.00356 ± 0.00007	0.0036

(2) Uncertainties propagated from replacement of cylindrical shaped experimental tube with water

Table A.2.2 lists the uncertainties in k_{eff} propagated from the replacement of the cylindrical shaped experimental tube with water. The uncertainties in k_{eff} propagated from the replacement are evaluated to be 0.0002 Δk_{eff} for all cores. It is considered that the cylindrical shaped experimental tube may be replaced with water because of trivial effect on the overall uncertainties in k_{eff} shown in Table 6.4.1.

Table A.2.2 Uncertainties in k_{eff} propagated from the replacement of the cylindrical shaped experimental tube with water.

Source of uncertainty	Core	Averaged bias ($\Delta k_{eff} \pm 1\sigma$)	Uncertainty in k_{eff} (Δk_{eff})
Replacement of cylindrical shaped experimental tube with water	Minimum	+0.00014 ± 0.00007	0.0002
	Standard	+0.00015 ± 0.00007	0.0002
	Intermediate	+0.00018 ± 0.00007	0.0002

Appendix-3 Effect of Impurities on Uncertainties

For reference, the effect of the impurities in the uranium-zirconium hydride, zirconium rod, and molybdenum disc on the uncertainties in k_{eff} were evaluated by the same method as described in Chap. 6. The evaluated uncertainties in k_{eff} are shown below.

(1) Uncertainties in k_{eff} propagated from ignoring impurities in uranium-zirconium hydride

Table A.3.1 lists the uncertainties in k_{eff} propagated from the ignoring the impurities in the uranium-zirconium hydride, which are shown in Tables 3.1.1(1) and 3.1.2(2). It is confirmed that the evaluated uncertainties in k_{eff} are 0.0016 Δk_{eff} for all cores. It is considered that the impurities in the uranium-zirconium hydride may not be ignored since the impurities significantly affect the overall uncertainties in k_{eff} shown in Table 6.4.1.

Table A.3.1 Uncertainties in k_{eff} propagated from the ignoring the impurities in the uranium-zirconium hydride.

Source of uncertainty	Core	Averaged bias ($\Delta k_{eff} \pm 1\sigma$)	Uncertainty in k_{eff} (Δk_{eff})
Ignoring impurities in U-ZrH	Minimum	+0.00156 ± 0.00007	0.0016
	Standard	+0.00158 ± 0.00007	0.0016
	Intermediate	+0.00160 ± 0.00007	0.0016

(2) Uncertainties in k_{eff} propagated from ignoring impurities in zirconium rod

Table A.3.2 lists the uncertainties in k_{eff} propagated from the ignoring the impurities in the zirconium rod, which are shown in Table 3.2.1. It is confirmed that the evaluated uncertainty in k_{eff} is 0.0001 Δk_{eff} for the minimum core. It is also confirmed that the uncertainties are negligibly small for the standard, and intermediate cores. It is considered that the impurities in the zirconium rod may be ignored because of little or no effect on the overall uncertainties in k_{eff} shown in Table 6.4.1.

Table A.3.2 Uncertainties in k_{eff} propagated from the ignoring the impurities in the zirconium rod.

Source of uncertainty	Core	Averaged bias ($\Delta k_{eff} \pm 1\sigma$)	Uncertainty in k_{eff} (Δk_{eff})
Ignoring impurities in Zr rod	Minimum	+0.00010 ± 0.00007	0.0001
	Standard	-0.00000 ± 0.00007	negligible
	Intermediate	+0.00007 ± 0.00007	negligible

(3) Uncertainties in k_{eff} propagated from ignoring impurities in molybdenum disc

Table A.3.3 lists the uncertainties in k_{eff} propagated from the ignoring the impurities in the molybdenum disc, which are shown in Table 3.5.1. It is confirmed that the evaluated uncertainties in k_{eff} are negligibly small for all cores. It is considered that the impurities in the molybdenum disc may be ignored because of no effect on the overall uncertainties in k_{eff} shown in Table 6.4.1.

Table A.3.3 Uncertainties in k_{eff} propagated from the ignoring the impurities in the molybdenum disc.

Source of uncertainty	Core	Averaged bias ($\Delta k_{eff} \pm 1\sigma$)	Uncertainty in k_{eff} (Δk_{eff})
Ignoring impurities in Mo disc	Minimum	-0.00004 ± 0.00007	negligible
	Standard	-0.00006 ± 0.00007	negligible
	Intermediate	+0.00000 ± 0.00007	negligible

Appendix-4 Sample Input List for MVP

A sample input list of the MVP version 3 code [6] is attached below. The input was prepared for the analyses on the standard core using the JENDL-5 library [7]. In the input, the absorber rod positions are specified by using the following 'symbolic parameters' [6], i.e., UZCR1' to 'UZCR6' for the control rods, UZSR1' and 'UZSR2' for the safety rods, UZTA1' for the adjustable transient rod, and 'UZTB1' and 'UZTC1' for the fast transient rods.

```
NSRR 19.89%EU standard core 23by23, initial type
50 million histories  JENDL-5
*
*--------+---------+---------+---------+---------+---------+---------+--
* OPTIONS
*--------+---------+---------+---------+---------+---------+---------+--
  BETA-EFFECTIVE DOPPLER-SCATTERING(EXACT)
  NEUTRON PERTURBATION DYNAMIC-MEMORY(550000000)
  EIGEN-VALUE  FREE-LATTICE-FRAME  LATTICE  FLUX-PRINT
  PRINT-SUPPRESS(6 7)

% NBT =   500  /* number of effective batches
% NSK =   200  /* number of skipped batches
% NHT = 100000  /* number of particles per batch
*
  NPART(<(NBT+NSK)*NHT>) /* total number of histories
  NHIST(<NHT>)          /* number of particles per batch
  NBANK(<NHT*2>)        /* length of particle bank
  NFBANK(<NHT*2>)       /* length of fission source bank
  NSKIP(<NSK>)          /* number of skipped batches
*
  NMEMO( 100 )          /* number of next-zone memory per zone
*  TCPU( 180 )            /* calculation CPU time limit (min)
  ETOP.N(2.0E7)         /* top of neutron energy (eV)
  EBOT.N(1.0E-5)        /* bottom of neutron energy (eV)
*
  NGROUP.N( 120 )
  ENGYB.N( 2.0000E+07 1.5795E+07 1.2474E+07 9.8515E+06 7.7803E+06
         6.1445E+06 4.8526E+06 3.8324E+06 3.0266E+06 2.3903E+06
         1.8877E+06 1.4909E+06 1.1774E+06 9.2986E+05 7.3436E+05
         5.7996E+05 4.5803E+05 3.6173E+05 2.8568E+05 2.2561E+05
         1.7818E+05 1.4072E+05 1.1113E+05 8.7767E+04 6.9315E+04
         5.4741E+04 4.3232E+04 3.4143E+04 2.6964E+04 2.1295E+04
         1.6818E+04 1.3282E+04 1.0490E+04 8.2841E+03 6.5424E+03
         5.1669E+03 4.0806E+03 3.2226E+03 2.5451E+03 2.0100E+03
         1.5874E+03 1.2537E+03 9.9008E+02 7.8192E+02 6.1752E+02
         4.8769E+02 3.8516E+02 3.0418E+02 2.4023E+02 1.8972E+02
         1.4983E+02 1.1833E+02 9.3451E+01 7.3803E+01 5.8286E+01
         4.6032E+01 3.6354E+01 2.8711E+01 2.2674E+01 1.7907E+01
         1.4142E+01 1.1169E+01 8.8206E+00 6.9661E+00 5.5015E+00
         4.3448E+00 3.4313E+00 2.7099E+00 2.1402E+00 1.6902E+00
         1.3348E+00 1.0542E+00 8.3255E-01 6.5751E-01 5.1927E-01
         4.1010E-01 3.2388E-01 2.5578E-01 2.0200E-01 1.5953E-01
         1.2599E-01 9.9503E-02 7.8583E-02 6.2061E-02 4.9013E-02
         3.8708E-02 3.0570E-02 2.4143E-02 1.9067E-02 1.5058E-02
         1.1892E-02 9.3918E-03 7.4172E-03 5.8578E-03 4.6262E-03
         3.6536E-03 2.8854E-03 2.2788E-03 1.7997E-03 1.4213E-03
         1.1225E-03 8.8647E-04 7.0009E-04 5.5290E-04 4.3666E-04
         3.4485E-04 2.7235E-04 2.1509E-04 1.6987E-04 1.3415E-04
         1.0595E-04 8.3672E-05 6.6080E-05 5.2187E-05 4.1215E-05
         3.2549E-05 2.5706E-05 2.0301E-05 1.6033E-05 1.2662E-05
         1.0000E-5)
*
*--------+---------+---------+---------+---------+---------+---------+--
* PARAMETERS FOR CONTROL ROD POSITION
*--------+---------+---------+---------+---------+---------+---------+--
*
% UZCR1  =  218        /* cr1 unit (100-900)
% UZCR2  =  211        /* cr2 unit (100-900)
% UZCR3  =  216        /* cr3 unit (100-900)
% UZCR4  =  211        /* cr4 unit (100-900)
% UZCR5  =  209        /* cr5 unit (100-900)
% UZCR6  =  213        /* cr6 unit (100-900)
% UZSR1  =  899        /* sr1 unit (100-900)
% UZSR2  =  897        /* sr2 unit (100-900)
% UZTA1  =  895        /* ta unit  (100-900)
% UZTB1  =  900        /* tb pos. (100:dn, 900:up)
% UZTC1  =  900        /* tc pos. (100:dn, 900:up)
*
% BZCR1  = <(900-UZCR1)*38.1/800>   /* cr1 bias (cm)
% BZCR2  = <(900-UZCR2)*38.1/800>   /* cr2 bias (cm)
% BZCR3  = <(900-UZCR3)*38.1/800>   /* cr3 bias (cm)
% BZCR4  = <(900-UZCR4)*38.1/800>   /* cr4 bias (cm)
% BZCR5  = <(900-UZCR5)*38.1/800>   /* cr5 bias (cm)
% BZCR6  = <(900-UZCR6)*38.1/800>   /* cr6 bias (cm)
% BZSR1  = <(900-UZSR1)*38.1/800>   /* sr1 bias (cm)
% BZSR2  = <(900-UZSR2)*38.1/800>   /* sr2 bias (cm)
% BZTA1  = <(900-UZTA1)*38.1/800>  /* ta bias (cm)
% BZTB1  = <(900-UZTB1)*76.2/800>  /* tb bias (cm)
% BZTC1  = <(900-UZTC1)*76.2/800>  /* tc bias (cm)
*
*--------+---------+---------+---------+---------+---------+---------+--
* PARAMETERS FOR CONTROL ROD (INITIAL TYPE)
*--------+---------+---------+---------+---------+---------+---------+--
*
% CR1   =   0.285      /* radius of zirconium (cm)
% CR2   =   0.32       /* inner radius of U-ZrH (cm)
% CR3   =   1.78       /* outer radius of U-ZrH (cm)
% CR4   =   1.83       /* inner radius of cladding (cm)
% CR5   =   1.88       /* outer radius of cladding (cm)
% CR6   =   1.815      /* radius of B4C (cm)
% CR7   =   1.655      /* inner radius of spacer tube (cm)
% CR8   =   1.745      /* outer radius of spacer tube (cm)
```

```
*
*--------+---------+---------+---------+---------+---------+---------+--
* PARAMETERS FOR CR1 (INITIAL TYPE)
*--------+---------+---------+---------+---------+---------+---------+--
*
% C1Z1   = -20.95 - <BZCR1>  /* height of bottom of u-zrh (cm)
% C1Z2   = <C1Z1> + 38.1    /* height of top of u-zrh (cm)
% C1Z3   = <C1Z1> -  3.18   /* height of bottom of sp1 (cm)
% C1Z4   = <C1Z3> - 65.12   /* height of bottom of spacer tube (cm)
% C1Z5   = <C1Z4> -  2.21   /* height of bottom of bottom plug (cm)
*
% C1Z7   = <C1Z2> +  0.63   /* height of bottom of sp2 (cm)
% C1Z8   = <C1Z7> +  1.27   /* height of bottom of b4c (cm)
% C1Z9   = <C1Z8> + 38.1    /* height of top of b4c (cm)
% C1Z10  = <C1Z9> +  0.3    /* height of bottom of sp3 (cm)
% C1Z11  = <C1Z10> +  1.27  /* height of top of sp3 (cm)
% C1Z12  = <C1Z11> + 13.61  /* height of bottom of top plug (cm)
% C1Z13  = <C1Z12> +  3.81  /* height of top of top plug (cm)
*
*--------+---------+---------+---------+---------+---------+---------+--
* PARAMETERS FOR CR2 (INITIAL TYPE)
*--------+---------+---------+---------+---------+---------+---------+--
*
% C2Z1   = -20.95 - <BZCR2>  /* height of bottom of u-zrh (cm)
% C2Z2   = <C2Z1> + 38.1    /* height of top of u-zrh (cm)
% C2Z3   = <C2Z1> -  3.18   /* height of bottom of sp1 (cm)
% C2Z4   = <C2Z3> - 65.12   /* height of bottom of spacer tube (cm)
% C2Z5   = <C2Z4> -  2.21   /* height of bottom of bottom plug (cm)
*
% C2Z7   = <C2Z2> +  0.63   /* height of bottom of sp2 (cm)
% C2Z8   = <C2Z7> +  1.27   /* height of bottom of b4c (cm)
% C2Z9   = <C2Z8> + 38.1    /* height of top of b4c (cm)
% C2Z10  = <C2Z9> +  0.3    /* height of bottom of sp3 (cm)
% C2Z11  = <C2Z10> +  1.27  /* height of top of sp3 (cm)
% C2Z12  = <C2Z11> + 13.61  /* height of bottom of top plug (cm)
% C2Z13  = <C2Z12> +  3.81  /* height of top of top plug (cm)
*
*--------+---------+---------+---------+---------+---------+---------+--
* PARAMETERS FOR CR3 (INITIAL TYPE)
*--------+---------+---------+---------+---------+---------+---------+--
*
% C3Z1   = -20.95 - <BZCR3>  /* height of bottom of u-zrh (cm)
% C3Z2   = <C3Z1> + 38.1    /* height of top of u-zrh (cm)
% C3Z3   = <C3Z1> -  3.18   /* height of bottom of sp1 (cm)
% C3Z4   = <C3Z3> - 65.12   /* height of bottom of spacer tube (cm)
% C3Z5   = <C3Z4> -  2.21   /* height of bottom of bottom plug (cm)
*
% C3Z7   = <C3Z2> +  0.63   /* height of bottom of sp2 (cm)
% C3Z8   = <C3Z7> +  1.27   /* height of bottom of b4c (cm)
% C3Z9   = <C3Z8> + 38.1    /* height of top of b4c (cm)
% C3Z10  = <C3Z9> +  0.3    /* height of bottom of sp3 (cm)
% C3Z11  = <C3Z10> +  1.27   /* height of top of sp3 (cm)
% C3Z12  = <C3Z11> + 13.61   /* height of bottom of top plug (cm)
% C3Z13  = <C3Z12> +  3.81   /* height of top of top plug (cm)
*
*--------+---------+---------+---------+---------+---------+---------+--
* PARAMETERS FOR CR4 (INITIAL TYPE)
*--------+---------+---------+---------+---------+---------+---------+--
*
% C4Z1   = -20.95 - <BZCR4>  /* height of bottom of u-zrh (cm)
% C4Z2   = <C4Z1> + 38.1    /* height of top of u-zrh (cm)
% C4Z3   = <C4Z1> -  3.18   /* height of bottom of sp1 (cm)
% C4Z4   = <C4Z3> - 65.12   /* height of bottom of spacer tube (cm)
% C4Z5   = <C4Z4> -  2.21   /* height of bottom of bottom plug (cm)
*
% C4Z7   = <C4Z2> +  0.63   /* height of bottom of sp2 (cm)
% C4Z8   = <C4Z7> +  1.27   /* height of bottom of b4c (cm)
% C4Z9   = <C4Z8> + 38.1    /* height of top of b4c (cm)
% C4Z10  = <C4Z9> +  0.3    /* height of bottom of sp3 (cm)
% C4Z11  = <C4Z10> +  1.27   /* height of top of sp3 (cm)
% C4Z12  = <C4Z11> + 13.61   /* height of bottom of top plug (cm)
% C4Z13  = <C4Z12> +  3.81   /* height of top of top plug (cm)
*
*--------+---------+---------+---------+---------+---------+---------+--
* PARAMETERS FOR CR5 (INITIAL TYPE)
*--------+---------+---------+---------+---------+---------+---------+--
*
% C5Z1   = -20.95 - <BZCR5>  /* height of bottom of u-zrh (cm)
% C5Z2   = <C5Z1> + 38.1    /* height of top of u-zrh (cm)
% C5Z3   = <C5Z1> -  3.18   /* height of bottom of sp1 (cm)
% C5Z4   = <C5Z3> - 65.12   /* height of bottom of spacer tube (cm)
% C5Z5   = <C5Z4> -  2.21   /* height of bottom of bottom plug (cm)
*
% C5Z7   = <C5Z2> +  0.63   /* height of bottom of sp2 (cm)
% C5Z8   = <C5Z7> +  1.27   /* height of bottom of b4c (cm)
% C5Z9   = <C5Z8> + 38.1    /* height of top of b4c (cm)
% C5Z10  = <C5Z9> +  0.3    /* height of bottom of sp3 (cm)
% C5Z11  = <C5Z10> +  1.27   /* height of top of sp3 (cm)
% C5Z12  = <C5Z11> + 13.61   /* height of bottom of top plug (cm)
% C5Z13  = <C5Z12> +  3.81   /* height of top of top plug (cm)
*
*--------+---------+---------+---------+---------+---------+---------+--
* PARAMETERS FOR CR6 (INITIAL TYPE)
```

```
*--------+---------+---------+---------+---------+---------+---------+--
*
% C6Z1   = -20.95 - <BZCR6>  /* height of bottom of u-zrh (cm)
% C6Z2   = <C6Z1> + 38.1    /* height of top of u-zrh (cm)
% C6Z3   = <C6Z1> -  3.18   /* height of bottom of sp1 (cm)
% C6Z4   = <C6Z3> - 65.12   /* height of bottom of spacer tube (cm)
% C6Z5   = <C6Z4> -  2.21   /* height of bottom of bottom plug (cm)
*
% C6Z7   = <C6Z2> +  0.63   /* height of bottom of sp2 (cm)
% C6Z8   = <C6Z7> +  1.27   /* height of bottom of b4c (cm)
% C6Z9   = <C6Z8> + 38.1    /* height of top of b4c (cm)
% C6Z10  = <C6Z9> +  0.3    /* height of bottom of sp3 (cm)
% C6Z11  = <C6Z10> +  1.27   /* height of top of sp3 (cm)
% C6Z12  = <C6Z11> + 13.61   /* height of bottom of top plug (cm)
% C6Z13  = <C6Z12> +  3.81   /* height of top of top plug (cm)
*
*--------+---------+---------+---------+---------+---------+---------+--
* PARAMETERS FOR SR1 (INITIAL TYPE)
*--------+---------+---------+---------+---------+---------+---------+--
*
% S1Z1   = -20.95 - <BZSR1>  /* height of bottom of u-zrh (cm)
% S1Z2   = <S1Z1> + 38.1    /* height of top of u-zrh (cm)
% S1Z3   = <S1Z1> -  3.18   /* height of bottom of sp1 (cm)
% S1Z4   = <S1Z3> - 65.12   /* height of bottom of spacer tube (cm)
% S1Z5   = <S1Z4> -  2.21   /* height of bottom of bottom plug (cm)
*
% S1Z7   = <S1Z2> +  0.63   /* height of bottom of sp2 (cm)
% S1Z8   = <S1Z7> +  1.27   /* height of bottom of b4c (cm)
% S1Z9   = <S1Z8> + 38.1    /* height of top of b4c (cm)
% S1Z10  = <S1Z9> +  0.3    /* height of bottom of sp3 (cm)
% S1Z11  = <S1Z10> +  1.27   /* height of top of sp3 (cm)
% S1Z12  = <S1Z11> + 13.61   /* height of bottom of top plug (cm)
% S1Z13  = <S1Z12> +  3.81   /* height of top of top plug (cm)
*
*--------+---------+---------+---------+---------+---------+---------+--
* PARAMETERS FOR SR2 (INITIAL TYPE)
*--------+---------+---------+---------+---------+---------+---------+--
*
% S2Z1   = -20.95 - <BZSR2>  /* height of bottom of u-zrh (cm)
% S2Z2   = <S2Z1> + 38.1    /* height of top of u-zrh (cm)
% S2Z3   = <S2Z1> -  3.18   /* height of bottom of sp1 (cm)
% S2Z4   = <S2Z3> - 65.12   /* height of bottom of spacer tube (cm)
% S2Z5   = <S2Z4> -  2.21   /* height of bottom of bottom plug (cm)
*
% S2Z7   = <S2Z2> +  0.63   /* height of bottom of sp2 (cm)
% S2Z8   = <S2Z7> +  1.27   /* height of bottom of b4c (cm)
% S2Z9   = <S2Z8> + 38.1    /* height of top of b4c (cm)
% S2Z10  = <S2Z9> +  0.3    /* height of bottom of sp3 (cm)
% S2Z11  = <S2Z10> +  1.27   /* height of top of sp3 (cm)
% S2Z12  = <S2Z11> + 13.61   /* height of bottom of top plug (cm)
% S2Z13  = <S2Z12> +  3.81   /* height of top of top plug (cm)
*
*--------+---------+---------+---------+---------+---------+---------+--
* PARAMETERS FOR TA ROD (INITIAL TYPE)
*--------+---------+---------+---------+---------+---------+---------+--
*
% AR1    =   1.815       /* radius of b4c (cm)
% AR2    =   1.655       /* inner radius of spacer tube (cm)
% AR3    =   1.745       /* outer radius of spacer tube (cm)
% AR4    =   1.655       /* inner radius of follower tube (cm)
% AR5    =   1.745       /* outer radius of follower tube (cm)
% AR6    =   1.815       /* inner radius of cladding (cm)
% AR7    =   1.905       /* outer radius of cladding (cm)
*
*--------+---------+---------+---------+---------+---------+---------+--
* PARAMETERS FOR TB AND TC ROD (INITIAL TYPE)
*--------+---------+---------+---------+---------+---------+---------+--
*
% TR1    =   1.815       /* radius of b4c (cm)
% TR2    =   1.655       /* inner radius of spacer tube (cm)
% TR3    =   1.745       /* outer radius of spacer tube (cm)
% TR4    =   1.655       /* inner radius of follower tube (cm)
% TR5    =   1.745       /* outer radius of follower tube (cm)
% TR6    =   1.815       /* inner radius of cladding (cm)
% TR7    =   1.905       /* outer radius of cladding (cm)
*
*--------+---------+---------+---------+---------+---------+---------+--
* PARAMETERS FOR TA (INITIAL TYPE)
*--------+---------+---------+---------+---------+---------+---------+--
*
% TAZ1   = 19.05  - <BZTA1>  /* height of bottom of b4c (cm)
% TAZ2   = <TAZ1> + 38.1    /* height of top of b4c (cm)
% TAZ3   = <TAZ1> -  2.54   /* height of bottom of sp1 (cm)
% TAZ4   = <TAZ3> - 106.33   /* height of bottom of follower tube (cm)
% TAZ5   = <TAZ4> -  1.58   /* height of bottom of ta (cm)
*
% TAZ6   = <TAZ2> +  1.27   /* height of bottom of spacer tube (cm)
% TAZ7   = <TAZ6> + 13.33   /* height of bottom of top plug (cm)
% TAZ8   = <TAZ7> +  4.45   /* height of top of ta (cm)
*
*--------+---------+---------+---------+---------+---------+---------+--
* PARAMETERS FOR TB (INITIAL TYPE)
*--------+---------+---------+---------+---------+---------+---------+--
*
% TBZ1   = 19.05  - <BZTB1>  /* height of bottom of b4c (cm)
% TBZ2   = <TBZ1> + 76.2    /* height of top of b4c (cm)
% TBZ3   = <TBZ1> -  2.54   /* height of bottom of sp1 (cm)
% TBZ4   = <TBZ3> - 68.23   /* height of bottom of follower tube (cm)
% TBZ5   = <TBZ4> -  1.58   /* height of bottom of tb (cm)
*
% TBZ6   = <TBZ2> +  1.27   /* height of bottom of spacer tube (cm)
% TBZ7   = <TBZ6> + 13.33   /* height of bottom of top plug (cm)
% TBZ8   = <TBZ7> +  4.45   /* height of top of tb (cm)
*
*--------+---------+---------+---------+---------+---------+---------+--
* PARAMETERS FOR TC (INITIAL TYPE)
*--------+---------+---------+---------+---------+---------+---------+--
*
% TCZ1   = 19.05  - <BZTC1>  /* height of bottom of b4c (cm)
% TCZ2   = <TCZ1> + 76.2    /* height of top of b4c (cm)
% TCZ3   = <TCZ1> -  2.54   /* height of bottom of sp1 (cm)
% TCZ4   = <TCZ3> - 68.23   /* height of bottom of follower tube (cm)
% TCZ5   = <TCZ4> -  1.58   /* height of bottom of tc (cm)
*
% TCZ6   = <TCZ2> +  1.27   /* height of bottom of spacer tube (cm)
% TCZ7   = <TCZ6> + 13.33   /* height of bottom of top plug (cm)
% TCZ8   = <TCZ7> +  4.45   /* height of top of tc (cm)
*
*--------+---------+---------+---------+---------+---------+---------+--
* PARAMETERS FOR FUEL PIN
*--------+---------+---------+---------+---------+---------+---------+--
*
% FR1    =   0.285       /* radius of zirconium (cm)
% FR2    =   0.32        /* inner radius of U-ZrH (cm)
% FR3    =   1.775       /* outer radius of U-ZrH (cm)
% FR4    =   1.82        /* inner radius of cladding (cm)
% FR5    =   1.875       /* outer radius of cladding (cm)
% FR6    =   1.815       /* radius of Mo disc (cm)
% FR7    =   1.715       /* radius of axial graphite reflector (cm)
% FR8    =   0.8775      /* rad_1 ot top end cap (cm)
% FR9    =   1.937       /* rad_2 of top end cap (cm)
% FR10   =   0.795       /* rad_1 of bottom end cap (cm)
% FR11   =   1.855       /* rad_2 of bottom end cap (cm)
% FR12   =   0.32        /* rad_3 of bottom end cap (cm)
*
% FZ1    = -19.05        /* height of bottom of core (cm)
% FZ2    =  19.05        /* height of top of core (cm)
% FZ3    = <FZ1> - 0.08   /* height of bottom of Mo disc (cm)
% FZ4    = <FZ3> - 8.69   /* height of bottom of bottom graphite (cm)
% FZ5    = <FZ4> - 0.91   /* height of bottom of cladding (cm)
% FZ6    = <FZ5> - 1.01   /* h1 of bottom end cap (cm)
% FZ7    = <FZ6> - 3.345  /* h2 of bottom end cap and top of b_grid (cm)
% FZ8    = <FZ7> - 1.535  /* h3 of bottom end cap (cm)
% FZ9    = <FZ8> - 1.7    /* height of bottom of fuel rod (cm)
*
% FZ10   = <FZ2>  + 8.69  /* height of top of top graphite (cm)
% FZ11   = <FZ10> + 0.63  /* height of bottom of top plug (cm)
% FZ12   = <FZ11> + 0.9   /* height of top of cladding (cm)
% FZ13   = <FZ12> + 1.01  /* h1 of top end cap (cm)
% FZ14   = <FZ13> + 2.15  /* h2 of top end cap (cm)
% FZ15   = <FZ14> + 4.34  /* height of top of fuel rod (cm)
*
*--------+---------+---------+---------+---------+---------+---------+--
* PARAMETERS FOR FUEL LATTICE
*--------+---------+---------+---------+---------+---------+---------+--
*
% FPN    =   23          /* number of cells in lattice (FPN by FPN)
% FPP    =    4.175       /* lattice pitch (cm)
*
% PPP    = <FPP>/SQRT(3)
*
*--------+---------+---------+---------+---------+---------+---------+--
* PARAMETERS FOR GRID PLATE
*--------+---------+---------+---------+---------+---------+---------+--
*
% GTRF   =    1.95        /* radius of fuel hole (cm)
% GTRC   =    2.0575       /* radius of crd hole (cm)
% GTB    =   28.59        /* height of bottom of t_grid (cm)
% GTT    =   31.025       /* height of top of t_grid (cm)
*
% GBRF   =    1.589        /* radius of fuel hole (cm)
% GBRC   =    2.055        /* radius of crd hole (cm)
% GBB    =  -38.135        /* height of bottom of b_grid (cm)
% GBT    = <FZ7-FR11+GBRF>  /* height of top of fuel hole (cm)
*
*--------+---------+---------+---------+---------+---------+---------+--
* PARAMETERS FOR EXPERIMENTAL TUBE
*--------+---------+---------+---------+---------+---------+---------+--
*
% EH1    =   24.465       /* outer width of hex tube (cm)
% EH2    =   23.185       /* inner width of hex tube (cm)
% EC1    =   12.4575      /* outer radius of cyl tube (cm)
% EC2    =   11.8175      /* inner radius of cyl tube (cm)
*
% EHB   =  -130.56        /* bottom of hex tube (cm)
% EHT   =    41.90       /* top of hex tube (cm)
% ECT    =  115.30       /* top of cyl tube (cm)
*
*--------+---------+---------+---------+---------+---------+---------+--
* PARAMETERS FOR SHROUD
*--------+---------+---------+---------+---------+---------+---------+--
*
% SH1    =   48.4475      /* outer radius of shroud (cm)
% SH2    =   47.45       /* inner radius of shroud (cm)
*
*
*--------+---------+---------+---------+---------+---------+---------+--
* PARAMETERS FOR TRANSIENT ROD GUIDE TUBE
*--------+---------+---------+---------+---------+---------+---------+--
*
% GR1    =   2.2225       /* outer radius of guide tube (cm)
% GR2    =   2.0725       /* inner radius of guide tube (cm)
% GZB    =   <GTT+0.79>    /* height of bottom of guide tube (cm)
*
*--------+---------+---------+---------+---------+---------+---------+--
* TEMPERATURE
*--------+---------+---------+---------+---------+---------+---------+--
*
% TP      =   23.0       /* temperature (deg-C)
% TPF     =   23.0       /* fuel temperature (deg-C)
*
*--------+---------+---------+---------+---------+---------+---------+--
* CONSTANTS
*--------+---------+---------+---------+---------+---------+---------+--
*
% FRM    =  100.0        /* moderator density (%)
*
% FRR    =  100.0        /* reflector density (%)
*
*--------+---------+---------+---------+---------+---------+---------+--
* CROSS SECTION
*--------+---------+---------+---------+---------+---------+---------+--
$XSEC
* ZIRCONIUM
& IDMAT(1)
  TPRECS( 0.1 )
  TEMPMT( <273.15+TP> )
  ZR0900J50( 2.2145E-02 )
  ZR0910J50( 4.8293E-03 )
  ZR0920J50( 7.3816E-03 )
  ZR0940J50( 7.4806E-03 )
  ZR0960J50( 1.2052E-03 )
  B00100J50( 1.4455E-08 )
  B00110J50( 5.8182E-08 )
  C00120J50( 3.7180E-05 )
  C00130J50( 4.1353E-07 )
  N00140J50( 1.1171E-05 )
  N00150J50( 4.1488E-08 )
  CR0500J50( 2.3460E-07 )
  CR0520J50( 4.5240E-06 )
  CR0530J50( 5.1293E-07 )
  CR0540J50( 1.2769E-07 )
  FE0540J50( 2.3251E-06 )
  FE0560J50( 3.6146E-05 )
  FE0570J50( 8.2759E-07 )
  FE0580J50( 1.1035E-07 )
  CU0630J50( 5.1287E-07 )
  CU0650J50( 2.2859E-07 )
  HF1740J50( 1.1582E-09 )
  HF1760J50( 3.7220E-08 )
  HF1770J50( 1.3302E-07 )
  HF1780J50( 1.9516E-07 )
  HF1790J50( 9.7440E-08 )
  HF1800J50( 2.5095E-07 )
*
* U-ZrH
& IDMAT(2)
  TPRECS( 0.1 )
```

```
  TEMPMT( <273.15+TPF> )
  H0001ZJ50( 5.5586E-02 )
  ZR090ZJ50( 1.7678E-02 )
  ZR091ZJ50( 3.8552E-03 )
  ZR092ZJ50( 5.8928E-03 )
  ZR094ZJ50( 5.9718E-03 )
  ZR096ZJ50( 9.6209E-04 )
  U02350J50( 3.6389E-04 )
  U02380J50( 1.4505E-03 )
  C00120J50( 3.6133E-05 )
  C00130J50( 4.0189E-07 )
  N00140J50( 4.9050E-06 )
  N00150J50( 1.8216E-08 )
  O00160J50( 1.5673E-04 )
  MG0240J50( 5.7755E-06 )
  MG0250J50( 7.3116E-07 )
  MG0260J50( 8.0501E-07 )
  AL0270J50( 5.7067E-06 )
  SI0280J50( 2.4758E-06 )
  SI0290J50( 1.2536E-07 )
  SI0300J50( 8.3215E-08 )
  CL0350J50( 6.6990E-06 )
  CL0370J50( 2.1422E-06 )
  CR0500J50( 1.3069E-07 )
  CR0520J50( 2.5202E-06 )
  CR0530J50( 2.8574E-07 )
  CR0540J50( 7.1134E-08 )
  FE0540J50( 1.1152E-06 )
  FE0560J50( 1.7337E-05 )
  FE0570J50( 3.9695E-07 )
  FE0580J50( 5.2926E-08 )
  NI0580J50( 2.5893E-07 )
  NI0600J50( 9.8989E-08 )
  NI0610J50( 4.2858E-09 )
  NI0620J50( 1.3616E-08 )
  NI0640J50( 3.4514E-09 )
  HF1740J50( 7.9659E-10 )
  HF1760J50( 2.5599E-08 )
  HF1770J50( 9.1490E-08 )
  HF1780J50( 1.3422E-07 )
  HF1790J50( 6.7017E-08 )
  HF1800J50( 1.7259E-07 )
*
* SUS304 CLADDING
& IDMAT(3)
  TPRECS( 0.1 )
  TEMPMT( <273.15+TP> )
  B00100J50( 1.4944E-06 )
  B00110J50( 6.0150E-06 )
  C00120J50( 2.0959E-04 )
  C00130J50( 2.3311E-06 )
  SI0280J50( 8.4167E-04 )
  SI0290J50( 4.2617E-05 )
  SI0300J50( 2.8290E-05 )
  P00310J50( 3.2378E-05 )
  S00320J50( 1.9388E-05 )
  S00330J50( 1.5303E-07 )
  S00340J50( 8.5901E-07 )
  S00360J50( 4.0808E-09 )
  CR0500J50( 7.3760E-04 )
  CR0520J50( 1.4224E-02 )
  CR0530J50( 1.6127E-03 )
  CR0540J50( 4.0148E-04 )
  MN0550J50( 1.1880E-03 )
  FE0540J50( 3.5498E-03 )
  FE0560J50( 5.5184E-02 )
  FE0570J50( 1.2635E-03 )
  FE0580J50( 1.6847E-04 )
  NI0580J50( 5.0923E-03 )
  NI0600J50( 1.9468E-03 )
  NI0610J50( 8.4288E-05 )
  NI0620J50( 2.6778E-04 )
  NI0640J50( 6.7878E-05 )
*
* SUS304 PLUG
& IDMAT(4)
  TPRECS( 0.1 )
  TEMPMT( <273.15+TP> )
  C00120J50( 1.0617E-04 )
  C00130J50( 1.1809E-06 )
  SI0280J50( 8.6253E-04 )
  SI0290J50( 4.3674E-05 )
  SI0300J50( 2.8991E-05 )
  P00310J50( 2.4669E-05 )
  S00320J50( 2.8304E-05 )
  S00330J50( 2.2340E-07 )
  S00340J50( 1.2540E-06 )
  S00360J50( 5.9574E-09 )
  CR0500J50( 7.4225E-04 )
  CR0520J50( 1.4314E-02 )
  CR0530J50( 1.6229E-03 )
  CR0540J50( 4.0401E-04 )
  MN0550J50( 1.1126E-03 )
  FE0540J50( 3.5599E-03 )
  FE0560J50( 5.5341E-02 )
  FE0570J50( 1.2671E-03 )
  FE0580J50( 1.6894E-04 )
  NI0580J50( 4.9719E-03 )
  NI0600J50( 1.9008E-03 )
  NI0610J50( 8.2295E-05 )
  NI0620J50( 2.6145E-04 )
  NI0640J50( 6.6273E-05 )
*
* MO DISC
& IDMAT(5)
  TPRECS( 0.1 )
  TEMPMT( <273.15+TP> )
  MO0920J50( 9.5767E-03 )
  MO0940J50( 5.9693E-03 )
  MO0950J50( 1.0274E-02 )
  MO0960J50( 1.0764E-02 )
  MO0970J50( 6.1629E-03 )
  MO0980J50( 1.5572E-02 )
  MO1000J50( 6.2145E-03 )
  H00010J50( 1.2284E-05 )
  O00160J50( 9.6734E-06 )
  N00140J50( 2.2017E-06 )
  N00150J50( 8.1766E-09 )
  NA0230J50( 2.1542E-06 )
  AL0270J50( 3.5532E-06 )
  SI0280J50( 5.3522E-06 )
  SI0290J50( 2.7100E-07 )
  SI0300J50( 1.7990E-07 )
  P00310J50( 5.9961E-07 )
  CA0400J50( 3.1479E-08 )
  CA0420J50( 6.4050E-09 )
  CA0430J50( 9.8908E-08 )
  CA0440J50( 1.9379E-10 )
  CA0460J50( 9.0425E-09 )
  CA0480J50( 8.6656E-09 )
  CR0500J50( 5.1732E-08 )
  CR0520J50( 9.9761E-07 )
  CR0530J50( 1.1311E-07 )
  CR0540J50( 2.8158E-08 )
  MN0550J50( 1.1269E-06 )
  FE0540J50( 2.6162E-07 )
  FE0560J50( 4.0672E-06 )
  FE0570J50( 9.3121E-08 )
  FE0580J50( 1.2416E-08 )
  NI0580J50( 7.2015E-07 )
  NI0600J50( 2.7532E-07 )
  NI0610J50( 1.1920E-08 )
  NI0620J50( 3.7869E-08 )
  NI0640J50( 9.5992E-09 )
  CU0630J50( 8.0864E-07 )
  CU0650J50( 3.6042E-07 )
  W01800J50( 3.6367E-09 )
  W01820J50( 7.9703E-07 )
  W01830J50( 4.3276E-07 )
  W01840J50( 9.3038E-07 )
  W01860J50( 8.6674E-07 )
*
* GRAPHITE
& IDMAT(6)
  TPRECS( 1.0 )
  TEMPMT( <273.15+TP> )
  C0012CJ50P00( 8.5785E-02 )
  C0013CJ50P00( 9.5413E-04 )
*
* MODERATOR
& IDMAT(7)
  TPRECS( 0.1 )
  TEMPMT( <273.15+TP> )
  H0001HJ50( <6.6689E-02*FRM/100.0> )
  O0016HJ50( <3.3346E-02*FRM/100.0> )
*
* REFLECTOR
& IDMAT(8)
  TPRECS( 0.1 )
  TEMPMT( <273.15+TP> )
  H0001HJ50( <6.6689E-02*FRR/100.0> )
  O0016HJ50( <3.3346E-02*FRR/100.0> )
*
* A6061 STD
& IDMAT(9)
  TPRECS( 0.1 )
  TEMPMT( <273.15+TP> )
  MG0240J50( 5.2843E-04 )
  MG0250J50( 6.6898E-05 )
  MG0260J50( 7.3655E-05 )
  AL0270J50( 5.8261E-02 )
  SI0280J50( 3.2037E-04 )
  SI0290J50( 1.6222E-05 )
  SI0300J50( 1.0768E-05 )
  TI0460J50( 4.0752E-06 )
  TI0470J50( 3.7187E-06 )
  TI0480J50( 3.7594E-05 )
  TI0490J50( 2.8017E-06 )
  TI0500J50( 2.7508E-06 )
  CR0500J50( 2.6495E-06 )
  CR0520J50( 5.1094E-05 )
  CR0530J50( 5.7929E-06 )
  CR0540J50( 1.4421E-06 )
  MN0550J50( 4.4395E-05 )
  FE0540J50( 1.2025E-05 )
  FE0560J50( 1.8694E-04 )
  FE0570J50( 4.2801E-06 )
  FE0580J50( 5.7068E-07 )
  CU0630J50( 4.8672E-05 )
  CU0650J50( 2.1694E-05 )
  ZN0640J50( 3.0209E-05 )
  ZN0660J50( 1.7342E-05 )
  ZN0670J50( 2.5485E-06 )
  ZN0680J50( 1.1686E-05 )
  ZN0700J50( 3.7295E-07 )
*
* SUS304 STD
& IDMAT(10)
  TPRECS( 0.1 )
  TEMPMT( <273.15+TP> )
  C00120J50( 3.1458E-04 )
  C00130J50( 3.4988E-06 )
  SI0280J50( 1.1762E-03 )
  SI0290J50( 5.9555E-05 )
  SI0300J50( 3.9533E-05 )
  P00310J50( 6.1672E-05 )
  S00320J50( 4.2456E-05 )
  S00330J50( 3.3510E-07 )
  S00340J50( 1.8811E-06 )
  S00360J50( 8.9361E-09 )
  CR0500J50( 7.5822E-04 )
  CR0520J50( 1.4622E-02 )
  CR0530J50( 1.6578E-03 )
  CR0540J50( 4.1270E-04 )
  MN0550J50( 1.7385E-03 )
  FE0540J50( 3.4612E-03 )
  FE0560J50( 5.3806E-02 )
  FE0570J50( 1.2319E-03 )
  FE0580J50( 1.6426E-04 )
  NI0580J50( 5.2775E-03 )
  NI0600J50( 2.0176E-03 )
  NI0610J50( 8.7352E-05 )
  NI0620J50( 2.7752E-04 )
  NI0640J50( 7.0346E-05 )
*
* NATURAL B4C
& IDMAT(11)
  TPRECS( 0.1 )
  TEMPMT( <273.15+TP> )
  B00100J50( 2.1688E-02 )
  B00110J50( 8.7299E-02 )
  C00120J50( 2.6947E-02 )
  C00130J50( 2.9971E-04 )
*
* ENRICHED B4C
& IDMAT(12)
  TPRECS( 0.1 )
  TEMPMT( <273.15+TP> )
  B00100J50( 9.8082E-02 )
  B00110J50( 7.7570E-03 )
  C00120J50( 2.6151E-02 )
  C00130J50( 2.9086E-04 )
*
$END XSEC
*
*--------+---------+---------+---------+---------+---------+---------+--
* GEOMETRY
*--------+---------+---------+---------+---------+---------+---------+--
```

```
$GEOMETRY
*
% DH1 = 32.0*<FPP>/SQRT(3)
% DH2 = 23.0*<FPP>/SQRT(3)
*
* hexagonal lattice (U-ZrH)
*
IDLAT(100)
 LTYP(2) NVLAT(<FPN> <FPN> 1)
 SZLAT(<FPP> 0.0 <FZ2-FZ1>)
 RCELL(12 12)
 SZHEX( 0.0 0.0 <DH1> <FZ2-FZ1> 0.0)
 CELLIDS(  0 1 2 3 4 5 )
 CELLSYMS( 0 1 2 3 X A )
 CKLATT(
                      A A A A A A A A A A A A 0 0 0 0 0 0 0 0 0 0 0
                     A A 3 3 3 3 3 3 3 3 3 A A 0 0 0 0 0 0 0 0 0 0
                    A 3 3 3 3 3 3 3 3 3 3 3 3 A 0 0 0 0 0 0 0 0 0
                   A 3 3 3 3 1 1 1 1 3 3 3 3 3 A 0 0 0 0 0 0 0 0
                  A 3 3 3 1 1 1 1 1 1 1 1 3 3 3 A 0 0 0 0 0 0 0
                 A 3 3 1 1 X 1 1 1 1 1 X 1 1 3 3 A 0 0 0 0 0 0
                A 3 3 1 1 1 1 1 1 1 1 1 1 1 1 3 3 A 0 0 0 0 0
               A 3 3 1 1 1 1 1 1 1 1 1 1 1 1 1 3 3 A 0 0 0 0
              A 3 3 1 1 X 1 1 2 2 2 2 1 1 X 1 1 3 3 A 0 0 0
             A 3 3 1 1 1 1 1 2 2 2 2 2 1 1 1 1 1 3 3 A 0 0
            A 3 3 3 1 1 1 1 2 2 2 2 2 2 1 1 1 1 3 3 3 A 0
           A A 3 3 1 X 1 1 2 2 2 2 2 2 2 1 1 X 1 3 3 A A
          0 A 3 3 3 1 1 1 1 2 2 2 2 2 2 1 1 1 1 3 3 3 A
         0 0 A 3 3 1 1 1 1 1 2 2 2 2 2 1 1 1 1 1 3 3 A
        0 0 0 A 3 3 1 1 X 1 1 2 2 2 2 1 1 X 1 1 3 3 A
       0 0 0 0 A 3 3 1 1 1 1 1 1 1 1 1 1 1 1 1 3 3 A
      0 0 0 0 0 A 3 3 1 1 1 1 1 1 1 1 1 1 1 1 3 3 A
     0 0 0 0 0 0 A 3 3 1 1 X 1 1 X 1 1 X 1 1 3 3 A
    0 0 0 0 0 0 0 A 3 3 3 1 1 1 1 1 1 1 1 3 3 3 A
   0 0 0 0 0 0 0 0 A 3 3 3 3 3 1 1 1 1 3 3 3 3 A
  0 0 0 0 0 0 0 0 0 A 3 3 3 3 3 3 3 3 3 3 3 3 A
 0 0 0 0 0 0 0 0 0 0 A A 3 3 3 3 3 3 3 3 3 A A
0 0 0 0 0 0 0 0 0 0 0 A A A A A A A A A A A A
  )
 KSLAT (<23*23>(0))
*
* hexagonal lattice (over U-ZrH)
*
IDLAT(200)
 LTYP(2) NVLAT(<FPN> <FPN> 1)
 SZLAT(<FPP> 0.0 <FZ15-FZ2>)
 RCELL(12 12)
 SZHEX( 0.0 0.0 <DH1> <FZ15-FZ2> 0.0)
 CELLIDS(  0 6 7 8 9 10 )
 CELLSYMS( 0 4 5 6 Y B )
 CKLATT(
                      B B B B B B B B B B B B 0 0 0 0 0 0 0 0 0 0 0
                     B B 6 6 6 6 6 6 6 6 6 B B 0 0 0 0 0 0 0 0 0 0
                    B 6 6 6 6 6 6 6 6 6 6 6 6 B 0 0 0 0 0 0 0 0 0
                   B 6 6 6 6 4 4 4 4 6 6 6 6 6 B 0 0 0 0 0 0 0 0
                  B 6 6 6 4 4 4 4 4 4 4 4 6 6 6 B 0 0 0 0 0 0 0
                 B 6 6 4 4 Y 4 4 4 4 4 Y 4 4 6 6 B 0 0 0 0 0 0
                B 6 6 4 4 4 4 4 4 4 4 4 4 4 4 6 6 B 0 0 0 0 0
               B 6 6 4 4 4 4 4 4 4 4 4 4 4 4 4 6 6 B 0 0 0 0
              B 6 6 4 4 Y 4 4 5 5 5 5 4 4 Y 4 4 6 6 B 0 0 0
             B 6 6 4 4 4 4 4 5 5 5 5 5 4 4 4 4 4 6 6 B 0 0
            B 6 6 6 4 4 4 4 5 5 5 5 5 5 4 4 4 4 6 6 6 B 0
           B B 6 6 4 Y 4 4 5 5 5 5 5 5 5 4 4 Y 4 6 6 B B
          0 B 6 6 6 4 4 4 4 5 5 5 5 5 5 4 4 4 4 6 6 6 B
         0 0 B 6 6 4 4 4 4 4 5 5 5 5 5 4 4 4 4 4 6 6 B
        0 0 0 B 6 6 4 4 Y 4 4 5 5 5 5 4 4 Y 4 4 6 6 B
       0 0 0 0 B 6 6 4 4 4 4 4 4 4 4 4 4 4 4 4 6 6 B
      0 0 0 0 0 B 6 6 4 4 4 4 4 4 4 4 4 4 4 4 6 6 B
     0 0 0 0 0 0 B 6 6 4 4 Y 4 4 Y 4 4 Y 4 4 6 6 B
    0 0 0 0 0 0 0 B 6 6 6 4 4 4 4 4 4 4 4 6 6 6 B
   0 0 0 0 0 0 0 0 B 6 6 6 6 6 4 4 4 4 6 6 6 6 B
  0 0 0 0 0 0 0 0 0 B 6 6 6 6 6 6 6 6 6 6 6 6 B
 0 0 0 0 0 0 0 0 0 0 B B 6 6 6 6 6 6 6 6 6 B B
0 0 0 0 0 0 0 0 0 0 0 B B B B B B B B B B B B
  )
 KSLAT (<23*23>(0))
*
* hexagonal lattice (under U-ZrH)
*
IDLAT(300)
 LTYP(2) NVLAT(<FPN> <FPN> 1)
 SZLAT(<FPP> 0.0 <FZ1-GBB>)
 RCELL(12 12)
 SZHEX( 0.0 0.0 <DH1> <FZ1-GBB> 0.0)
 CELLIDS(  0 11 12 13 14 15 )
 CELLSYMS( 0 7 8 9 Z C )
 CKLATT(
                      C C C C C C C C C C C C 0 0 0 0 0 0 0 0 0 0 0
                     C C 9 9 9 9 9 9 9 9 9 C C 0 0 0 0 0 0 0 0 0 0
                    C 9 9 9 9 9 9 9 9 9 9 9 9 C 0 0 0 0 0 0 0 0 0
                   C 9 9 9 9 7 7 7 7 9 9 9 9 9 C 0 0 0 0 0 0 0 0
                  C 9 9 9 7 7 7 7 7 7 7 7 9 9 9 C 0 0 0 0 0 0 0
                 C 9 9 7 7 Z 7 7 7 7 7 Z 7 7 9 9 C 0 0 0 0 0 0
                C 9 9 7 7 7 7 7 7 7 7 7 7 7 7 9 9 C 0 0 0 0 0
               C 9 9 7 7 7 7 7 7 7 7 7 7 7 7 7 9 9 C 0 0 0 0
              C 9 9 7 7 Z 7 7 8 8 8 8 7 7 Z 7 7 9 9 C 0 0 0
             C 9 9 7 7 7 7 7 8 8 8 8 8 7 7 7 7 7 9 9 C 0 0
            C 9 9 9 7 7 7 7 8 8 8 8 8 8 7 7 7 7 9 9 9 C 0
           C C 9 9 7 Z 7 7 8 8 8 8 8 8 8 7 7 Z 7 9 9 C C
          0 C 9 9 9 7 7 7 7 8 8 8 8 8 8 7 7 7 7 9 9 9 C
         0 0 C 9 9 7 7 7 7 7 8 8 8 8 8 7 7 7 7 7 9 9 C
        0 0 0 C 9 9 7 7 Z 7 7 8 8 8 8 7 7 Z 7 7 9 9 C
       0 0 0 0 C 9 9 7 7 7 7 7 7 7 7 7 7 7 7 7 9 9 C
      0 0 0 0 0 C 9 9 7 7 7 7 7 7 7 7 7 7 7 7 9 9 C
     0 0 0 0 0 0 C 9 9 7 7 Z 7 7 Z 7 7 Z 7 7 9 9 C
    0 0 0 0 0 0 0 C 9 9 9 7 7 7 7 7 7 7 7 9 9 9 C
   0 0 0 0 0 0 0 0 C 9 9 9 9 9 7 7 7 7 9 9 9 9 C
  0 0 0 0 0 0 0 0 0 C 9 9 9 9 9 9 9 9 9 9 9 9 C
 0 0 0 0 0 0 0 0 0 0 C C 9 9 9 9 9 9 9 9 9 C C
0 0 0 0 0 0 0 0 0 0 0 C C C C C C C C C C C C
  )
 KSLAT (<23*23>(0))
*
END
*--------+---------+---------+---------+---------+---------+---------+--
* BODY
*--------+---------+---------+---------+---------+---------+---------+--
*
* outer boundary
CYL (100000  0.0  0.0  <EHB>      <ECT-EHB>      <SH1+30.0> )
* experimental tube
RHP ( 10000  0.0  0.0  <EHB>      <EHT-EHB>      <EH1>      )
RHP ( 20000  0.0  0.0  <EHB>      <EHT-EHB>      <EH2>      )
CYL ( 30000  0.0  0.0  <EHT>      <ECT-EHT>      <EC1>      )
CYL ( 40000  0.0  0.0  <EHT>      <ECT-EHT>      <EC2>      )
* shroud
CYL ( 50000  0.0  0.0  <GBB>      <GTT-GBB>      <SH1>      )
CYL ( 51000  0.0  0.0  <GBB>      <GTT-GBB>      <SH2>      )
* grid
CYL ( 60000  0.0  0.0  <GTB>      <GTT-GTB>      <SH2>      ) /* t_g
CYL ( 61000  0.0  0.0  <GBB>      <FZ7-GBB>      <SH2>      ) /* b-g
* over shroud
CYL ( 70000  0.0  0.0  <GTT>      <FZ15-GTT>     <SH1>      )
CYL ( 71000  0.0  0.0  <GTT>      <FZ15-GTT>     <SH2>      )
* guide tube TA
CYL (   500 < 9.0*PPP> 0.0       <GZB> <ECT-GZB>  <GR1>      )
CYL (   501 < 9.0*PPP> 0.0       <GZB> <ECT-GZB>  <GR2>      )
* guide tube TB
CYL (   510 <-4.5*PPP> <-4.5*FPP> <GZB> <ECT-GZB>  <GR1>      )
CYL (   511 <-4.5*PPP> <-4.5*FPP> <GZB> <ECT-GZB>  <GR2>      )
* guide tube TC
CYL (   520 <-4.5*PPP> < 4.5*FPP> <GZB> <ECT-GZB>  <GR1>      )
CYL (   521 <-4.5*PPP> < 4.5*FPP> <GZB> <ECT-GZB>  <GR2>      )
* grid water hole 1
CYL ( 60110 <  4.5*PPP> < 9.5*FPP> <GTB> <GTT-GTB>  <GTRF>    ) /* tg
TRC ( 60111 <  4.5*PPP> < 9.5*FPP> <GBT>   0.0  0.0  <FZ7-GBT>
                                   <GBRF>  <FR11>    ) /* bg1
CYL ( 60112 <  4.5*PPP> < 9.5*FPP> <GBB> <GBT-GBB>  <GBRF>    ) /* bg2
CYL ( 60120 <  6.0*PPP> < 9.0*FPP> <GTB> <GTT-GTB>  <GTRF>    ) /* tg
TRC ( 60121 <  6.0*PPP> < 9.0*FPP> <GBT>   0.0  0.0  <FZ7-GBT>
                                   <GBRF>  <FR11>    ) /* bg1
CYL ( 60122 <  6.0*PPP> < 9.0*FPP> <GBB> <GBT-GBB>  <GBRF>    ) /* bg2
CYL ( 60130 <  7.5*PPP> < 8.5*FPP> <GTB> <GTT-GTB>  <GTRF>    ) /* tg
TRC ( 60131 <  7.5*PPP> < 8.5*FPP> <GBT>   0.0  0.0  <FZ7-GBT>
                                   <GBRF>  <FR11>    ) /* bg1
CYL ( 60132 <  7.5*PPP> < 8.5*FPP> <GBB> <GBT-GBB>  <GBRF>    ) /* bg2
CYL ( 60140 <  9.0*PPP> < 8.0*FPP> <GTB> <GTT-GTB>  <GTRF>    ) /* tg
TRC ( 60141 <  9.0*PPP> < 8.0*FPP> <GBT>   0.0  0.0  <FZ7-GBT>
                                   <GBRF>  <FR11>    ) /* bg1
CYL ( 60142 <  9.0*PPP> < 8.0*FPP> <GBB> <GBT-GBB>  <GBRF>    ) /* bg2
CYL ( 60150 < 10.5*PPP> < 7.5*FPP> <GTB> <GTT-GTB>  <GTRF>    ) /* tg
TRC ( 60151 < 10.5*PPP> < 7.5*FPP> <GBT>   0.0  0.0  <FZ7-GBT>
                                   <GBRF>  <FR11>    ) /* bg1
CYL ( 60152 < 10.5*PPP> < 7.5*FPP> <GBB> <GBT-GBB>  <GBRF>    ) /* bg2
CYL ( 60160 < 12.0*PPP> < 7.0*FPP> <GTB> <GTT-GTB>  <GTRF>    ) /* tg
TRC ( 60161 < 12.0*PPP> < 7.0*FPP> <GBT>   0.0  0.0  <FZ7-GBT>
                                   <GBRF>  <FR11>    ) /* bg1
CYL ( 60162 < 12.0*PPP> < 7.0*FPP> <GBB> <GBT-GBB>  <GBRF>    ) /* bg2
* grid water hole 2
CYL ( 60210 < 16.5*PPP> < 2.5*FPP> <GTB> <GTT-GTB>  <GTRF>    ) /* tg
TRC ( 60211 < 16.5*PPP> < 2.5*FPP> <GBT>   0.0  0.0  <FZ7-GBT>
                                   <GBRF>  <FR11>    ) /* bg1
CYL ( 60212 < 16.5*PPP> < 2.5*FPP> <GBB> <GBT-GBB>  <GBRF>    ) /* bg2
CYL ( 60220 < 16.5*PPP> < 1.5*FPP> <GTB> <GTT-GTB>  <GTRF>    ) /* tg
TRC ( 60221 < 16.5*PPP> < 1.5*FPP> <GBT>   0.0  0.0  <FZ7-GBT>
                                   <GBRF>  <FR11>    ) /* bg1
CYL ( 60222 < 16.5*PPP> < 1.5*FPP> <GBB> <GBT-GBB>  <GBRF>    ) /* bg2
CYL ( 60230 < 16.5*PPP> < 0.5*FPP> <GTB> <GTT-GTB>  <GTRF>    ) /* tg
TRC ( 60231 < 16.5*PPP> < 0.5*FPP> <GBT>   0.0  0.0  <FZ7-GBT>
                                   <GBRF>  <FR11>    ) /* bg1
CYL ( 60232 < 16.5*PPP> < 0.5*FPP> <GBB> <GBT-GBB>  <GBRF>    ) /* bg2
CYL ( 60240 < 16.5*PPP> <-0.5*FPP> <GTB> <GTT-GTB>  <GTRF>    ) /* tg
TRC ( 60241 < 16.5*PPP> <-0.5*FPP> <GBT>   0.0  0.0  <FZ7-GBT>
                                   <GBRF>  <FR11>    ) /* bg1
CYL ( 60242 < 16.5*PPP> <-0.5*FPP> <GBB> <GBT-GBB>  <GBRF>    ) /* bg2
CYL ( 60250 < 16.5*PPP> <-1.5*FPP> <GTB> <GTT-GTB>  <GTRF>    ) /* tg
TRC ( 60251 < 16.5*PPP> <-1.5*FPP> <GBT>   0.0  0.0  <FZ7-GBT>
                                   <GBRF>  <FR11>    ) /* bg1
CYL ( 60252 < 16.5*PPP> <-1.5*FPP> <GBB> <GBT-GBB>  <GBRF>    ) /* bg2
CYL ( 60260 < 16.5*PPP> <-2.5*FPP> <GTB> <GTT-GTB>  <GTRF>    ) /* tg
TRC ( 60261 < 16.5*PPP> <-2.5*FPP> <GBT>   0.0  0.0  <FZ7-GBT>
                                   <GBRF>  <FR11>    ) /* bg1
CYL ( 60262 < 16.5*PPP> <-2.5*FPP> <GBB> <GBT-GBB>  <GBRF>    ) /* bg2
* grid water hole 3
CYL ( 60310 <  4.5*PPP> <-9.5*FPP> <GTB> <GTT-GTB>  <GTRF>    ) /* tg
TRC ( 60311 <  4.5*PPP> <-9.5*FPP> <GBT>   0.0  0.0  <FZ7-GBT>
                                   <GBRF>  <FR11>    ) /* bg1
CYL ( 60312 <  4.5*PPP> <-9.5*FPP> <GBB> <GBT-GBB>  <GBRF>    ) /* bg2
CYL ( 60320 <  6.0*PPP> <-9.0*FPP> <GTB> <GTT-GTB>  <GTRF>    ) /* tg
TRC ( 60321 <  6.0*PPP> <-9.0*FPP> <GBT>   0.0  0.0  <FZ7-GBT>
                                   <GBRF>  <FR11>    ) /* bg1
CYL ( 60322 <  6.0*PPP> <-9.0*FPP> <GBB> <GBT-GBB>  <GBRF>    ) /* bg2
CYL ( 60330 <  7.5*PPP> <-8.5*FPP> <GTB> <GTT-GTB>  <GTRF>    ) /* tg
TRC ( 60331 <  7.5*PPP> <-8.5*FPP> <GBT>   0.0  0.0  <FZ7-GBT>
                                   <GBRF>  <FR11>    ) /* bg1
CYL ( 60332 <  7.5*PPP> <-8.5*FPP> <GBB> <GBT-GBB>  <GBRF>    ) /* bg2
CYL ( 60340 <  9.0*PPP> <-8.0*FPP> <GTB> <GTT-GTB>  <GTRF>    ) /* tg
TRC ( 60341 <  9.0*PPP> <-8.0*FPP> <GBT>   0.0  0.0  <FZ7-GBT>
                                   <GBRF>  <FR11>    ) /* bg1
CYL ( 60342 <  9.0*PPP> <-8.0*FPP> <GBB> <GBT-GBB>  <GBRF>    ) /* bg2
CYL ( 60350 < 10.5*PPP> <-7.5*FPP> <GTB> <GTT-GTB>  <GTRF>    ) /* tg
TRC ( 60351 < 10.5*PPP> <-7.5*FPP> <GBT>   0.0  0.0  <FZ7-GBT>
                                   <GBRF>  <FR11>    ) /* bg1
CYL ( 60352 < 10.5*PPP> <-7.5*FPP> <GBB> <GBT-GBB>  <GBRF>    ) /* bg2
CYL ( 60360 < 12.0*PPP> <-7.0*FPP> <GTB> <GTT-GTB>  <GTRF>    ) /* tg
TRC ( 60361 < 12.0*PPP> <-7.0*FPP> <GBT>   0.0  0.0  <FZ7-GBT>
                                   <GBRF>  <FR11>    ) /* bg1
CYL ( 60362 < 12.0*PPP> <-7.0*FPP> <GBB> <GBT-GBB>  <GBRF>    ) /* bg2
* grid water hole 4
CYL ( 60410 < -4.5*PPP> <-9.5*FPP> <GTB> <GTT-GTB>  <GTRF>    ) /* tg
TRC ( 60411 < -4.5*PPP> <-9.5*FPP> <GBT>   0.0  0.0  <FZ7-GBT>
                                   <GBRF>  <FR11>    ) /* bg1
CYL ( 60412 < -4.5*PPP> <-9.5*FPP> <GBB> <GBT-GBB>  <GBRF>    ) /* bg2
CYL ( 60420 < -6.0*PPP> <-9.0*FPP> <GTB> <GTT-GTB>  <GTRF>    ) /* tg
TRC ( 60421 < -6.0*PPP> <-9.0*FPP> <GBT>   0.0  0.0  <FZ7-GBT>
                                   <GBRF>  <FR11>    ) /* bg1
CYL ( 60422 < -6.0*PPP> <-9.0*FPP> <GBB> <GBT-GBB>  <GBRF>    ) /* bg2
CYL ( 60430 < -7.5*PPP> <-8.5*FPP> <GTB> <GTT-GTB>  <GTRF>    ) /* tg
TRC ( 60431 < -7.5*PPP> <-8.5*FPP> <GBT>   0.0  0.0  <FZ7-GBT>
                                   <GBRF>  <FR11>    ) /* bg1
CYL ( 60432 < -7.5*PPP> <-8.5*FPP> <GBB> <GBT-GBB>  <GBRF>    ) /* bg2
CYL ( 60440 < -9.0*PPP> <-8.0*FPP> <GTB> <GTT-GTB>  <GTRF>    ) /* tg
TRC ( 60441 < -9.0*PPP> <-8.0*FPP> <GBT>   0.0  0.0  <FZ7-GBT>
                                   <GBRF>  <FR11>    ) /* bg1
CYL ( 60442 < -9.0*PPP> <-8.0*FPP> <GBB> <GBT-GBB>  <GBRF>    ) /* bg2
CYL ( 60450 <-10.5*PPP> <-7.5*FPP> <GTB> <GTT-GTB>  <GTRF>    ) /* tg
TRC ( 60451 <-10.5*PPP> <-7.5*FPP> <GBT>   0.0  0.0  <FZ7-GBT>
                                   <GBRF>  <FR11>    ) /* bg1
CYL ( 60452 <-10.5*PPP> <-7.5*FPP> <GBB> <GBT-GBB>  <GBRF>    ) /* bg2
CYL ( 60460 <-12.0*PPP> <-7.0*FPP> <GTB> <GTT-GTB>  <GTRF>    ) /* tg
TRC ( 60461 <-12.0*PPP> <-7.0*FPP> <GBT>   0.0  0.0  <FZ7-GBT>
                                   <GBRF>  <FR11>    ) /* bg1
CYL ( 60462 <-12.0*PPP> <-7.0*FPP> <GBB> <GBT-GBB>  <GBRF>    ) /* bg2
* grid water hole 5
CYL ( 60510 <-16.5*PPP> < 2.5*FPP> <GTB> <GTT-GTB>  <GTRF>    ) /* tg
TRC ( 60511 <-16.5*PPP> < 2.5*FPP> <GBT>   0.0  0.0  <FZ7-GBT>
                                   <GBRF>  <FR11>    ) /* bg1
CYL ( 60512 <-16.5*PPP> < 2.5*FPP> <GBB> <GBT-GBB>  <GBRF>    ) /* bg2
CYL ( 60520 <-16.5*PPP> < 1.5*FPP> <GTB> <GTT-GTB>  <GTRF>    ) /* tg
TRC ( 60521 <-16.5*PPP> < 1.5*FPP> <GBT>   0.0  0.0  <FZ7-GBT>
                                   <GBRF>  <FR11>    ) /* bg1
CYL ( 60522 <-16.5*PPP> < 1.5*FPP> <GBB> <GBT-GBB>  <GBRF>    ) /* bg2
CYL ( 60530 <-16.5*PPP> < 0.5*FPP> <GTB> <GTT-GTB>  <GTRF>    ) /* tg
TRC ( 60531 <-16.5*PPP> < 0.5*FPP> <GBT>   0.0  0.0  <FZ7-GBT>
                                   <GBRF>  <FR11>    ) /* bg1
CYL ( 60532 <-16.5*PPP> < 0.5*FPP> <GBB> <GBT-GBB>  <GBRF>    ) /* bg2
CYL ( 60540 <-16.5*PPP> <-0.5*FPP> <GTB> <GTT-GTB>  <GTRF>    ) /* tg
TRC ( 60541 <-16.5*PPP> <-0.5*FPP> <GBT>   0.0  0.0  <FZ7-GBT>
```

```
                                     <GBRF>  <FR11>    ) /* bg1
CYL ( 60542 <-16.5*PPP> <-0.5*FPP> <GBB> <GBT-GBB>  <GBRF>    ) /* bg2
CYL ( 60550 <-16.5*PPP> <-1.5*FPP> <GTB> <GTT-GTB>  <GTRF>    ) /* tg
TRC ( 60551 <-16.5*PPP> <-1.5*FPP> <GBT>   0.0  0.0  <FZ7-GBT>
                                     <GBRF>  <FR11>    ) /* bg1
CYL ( 60552 <-16.5*PPP> <-1.5*FPP> <GBB> <GBT-GBB>  <GBRF>    ) /* bg2
CYL ( 60560 <-16.5*PPP> <-2.5*FPP> <GTB> <GTT-GTB>  <GTRF>    ) /* tg
TRC ( 60561 <-16.5*PPP> <-2.5*FPP> <GBT>   0.0  0.0  <FZ7-GBT>
                                     <GBRF>  <FR11>    ) /* bg1
CYL ( 60562 <-16.5*PPP> <-2.5*FPP> <GBB> <GBT-GBB>  <GBRF>    ) /* bg2
* grid water hole 6
CYL ( 60610 < -4.5*PPP> < 9.5*FPP> <GTB> <GTT-GTB>  <GTRF>    ) /* tg
TRC ( 60611 < -4.5*PPP> < 9.5*FPP> <GBT>   0.0  0.0  <FZ7-GBT>
                                     <GBRF>  <FR11>    ) /* bg1
CYL ( 60612 < -4.5*PPP> < 9.5*FPP> <GBB> <GBT-GBB>  <GBRF>    ) /* bg2
CYL ( 60620 < -6.0*PPP> < 9.0*FPP> <GTB> <GTT-GTB>  <GTRF>    ) /* tg
TRC ( 60621 < -6.0*PPP> < 9.0*FPP> <GBT>   0.0  0.0  <FZ7-GBT>
                                     <GBRF>  <FR11>    ) /* bg1
CYL ( 60622 < -6.0*PPP> < 9.0*FPP> <GBB> <GBT-GBB>  <GBRF>    ) /* bg2
CYL ( 60630 < -7.5*PPP> < 8.5*FPP> <GTB> <GTT-GTB>  <GTRF>    ) /* tg
TRC ( 60631 < -7.5*PPP> < 8.5*FPP> <GBT>   0.0  0.0  <FZ7-GBT>
                                     <GBRF>  <FR11>    ) /* bg1
CYL ( 60632 < -7.5*PPP> < 8.5*FPP> <GBB> <GBT-GBB>  <GBRF>    ) /* bg2
CYL ( 60640 < -9.0*PPP> < 8.0*FPP> <GTB> <GTT-GTB>  <GTRF>    ) /* tg
TRC ( 60641 < -9.0*PPP> < 8.0*FPP> <GBT>   0.0  0.0  <FZ7-GBT>
                                     <GBRF>  <FR11>    ) /* bg1
CYL ( 60642 < -9.0*PPP> < 8.0*FPP> <GBB> <GBT-GBB>  <GBRF>    ) /* bg2
CYL ( 60650 <-10.5*PPP> < 7.5*FPP> <GTB> <GTT-GTB>  <GTRF>    ) /* tg
TRC ( 60651 <-10.5*PPP> < 7.5*FPP> <GBT>   0.0  0.0  <FZ7-GBT>
                                     <GBRF>  <FR11>    ) /* bg1
CYL ( 60652 <-10.5*PPP> < 7.5*FPP> <GBB> <GBT-GBB>  <GBRF>    ) /* bg2
CYL ( 60660 <-12.0*PPP> < 7.0*FPP> <GTB> <GTT-GTB>  <GTRF>    ) /* tg
TRC ( 60661 <-12.0*PPP> < 7.0*FPP> <GBT>   0.0  0.0  <FZ7-GBT>
                                     <GBRF>  <FR11>    ) /* bg1
CYL ( 60662 <-12.0*PPP> < 7.0*FPP> <GBB> <GBT-GBB>  <GBRF>    ) /* bg2
* control rod 1
CYL (  1001 0.0       < 6.0*FPP> <C1Z1> <C1Z2-C1Z1> <CR1>    ) /* zr
CYL (  1002 0.0       < 6.0*FPP> <C1Z1> <C1Z2-C1Z1> <CR2>    ) /* v
CYL (  1003 0.0       < 6.0*FPP> <C1Z1> <C1Z2-C1Z1> <CR3>    ) /* UZrH
CYL (  1004 0.0       < 6.0*FPP> <C1Z1> <C1Z7-C1Z1> <CR4>    ) /* v
CYL (  1005 0.0       < 6.0*FPP> <C1Z3> <C1Z1-C1Z3> <CR4>    ) /* sp1
CYL (  1006 0.0       < 6.0*FPP> <C1Z4> <C1Z3-C1Z4> <CR7>    ) /* v
CYL (  1007 0.0       < 6.0*FPP> <C1Z4> <C1Z3-C1Z4> <CR8>    ) /* st
CYL (  1008 0.0       < 6.0*FPP> <C1Z4> <C1Z3-C1Z4> <CR4>    ) /* v
CYL (  1009 0.0       < 6.0*FPP> <C1Z5> <C1Z4-C1Z5> <CR4>    ) /* bp
CYL (  1010 0.0       < 6.0*FPP> <C1Z7> <C1Z8-C1Z7> <CR4>    ) /* sp2
CYL (  1011 0.0       < 6.0*FPP> <C1Z8> <C1Z9-C1Z8> <CR6>    ) /* b4c
CYL (  1012 0.0       < 6.0*FPP> <C1Z8> <C1Z10-C1Z8> <CR4>   ) /* v
CYL (  1013 0.0       < 6.0*FPP> <C1Z10> <C1Z11-C1Z10> <CR4> ) /* sp3
CYL (  1014 0.0       < 6.0*FPP> <C1Z11> <C1Z12-C1Z11> <CR4> ) /* v
CYL (  1015 0.0       < 6.0*FPP> <C1Z12> <C1Z13-C1Z12> <CR4> ) /* tp
CYL (  1016 0.0       < 6.0*FPP> <C1Z5> <C1Z13-C1Z5> <CR5>   ) /* clad
* control rod 2
CYL (  2001 < 9.0*PPP> < 3.0*FPP> <C2Z1> <C2Z2-C2Z1> <CR1>    ) /* zr
CYL (  2002 < 9.0*PPP> < 3.0*FPP> <C2Z1> <C2Z2-C2Z1> <CR2>    ) /* v
CYL (  2003 < 9.0*PPP> < 3.0*FPP> <C2Z1> <C2Z2-C2Z1> <CR3>    ) /* UZrH
CYL (  2004 < 9.0*PPP> < 3.0*FPP> <C2Z1> <C2Z7-C2Z1> <CR4>    ) /* v
CYL (  2005 < 9.0*PPP> < 3.0*FPP> <C2Z3> <C2Z1-C2Z3> <CR4>    ) /* sp1
CYL (  2006 < 9.0*PPP> < 3.0*FPP> <C2Z4> <C2Z3-C2Z4> <CR7>    ) /* v
CYL (  2007 < 9.0*PPP> < 3.0*FPP> <C2Z4> <C2Z3-C2Z4> <CR8>    ) /* st
CYL (  2008 < 9.0*PPP> < 3.0*FPP> <C2Z4> <C2Z3-C2Z4> <CR4>    ) /* v
CYL (  2009 < 9.0*PPP> < 3.0*FPP> <C2Z5> <C2Z4-C2Z5> <CR4>    ) /* bp
CYL (  2010 < 9.0*PPP> < 3.0*FPP> <C2Z7> <C2Z8-C2Z7> <CR4>    ) /* sp2
CYL (  2011 < 9.0*PPP> < 3.0*FPP> <C2Z8> <C2Z9-C2Z8> <CR6>    ) /* b4c
CYL (  2012 < 9.0*PPP> < 3.0*FPP> <C2Z8> <C2Z10-C2Z8> <CR4>   ) /* v
CYL (  2013 < 9.0*PPP> < 3.0*FPP> <C2Z10> <C2Z11-C2Z10> <CR4> ) /* sp3
CYL (  2014 < 9.0*PPP> < 3.0*FPP> <C2Z11> <C2Z12-C2Z11> <CR4> ) /* v
CYL (  2015 < 9.0*PPP> < 3.0*FPP> <C2Z12> <C2Z13-C2Z12> <CR4> ) /* tp
CYL (  2016 < 9.0*PPP> < 3.0*FPP> <C2Z5> <C2Z13-C2Z5> <CR5>   ) /* clad
* control rod 3
CYL (  3001 < 9.0*PPP> <-3.0*FPP> <C3Z1> <C3Z2-C3Z1> <CR1>    ) /* zr
CYL (  3002 < 9.0*PPP> <-3.0*FPP> <C3Z1> <C3Z2-C3Z1> <CR2>    ) /* v
CYL (  3003 < 9.0*PPP> <-3.0*FPP> <C3Z1> <C3Z2-C3Z1> <CR3>    ) /* UZrH
CYL (  3004 < 9.0*PPP> <-3.0*FPP> <C3Z1> <C3Z7-C3Z1> <CR4>    ) /* v
CYL (  3005 < 9.0*PPP> <-3.0*FPP> <C3Z3> <C3Z1-C3Z3> <CR4>    ) /* sp1
CYL (  3006 < 9.0*PPP> <-3.0*FPP> <C3Z4> <C3Z3-C3Z4> <CR7>    ) /* v
CYL (  3007 < 9.0*PPP> <-3.0*FPP> <C3Z4> <C3Z3-C3Z4> <CR8>    ) /* st
CYL (  3008 < 9.0*PPP> <-3.0*FPP> <C3Z4> <C3Z3-C3Z4> <CR4>    ) /* v
CYL (  3009 < 9.0*PPP> <-3.0*FPP> <C3Z5> <C3Z4-C3Z5> <CR4>    ) /* bp
CYL (  3010 < 9.0*PPP> <-3.0*FPP> <C3Z7> <C3Z8-C3Z7> <CR4>    ) /* sp2
CYL (  3011 < 9.0*PPP> <-3.0*FPP> <C3Z8> <C3Z9-C3Z8> <CR6>    ) /* b4c
CYL (  3012 < 9.0*PPP> <-3.0*FPP> <C3Z8> <C3Z10-C3Z8> <CR4>   ) /* v
CYL (  3013 < 9.0*PPP> <-3.0*FPP> <C3Z10> <C3Z11-C3Z10> <CR4> ) /* sp3
CYL (  3014 < 9.0*PPP> <-3.0*FPP> <C3Z11> <C3Z12-C3Z11> <CR4> ) /* v
CYL (  3015 < 9.0*PPP> <-3.0*FPP> <C3Z12> <C3Z13-C3Z12> <CR4> ) /* tp
CYL (  3016 < 9.0*PPP> <-3.0*FPP> <C3Z5> <C3Z13-C3Z5> <CR5>   ) /* clad
* control rod 4
CYL (  4001 0.0       <-6.0*FPP> <C4Z1> <C4Z2-C4Z1> <CR1>    ) /* zr
CYL (  4002 0.0       <-6.0*FPP> <C4Z1> <C4Z2-C4Z1> <CR2>    ) /* v
CYL (  4003 0.0       <-6.0*FPP> <C4Z1> <C4Z2-C4Z1> <CR3>    ) /* UZrH
CYL (  4004 0.0       <-6.0*FPP> <C4Z1> <C4Z7-C4Z1> <CR4>    ) /* v
CYL (  4005 0.0       <-6.0*FPP> <C4Z3> <C4Z1-C4Z3> <CR4>    ) /* sp1
CYL (  4006 0.0       <-6.0*FPP> <C4Z4> <C4Z3-C4Z4> <CR7>    ) /* v
CYL (  4007 0.0       <-6.0*FPP> <C4Z4> <C4Z3-C4Z4> <CR8>    ) /* st
CYL (  4008 0.0       <-6.0*FPP> <C4Z4> <C4Z3-C4Z4> <CR4>    ) /* v
CYL (  4009 0.0       <-6.0*FPP> <C4Z5> <C4Z4-C4Z5> <CR4>    ) /* bp
CYL (  4010 0.0       <-6.0*FPP> <C4Z7> <C4Z8-C4Z7> <CR4>    ) /* sp2
CYL (  4011 0.0       <-6.0*FPP> <C4Z8> <C4Z9-C4Z8> <CR6>    ) /* b4c
CYL (  4012 0.0       <-6.0*FPP> <C4Z8> <C4Z10-C4Z8> <CR4>   ) /* v
CYL (  4013 0.0       <-6.0*FPP> <C4Z10> <C4Z11-C4Z10> <CR4> ) /* sp3
CYL (  4014 0.0       <-6.0*FPP> <C4Z11> <C4Z12-C4Z11> <CR4> ) /* v
CYL (  4015 0.0       <-6.0*FPP> <C4Z12> <C4Z13-C4Z12> <CR4> ) /* tp
CYL (  4016 0.0       <-6.0*FPP> <C4Z5> <C4Z13-C4Z5> <CR5>   ) /* clad
* control rod 5
CYL (  5001 <-9.0*PPP> <-3.0*FPP> <C5Z1> <C5Z2-C5Z1> <CR1>    ) /* zr
CYL (  5002 <-9.0*PPP> <-3.0*FPP> <C5Z1> <C5Z2-C5Z1> <CR2>    ) /* v
CYL (  5003 <-9.0*PPP> <-3.0*FPP> <C5Z1> <C5Z2-C5Z1> <CR3>    ) /* UZrH
CYL (  5004 <-9.0*PPP> <-3.0*FPP> <C5Z1> <C5Z7-C5Z1> <CR4>    ) /* v
CYL (  5005 <-9.0*PPP> <-3.0*FPP> <C5Z3> <C5Z1-C5Z3> <CR4>    ) /* sp1
CYL (  5006 <-9.0*PPP> <-3.0*FPP> <C5Z4> <C5Z3-C5Z4> <CR7>    ) /* v
CYL (  5007 <-9.0*PPP> <-3.0*FPP> <C5Z4> <C5Z3-C5Z4> <CR8>    ) /* st
CYL (  5008 <-9.0*PPP> <-3.0*FPP> <C5Z4> <C5Z3-C5Z4> <CR4>    ) /* v
CYL (  5009 <-9.0*PPP> <-3.0*FPP> <C5Z5> <C5Z4-C5Z5> <CR4>    ) /* bp
CYL (  5010 <-9.0*PPP> <-3.0*FPP> <C5Z7> <C5Z8-C5Z7> <CR4>    ) /* sp2
CYL (  5011 <-9.0*PPP> <-3.0*FPP> <C5Z8> <C5Z9-C5Z8> <CR6>    ) /* b4c
CYL (  5012 <-9.0*PPP> <-3.0*FPP> <C5Z8> <C5Z10-C5Z8> <CR4>   ) /* v
CYL (  5013 <-9.0*PPP> <-3.0*FPP> <C5Z10> <C5Z11-C5Z10> <CR4> ) /* sp3
CYL (  5014 <-9.0*PPP> <-3.0*FPP> <C5Z11> <C5Z12-C5Z11> <CR4> ) /* v
CYL (  5015 <-9.0*PPP> <-3.0*FPP> <C5Z12> <C5Z13-C5Z12> <CR4> ) /* tp
CYL (  5016 <-9.0*PPP> <-3.0*FPP> <C5Z5> <C5Z13-C5Z5> <CR5>   ) /* clad
* control rod 6
CYL (  6001 <-9.0*PPP> < 3.0*FPP> <C6Z1> <C6Z2-C6Z1> <CR1>    ) /* zr
CYL (  6002 <-9.0*PPP> < 3.0*FPP> <C6Z1> <C6Z2-C6Z1> <CR2>    ) /* v
CYL (  6003 <-9.0*PPP> < 3.0*FPP> <C6Z1> <C6Z2-C6Z1> <CR3>    ) /* UZrH
CYL (  6004 <-9.0*PPP> < 3.0*FPP> <C6Z1> <C6Z7-C6Z1> <CR4>    ) /* v
CYL (  6005 <-9.0*PPP> < 3.0*FPP> <C6Z3> <C6Z1-C6Z3> <CR4>    ) /* sp1
CYL (  6006 <-9.0*PPP> < 3.0*FPP> <C6Z4> <C6Z3-C6Z4> <CR7>    ) /* v
CYL (  6007 <-9.0*PPP> < 3.0*FPP> <C6Z4> <C6Z3-C6Z4> <CR8>    ) /* st
CYL (  6008 <-9.0*PPP> < 3.0*FPP> <C6Z4> <C6Z3-C6Z4> <CR4>    ) /* v
CYL (  6009 <-9.0*PPP> < 3.0*FPP> <C6Z5> <C6Z4-C6Z5> <CR4>    ) /* bp
CYL (  6010 <-9.0*PPP> < 3.0*FPP> <C6Z7> <C6Z8-C6Z7> <CR4>    ) /* sp2
CYL (  6011 <-9.0*PPP> < 3.0*FPP> <C6Z8> <C6Z9-C6Z8> <CR6>    ) /* b4c
CYL (  6012 <-9.0*PPP> < 3.0*FPP> <C6Z8> <C6Z10-C6Z8> <CR4>   ) /* v
CYL (  6013 <-9.0*PPP> < 3.0*FPP> <C6Z10> <C6Z11-C6Z10> <CR4> ) /* sp3
CYL (  6014 <-9.0*PPP> < 3.0*FPP> <C6Z11> <C6Z12-C6Z11> <CR4> ) /* v
CYL (  6015 <-9.0*PPP> < 3.0*FPP> <C6Z12> <C6Z13-C6Z12> <CR4> ) /* tp
CYL (  6016 <-9.0*PPP> < 3.0*FPP> <C6Z5> <C6Z13-C6Z5> <CR5>   ) /* clad
* safety rod 1
CYL (  7001 < 4.5*PPP> <-4.5*FPP> <S1Z1> <S1Z2-S1Z1> <CR1>    ) /* zr
CYL (  7002 < 4.5*PPP> <-4.5*FPP> <S1Z1> <S1Z2-S1Z1> <CR2>    ) /* v
CYL (  7003 < 4.5*PPP> <-4.5*FPP> <S1Z1> <S1Z2-S1Z1> <CR3>    ) /* UZrH
CYL (  7004 < 4.5*PPP> <-4.5*FPP> <S1Z1> <S1Z7-S1Z1> <CR4>    ) /* v
CYL (  7005 < 4.5*PPP> <-4.5*FPP> <S1Z3> <S1Z1-S1Z3> <CR4>    ) /* sp1
CYL (  7006 < 4.5*PPP> <-4.5*FPP> <S1Z4> <S1Z3-S1Z4> <CR7>    ) /* v
CYL (  7007 < 4.5*PPP> <-4.5*FPP> <S1Z4> <S1Z3-S1Z4> <CR8>    ) /* st
CYL (  7008 < 4.5*PPP> <-4.5*FPP> <S1Z4> <S1Z3-S1Z4> <CR4>    ) /* v
CYL (  7009 < 4.5*PPP> <-4.5*FPP> <S1Z5> <S1Z4-S1Z5> <CR4>    ) /* bp
CYL (  7010 < 4.5*PPP> <-4.5*FPP> <S1Z7> <S1Z8-S1Z7> <CR4>    ) /* sp2
CYL (  7011 < 4.5*PPP> <-4.5*FPP> <S1Z8> <S1Z9-S1Z8> <CR6>    ) /* b4c
CYL (  7012 < 4.5*PPP> <-4.5*FPP> <S1Z8> <S1Z10-S1Z8> <CR4>   ) /* v
CYL (  7013 < 4.5*PPP> <-4.5*FPP> <S1Z10> <S1Z11-S1Z10> <CR4> ) /* sp3
CYL (  7014 < 4.5*PPP> <-4.5*FPP> <S1Z11> <S1Z12-S1Z11> <CR4> ) /* v
CYL (  7015 < 4.5*PPP> <-4.5*FPP> <S1Z12> <S1Z13-S1Z12> <CR4> ) /* tp
CYL (  7016 < 4.5*PPP> <-4.5*FPP> <S1Z5> <S1Z13-S1Z5> <CR5>   ) /* clad
* safety rod 2
CYL (  8001 <-9.0*PPP> 0.0        <S2Z1> <S2Z2-S2Z1> <CR1>    ) /* zr
CYL (  8002 <-9.0*PPP> 0.0        <S2Z1> <S2Z2-S2Z1> <CR2>    ) /* v
CYL (  8003 <-9.0*PPP> 0.0        <S2Z1> <S2Z2-S2Z1> <CR3>    ) /* UZrH
CYL (  8004 <-9.0*PPP> 0.0        <S2Z1> <S2Z7-S2Z1> <CR4>    ) /* v
CYL (  8005 <-9.0*PPP> 0.0        <S2Z3> <S2Z1-S2Z3> <CR4>    ) /* sp1
CYL (  8006 <-9.0*PPP> 0.0        <S2Z4> <S2Z3-S2Z4> <CR7>    ) /* v
CYL (  8007 <-9.0*PPP> 0.0        <S2Z4> <S2Z3-S2Z4> <CR8>    ) /* st
CYL (  8008 <-9.0*PPP> 0.0        <S2Z4> <S2Z3-S2Z4> <CR4>    ) /* v
CYL (  8009 <-9.0*PPP> 0.0        <S2Z5> <S2Z4-S2Z5> <CR4>    ) /* bp
CYL (  8010 <-9.0*PPP> 0.0        <S2Z7> <S2Z8-S2Z7> <CR4>    ) /* sp2
CYL (  8011 <-9.0*PPP> 0.0        <S2Z8> <S2Z9-S2Z8> <CR6>    ) /* b4c
CYL (  8012 <-9.0*PPP> 0.0        <S2Z8> <S2Z10-S2Z8> <CR4>   ) /* v
CYL (  8013 <-9.0*PPP> 0.0        <S2Z10> <S2Z11-S2Z10> <CR4> ) /* sp3
CYL (  8014 <-9.0*PPP> 0.0        <S2Z11> <S2Z12-S2Z11> <CR4> ) /* v
CYL (  8015 <-9.0*PPP> 0.0        <S2Z12> <S2Z13-S2Z12> <CR4> ) /* tp
CYL (  8016 <-9.0*PPP> 0.0        <S2Z5> <S2Z13-S2Z5> <CR5>   ) /* clad
* ta rod
CYL ( 10001 < 9.0*PPP> 0.0        <TAZ1> <TAZ2-TAZ1> <AR1>    ) /* b4c
CYL ( 10002 < 9.0*PPP> 0.0        <TAZ1> <TAZ2-TAZ1> <AR6>    ) /* v
CYL ( 10003 < 9.0*PPP> 0.0        <TAZ3> <TAZ1-TAZ3> <AR6>    ) /* sp1
CYL ( 10004 < 9.0*PPP> 0.0        <TAZ4> <TAZ3-TAZ4> <AR4>    ) /* v
CYL ( 10005 < 9.0*PPP> 0.0        <TAZ4> <TAZ3-TAZ4> <AR5>    ) /* fol
CYL ( 10006 < 9.0*PPP> 0.0        <TAZ4> <TAZ3-TAZ4> <AR6>    ) /* v
CYL ( 10007 < 9.0*PPP> 0.0        <TAZ5> <TAZ4-TAZ5> <AR6>    ) /* bp
CYL ( 10008 < 9.0*PPP> 0.0        <TAZ2> <TAZ6-TAZ2> <AR6>    ) /* sp2
CYL ( 10009 < 9.0*PPP> 0.0        <TAZ6> <TAZ7-TAZ6> <AR2>    ) /* v
CYL ( 10010 < 9.0*PPP> 0.0        <TAZ6> <TAZ7-TAZ6> <AR3>    ) /* st
CYL ( 10011 < 9.0*PPP> 0.0        <TAZ6> <TAZ7-TAZ6> <AR6>    ) /* v
CYL ( 10012 < 9.0*PPP> 0.0        <TAZ7> <TAZ8-TAZ7> <AR6>    ) /* tp
CYL ( 10013 < 9.0*PPP> 0.0        <TAZ5> <TAZ8-TAZ5> <AR7>    ) /* clad
* tb rod
CYL ( 20001 <-4.5*PPP> <-4.5*FPP> <TBZ1> <TBZ2-TBZ1> <TR1>    ) /* b4c
CYL ( 20002 <-4.5*PPP> <-4.5*FPP> <TBZ1> <TBZ2-TBZ1> <TR6>    ) /* v
CYL ( 20003 <-4.5*PPP> <-4.5*FPP> <TBZ3> <TBZ1-TBZ3> <TR6>    ) /* sp1
CYL ( 20004 <-4.5*PPP> <-4.5*FPP> <TBZ4> <TBZ3-TBZ4> <TR4>    ) /* v
CYL ( 20005 <-4.5*PPP> <-4.5*FPP> <TBZ4> <TBZ3-TBZ4> <TR5>    ) /* fol
CYL ( 20006 <-4.5*PPP> <-4.5*FPP> <TBZ4> <TBZ3-TBZ4> <TR6>    ) /* v
CYL ( 20007 <-4.5*PPP> <-4.5*FPP> <TBZ5> <TBZ4-TBZ5> <TR6>    ) /* bp
CYL ( 20008 <-4.5*PPP> <-4.5*FPP> <TBZ2> <TBZ6-TBZ2> <TR6>    ) /* sp2
CYL ( 20009 <-4.5*PPP> <-4.5*FPP> <TBZ6> <TBZ7-TBZ6> <TR2>    ) /* v
CYL ( 20010 <-4.5*PPP> <-4.5*FPP> <TBZ6> <TBZ7-TBZ6> <TR3>    ) /* st
CYL ( 20011 <-4.5*PPP> <-4.5*FPP> <TBZ6> <TBZ7-TBZ6> <TR6>    ) /* v
CYL ( 20012 <-4.5*PPP> <-4.5*FPP> <TBZ7> <TBZ8-TBZ7> <TR6>    ) /* tp
CYL ( 20013 <-4.5*PPP> <-4.5*FPP> <TBZ5> <TBZ8-TBZ5> <TR7>    ) /* clad
* tc rod
CYL ( 30001 <-4.5*PPP> < 4.5*FPP> <TCZ1> <TCZ2-TCZ1> <TR1>    ) /* b4c
CYL ( 30002 <-4.5*PPP> < 4.5*FPP> <TCZ1> <TCZ2-TCZ1> <TR6>    ) /* v
CYL ( 30003 <-4.5*PPP> < 4.5*FPP> <TCZ3> <TCZ1-TCZ3> <TR6>    ) /* sp1
CYL ( 30004 <-4.5*PPP> < 4.5*FPP> <TCZ4> <TCZ3-TCZ4> <TR4>    ) /* v
CYL ( 30005 <-4.5*PPP> < 4.5*FPP> <TCZ4> <TCZ3-TCZ4> <TR5>    ) /* fol
CYL ( 30006 <-4.5*PPP> < 4.5*FPP> <TCZ4> <TCZ3-TCZ4> <TR6>    ) /* v
CYL ( 30007 <-4.5*PPP> < 4.5*FPP> <TCZ5> <TCZ4-TCZ5> <TR6>    ) /* bp
CYL ( 30008 <-4.5*PPP> < 4.5*FPP> <TCZ2> <TCZ6-TCZ2> <TR6>    ) /* sp2
CYL ( 30009 <-4.5*PPP> < 4.5*FPP> <TCZ6> <TCZ7-TCZ6> <TR2>    ) /* v
CYL ( 30010 <-4.5*PPP> < 4.5*FPP> <TCZ6> <TCZ7-TCZ6> <TR3>    ) /* st
CYL ( 30011 <-4.5*PPP> < 4.5*FPP> <TCZ6> <TCZ7-TCZ6> <TR6>    ) /* v
CYL ( 30012 <-4.5*PPP> < 4.5*FPP> <TCZ7> <TCZ8-TCZ7> <TR6>    ) /* tp
CYL ( 30013 <-4.5*PPP> < 4.5*FPP> <TCZ5> <TCZ8-TCZ5> <TR7>    ) /* clad
* lattice boundary
RHP (  1000  0.0  0.0  <FZ1>      <FZ2-FZ1>      <DH1>     )
RHP (  2000  0.0  0.0  <FZ2>      <FZ15-FZ2>     <DH1>     )
RHP (  3000  0.0  0.0  <GBB>      <FZ1-GBB>      <DH1>     )
* lattice 100
RHP (   100  0.0  0.0  <FZ1>      <FZ2-FZ1>      <FPP>     )
CYL (    10  0.0  0.0  <FZ1>      <FZ2-FZ1>      <FR1>     ) /* Zr
CYL (    11  0.0  0.0  <FZ1>      <FZ2-FZ1>      <FR2>     ) /* v
CYL (    12  0.0  0.0  <FZ1>      <FZ2-FZ1>      <FR3>     ) /* UZrH
CYL (    13  0.0  0.0  <FZ1>      <FZ2-FZ1>      <FR4>     ) /* v
CYL (    14  0.0  0.0  <FZ1>      <FZ2-FZ1>      <FR5>     ) /* clad
* lattice 200
RHP (   200  0.0  0.0  <FZ2>      <FZ15-FZ2>     <FPP>     )
RHP (   210  0.0  0.0  <FZ2>      <GTB-FZ2>      <FPP>     )
RHP (   220  0.0  0.0  <GTB>      <GTT-GTB>      <FPP>     )
RHP (   230  0.0  0.0  <GTT>      <FZ15-GTT>     <FPP>     )
CYL (    20  0.0  0.0  <FZ2>      <FZ10-FZ2>     <FR7>     )  /* C
CYL (    21  0.0  0.0  <FZ2>      <FZ11-FZ2>     <FR4>     )  /* v
CYL (    22  0.0  0.0  <FZ11>     <FZ12-FZ11>     <FR4>     )  /* cap
CYL (    23  0.0  0.0  <FZ2>      <FZ12-FZ2>     <FR5>     )  /* clad
CYL (    24  0.0  0.0  <FZ12>     <FZ13-FZ12>     <FR8>     )  /* c1
CYL (    25  0.0  0.0  <FZ13>     <FZ14-FZ13>     <FR9>     )  /* c2
CYL (    26  0.0  0.0  <FZ14>     <FZ15-FZ14>     <FR8>     )  /* c3
CYL (    27  0.0  0.0  <GTB>      <GTT-GTB>      <GTRF>    )  /* h_f
CYL (    28  0.0  0.0  <GTB>      <GTT-GTB>      <GTRC>    )  /* h_c
* lattice 300
RHP (   300  0.0  0.0  <GBB>      <FZ1-GBB>      <FPP>     )
RHP (   310  0.0  0.0  <GBB>      <FZ7-GBB>      <FPP>     )
RHP (   320  0.0  0.0  <FZ7>      <FZ1-FZ7>      <FPP>     )
CYL (    30  0.0  0.0  <FZ9>      <FZ8-FZ9>      <FR12>    )  /* c4
TRC (    31  0.0  0.0  <FZ8>   0.0  0.0  <FZ7-FZ8>
                                  <FR12>  <FR11>    )  /* c3
CYL (    32  0.0  0.0  <FZ7>      <FZ6-FZ7>      <FR11>    )  /* c2
CYL (    33  0.0  0.0  <FZ6>      <FZ5-FZ6>      <FR10>    )  /* c1
CYL (    34  0.0  0.0  <FZ5>      <FZ1-FZ5>      <FR5>     )  /* clad
CYL (    35  0.0  0.0  <FZ5>      <FZ4-FZ5>      <FR4>     )  /* cap
CYL (    36  0.0  0.0  <FZ4>      <FZ1-FZ4>      <FR4>     )  /* v
CYL (    37  0.0  0.0  <FZ4>      <FZ3-FZ4>      <FR7>     )  /* C
CYL (    38  0.0  0.0  <FZ3>      <FZ1-FZ3>      <FR6>     )  /* Mo
TRC (    39  0.0  0.0  <GBT>   0.0  0.0  <FZ7-GBT>
                                  <GBRF>  <FR11>    )  /* h_f1
CYL (    40  0.0  0.0  <GBB>      <GBT-GBB>      <GBRF>    )  /* h_f2
CYL (    41  0.0  0.0  <GBB>      <FZ7-GBB>      <GBRC>    )  /* h_c
*
END
```

```
*--------+---------+---------+---------+---------+---------+---------+--
* ZONE
*--------+---------+---------+---------+---------+---------+---------+--
*
  VOUT    :      : -1000 : -100000                 /* outer void
  REF1    : REFL :    8 :  100000 -50000 -70000
                             -10000 -30000
                             -500 -510 -520
                             -1016
                             -2016
                             -3016
                             -4016
                             -5016
                             -6016
                             -7016
                             -8016
                          -10013 -20013 -30013 /* water reflector
*
  SHRD    : SHRD :    9 :   50000 -51000          /* shroud
*
  GRIT    : GRIT :    9 :   60000 -2000
                        -60110 -60120 -60130 -60140 -60150 -60160
                        -60210 -60220 -60230 -60240 -60250 -60260
                        -60310 -60320 -60330 -60340 -60350 -60360
                        -60410 -60420 -60430 -60440 -60450 -60460
                        -60510 -60520 -60530 -60540 -60550 -60560
                        -60610 -60620 -60630 -60640 -60650 -60660
  GRIB    : GRIB :    9 :   61000 -3000
                        -60111 -60121 -60131 -60141 -60151 -60161
                        -60211 -60221 -60231 -60241 -60251 -60261
                        -60311 -60321 -60331 -60341 -60351 -60361
                        -60411 -60421 -60431 -60441 -60451 -60461
                        -60511 -60521 -60531 -60541 -60551 -60561
                        -60611 -60621 -60631 -60641 -60651 -60661
                        -60112 -60122 -60132 -60142 -60152 -60162
                        -60212 -60222 -60232 -60242 -60252 -60262
                        -60312 -60322 -60332 -60342 -60352 -60362
                        -60412 -60422 -60432 -60442 -60452 -60462
                        -60512 -60522 -60532 -60542 -60552 -60562
                        -60612 -60622 -60632 -60642 -60652 -60662
*
  REF2    : REFL :    8 :   70000 -2000  -10000    /* water reflector
  REF3    : REFL :    8 :   51000 -60000 -61000
                             -1000 -2000 -3000 /* grid wh 1
  REFG11   : REFL :    8 :   60110 OR 60111 OR 60112 /* grid wh 1
  REFG12   : REFL :    8 :   60120 OR 60121 OR 60122 /* grid wh 1
  REFG13   : REFL :    8 :   60130 OR 60131 OR 60132 /* grid wh 1
  REFG14   : REFL :    8 :   60140 OR 60141 OR 60142 /* grid wh 1
  REFG15   : REFL :    8 :   60150 OR 60151 OR 60152 /* grid wh 1
  REFG16   : REFL :    8 :   60160 OR 60161 OR 60162 /* grid wh 1
  REFG21   : REFL :    8 :   60210 OR 60211 OR 60212 /* grid wh 2
  REFG22   : REFL :    8 :   60220 OR 60221 OR 60222 /* grid wh 2
  REFG23   : REFL :    8 :   60230 OR 60231 OR 60232 /* grid wh 2
  REFG24   : REFL :    8 :   60240 OR 60241 OR 60242 /* grid wh 2
  REFG25   : REFL :    8 :   60250 OR 60251 OR 60252 /* grid wh 2
  REFG26   : REFL :    8 :   60260 OR 60261 OR 60262 /* grid wh 2
  REFG31   : REFL :    8 :   60310 OR 60311 OR 60312 /* grid wh 3
  REFG32   : REFL :    8 :   60320 OR 60321 OR 60322 /* grid wh 3
  REFG33   : REFL :    8 :   60330 OR 60331 OR 60332 /* grid wh 3
  REFG34   : REFL :    8 :   60340 OR 60341 OR 60342 /* grid wh 3
  REFG35   : REFL :    8 :   60350 OR 60351 OR 60352 /* grid wh 3
  REFG36   : REFL :    8 :   60360 OR 60361 OR 60362 /* grid wh 3
  REFG41   : REFL :    8 :   60410 OR 60411 OR 60412 /* grid wh 4
  REFG42   : REFL :    8 :   60420 OR 60421 OR 60422 /* grid wh 4
  REFG43   : REFL :    8 :   60430 OR 60431 OR 60432 /* grid wh 4
  REFG44   : REFL :    8 :   60440 OR 60441 OR 60442 /* grid wh 4
  REFG45   : REFL :    8 :   60450 OR 60451 OR 60452 /* grid wh 4
  REFG46   : REFL :    8 :   60460 OR 60461 OR 60462 /* grid wh 4
  REFG51   : REFL :    8 :   60510 OR 60511 OR 60512 /* grid wh 5
  REFG52   : REFL :    8 :   60520 OR 60521 OR 60522 /* grid wh 5
  REFG53   : REFL :    8 :   60530 OR 60531 OR 60532 /* grid wh 5
  REFG54   : REFL :    8 :   60540 OR 60541 OR 60542 /* grid wh 5
  REFG55   : REFL :    8 :   60550 OR 60551 OR 60552 /* grid wh 5
  REFG56   : REFL :    8 :   60560 OR 60561 OR 60562 /* grid wh 5
  REFG61   : REFL :    8 :   60610 OR 60611 OR 60612 /* grid wh 6
  REFG62   : REFL :    8 :   60620 OR 60621 OR 60622 /* grid wh 6
  REFG63   : REFL :    8 :   60630 OR 60631 OR 60632 /* grid wh 6
  REFG64   : REFL :    8 :   60640 OR 60641 OR 60642 /* grid wh 6
  REFG65   : REFL :    8 :   60650 OR 60651 OR 60652 /* grid wh 6
  REFG66   : REFL :    8 :   60660 OR 60661 OR 60662 /* grid wh 6
*
  ETB1    : VOIH :    0 :  20000                  /* void hex
  ETB2    : EBTU :    9 :  10000 -20000            /* tube hex
  ETB3    : VOIC :    0 :  40000                  /* void cyl
  ETB4    : EBTU :    9 :  30000 -40000            /* tube cyl
*
  GTTA    : GUTU :   10 :    500   -501            /* gt TA
  REF4    : REFL :    8 :    501 -10013            /* water reflector
*
  GTTB    : GUTU :   10 :    510   -511            /* gt TB
  REF5    : REFL :    8 :    511 -20013            /* water reflector
*
  GTTC    : GUTU :   10 :    520   -521            /* gt TC
  REF5    : REFL :    8 :    521 -30013            /* water reflector
*
  CR101   : CZIR :    1 :  1001                   /* zr
  CR102   : CVO1 :    0 :  1002 -1001              /* void
  CR103   : CFUE :    2 :  1003 -1002              /* U-ZrH
  CR104   : CVO2 :    0 :  1004 -1003              /* vd
  CR105   : CSP1 :   10 :  1005                   /* sp1
  CR106   : CVO3 :    0 :  1006                   /* void
  CR107   : CSPT :    9 :  1007 -1006              /* spacer tube
  CR108   : CVO4 :    0 :  1008 -1007              /* void
  CR109   : CBPL :   10 :  1009                   /* bottom plug
  CR110   : CSP2 :   10 :  1010                   /* sp2
  CR111   : CB4C :   11 :  1011                   /* b4c
  CR112   : CVO5 :    0 :  1012 -1011              /* void
  CR113   : CSP3 :   10 :  1013                   /* sp3
  CR114   : CVO6 :    0 :  1014                   /* void
  CR115   : CTPL :   10 :  1015                   /* top plug
  CR116   : CCLA :   10 :  1016 -1015 -1014 -1013
                            -1012 -1010 -1009
                            -1008 -1005 -1004  /* clad
*
  CR201   : CZIR :    1 :  2001                   /* zr
  CR202   : CVO1 :    0 :  2002 -2001              /* void
  CR203   : CFUE :    2 :  2003 -2002              /* U-ZrH
  CR204   : CVO2 :    0 :  2004 -2003              /* vd
  CR205   : CSP1 :   10 :  2005                   /* sp1
  CR206   : CVO3 :    0 :  2006                   /* void
  CR207   : CSPT :    9 :  2007 -2006              /* spacer tube
  CR208   : CVO4 :    0 :  2008 -2007              /* void
  CR209   : CBPL :   10 :  2009                   /* bottom plug
  CR210   : CSP2 :   10 :  2010                   /* sp2
  CR211   : CB4C :   11 :  2011                   /* b4c
  CR212   : CVO5 :    0 :  2012 -2011              /* void
  CR213   : CSP3 :   10 :  2013                   /* sp3
  CR214   : CVO6 :    0 :  2014                   /* void
  CR215   : CTPL :   10 :  2015                   /* top plug
  CR216   : CCLA :   10 :  2016 -2015 -2014 -2013
                            -2012 -2010 -2009
                            -2008 -2005 -2004  /* clad
*
  CR301   : CZIR :    1 :  3001                   /* zr
  CR302   : CVO1 :    0 :  3002 -3001              /* void
  CR303   : CFUE :    2 :  3003 -3002              /* U-ZrH
  CR304   : CVO2 :    0 :  3004 -3003              /* vd
  CR305   : CSP1 :   10 :  3005                   /* sp1
  CR306   : CVO3 :    0 :  3006                   /* void
  CR307   : CSPT :    9 :  3007 -3006              /* spacer tube
  CR308   : CVO4 :    0 :  3008 -3007              /* void
  CR309   : CBPL :   10 :  3009                   /* bottom plug
  CR310   : CSP2 :   10 :  3010                   /* sp2
  CR311   : CB4C :   11 :  3011                   /* b4c
  CR312   : CVO5 :    0 :  3012 -3011              /* void
  CR313   : CSP3 :   10 :  3013                   /* sp3
  CR314   : CVO6 :    0 :  3014                   /* void
  CR315   : CTPL :   10 :  3015                   /* top plug
  CR316   : CCLA :   10 :  3016 -3015 -3014 -3013
                            -3012 -3010 -3009
                            -3008 -3005 -3004  /* clad
*
  CR401   : CZIR :    1 :  4001                   /* zr
  CR402   : CVO1 :    0 :  4002 -4001              /* void
  CR403   : CFUE :    2 :  4003 -4002              /* U-ZrH
  CR404   : CVO2 :    0 :  4004 -4003              /* vd
  CR405   : CSP1 :   10 :  4005                   /* sp1
  CR406   : CVO3 :    0 :  4006                   /* void
  CR407   : CSPT :    9 :  4007 -4006              /* spacer tube
  CR408   : CVO4 :    0 :  4008 -4007              /* void
  CR409   : CBPL :   10 :  4009                   /* bottom plug
  CR410   : CSP2 :   10 :  4010                   /* sp2
  CR411   : CB4C :   11 :  4011                   /* b4c
  CR412   : CVO5 :    0 :  4012 -4011              /* void
  CR413   : CSP3 :   10 :  4013                   /* sp3
  CR414   : CVO6 :    0 :  4014                   /* void
  CR415   : CTPL :   10 :  4015                   /* top plug
  CR416   : CCLA :   10 :  4016 -4015 -4014 -4013
                            -4012 -4010 -4009
                            -4008 -4005 -4004  /* clad
*
  CR501   : CZIR :    1 :  5001                   /* zr
  CR502   : CVO1 :    0 :  5002 -5001              /* void
  CR503   : CFUE :    2 :  5003 -5002              /* U-ZrH
  CR504   : CVO2 :    0 :  5004 -5003              /* vd
  CR505   : CSP1 :   10 :  5005                   /* sp1
  CR506   : CVO3 :    0 :  5006                   /* void
  CR507   : CSPT :    9 :  5007 -5006              /* spacer tube
  CR508   : CVO4 :    0 :  5008 -5007              /* void
  CR509   : CBPL :   10 :  5009                   /* bottom plug
  CR510   : CSP2 :   10 :  5010                   /* sp2
  CR511   : CB4C :   11 :  5011                   /* b4c
  CR512   : CVO5 :    0 :  5012 -5011              /* void
  CR513   : CSP3 :   10 :  5013                   /* sp3
  CR514   : CVO6 :    0 :  5014                   /* void
  CR515   : CTPL :   10 :  5015                   /* top plug
  CR516   : CCLA :   10 :  5016 -5015 -5014 -5013
                            -5012 -5010 -5009
                            -5008 -5005 -5004  /* clad
*
  CR601   : CZIR :    1 :  6001                   /* zr
  CR602   : CVO1 :    0 :  6002 -6001              /* void
  CR603   : CFUE :    2 :  6003 -6002              /* U-ZrH
  CR604   : CVO2 :    0 :  6004 -6003              /* vd
  CR605   : CSP1 :   10 :  6005                   /* sp1
  CR606   : CVO3 :    0 :  6006                   /* void
  CR607   : CSPT :    9 :  6007 -6006              /* spacer tube
  CR608   : CVO4 :    0 :  6008 -6007              /* void
  CR609   : CBPL :   10 :  6009                   /* bottom plug
  CR610   : CSP2 :   10 :  6010                   /* sp2
  CR611   : CB4C :   11 :  6011                   /* b4c
  CR612   : CVO5 :    0 :  6012 -6011              /* void
  CR613   : CSP3 :   10 :  6013                   /* sp3
  CR614   : CVO6 :    0 :  6014                   /* void
  CR615   : CTPL :   10 :  6015                   /* top plug
  CR616   : CCLA :   10 :  6016 -6015 -6014 -6013
                            -6012 -6010 -6009
                            -6008 -6005 -6004  /* clad
*
  SR101   : CZIR :    1 :  7001                   /* zr
  SR102   : CVO1 :    0 :  7002 -7001              /* void
  SR103   : CFUE :    2 :  7003 -7002              /* U-ZrH
  SR104   : CVO2 :    0 :  7004 -7003              /* vd
  SR105   : CSP1 :   10 :  7005                   /* sp1
  SR106   : CVO3 :    0 :  7006                   /* void
  SR107   : CSPT :    9 :  7007 -7006              /* spacer tube
  SR108   : CVO4 :    0 :  7008 -7007              /* void
  SR109   : CBPL :   10 :  7009                   /* bottom plug
  SR110   : CSP2 :   10 :  7010                   /* sp2
  SR111   : CB4C :   11 :  7011                   /* b4c
  SR112   : CVO5 :    0 :  7012 -7011              /* void
  SR113   : CSP3 :   10 :  7013                   /* sp3
  SR114   : CVO6 :    0 :  7014                   /* void
  SR115   : CTPL :   10 :  7015                   /* top plug
  SR116   : CCLA :   10 :  7016 -7015 -7014 -7013
                            -7012 -7010 -7009
                            -7008 -7005 -7004  /* clad
*
  SR201   : CZIR :    1 :  8001                   /* zr
  SR202   : CVO1 :    0 :  8002 -8001              /* void
  SR203   : CFUE :    2 :  8003 -8002              /* U-ZrH
  SR204   : CVO2 :    0 :  8004 -8003              /* vd
  SR205   : CSP1 :   10 :  8005                   /* sp1
  SR206   : CVO3 :    0 :  8006                   /* void
  SR207   : CSPT :    9 :  8007 -8006              /* spacer tube
  SR208   : CVO4 :    0 :  8008 -8007              /* void
  SR209   : CBPL :   10 :  8009                   /* bottom plug
  SR210   : CSP2 :   10 :  8010                   /* sp2
  SR211   : CB4C :   11 :  8011                   /* b4c
  SR212   : CVO5 :    0 :  8012 -8011              /* void
  SR213   : CSP3 :   10 :  8013                   /* sp3
  SR214   : CVO6 :    0 :  8014                   /* void
  SR215   : CTPL :   10 :  8015                   /* top plug
  SR216   : CCLA :   10 :  8016 -8015 -8014 -8013
                            -8012 -8010 -8009
                            -8008 -8005 -8004  /* clad
*
  TA101   : TB4C :   12 : 10001                   /* b4c
  TA102   : TVO1 :    0 : 10002 -10001             /* void
  TA103   : TSP1 :    9 : 10003                   /* sp1
  TA104   : TVO2 :    0 : 10004                   /* void
  TA105   : TFOL :    9 : 10005 -10004             /* follower tube
  TA106   : TVO3 :    0 : 10006 -10005             /* void
  TA107   : TBPL :    9 : 10007                   /* bottom plug
  TA108   : TSP2 :    9 : 10008                   /* sp2
  TA109   : TVO4 :    0 : 10009                   /* void
  TA110   : TSPT :    9 : 10010 -10009             /* spacer tube
  TA111   : TVO5 :    0 : 10011 -10010             /* void
```

```
  TA112   : TTPL :    9 : 10012                 /* top plug
  TA113   : TCLA :    9 : 10013 -10002 -10003 -10006
                            -10007 -10008 -10011
                            -10012           /* clad
*
  TB101   : TB4C :   12 : 20001                 /* b4c
  TB102   : TVO1 :    0 : 20002 -20001           /* void
  TB103   : TSP1 :    9 : 20003                 /* sp1
  TB104   : TVO2 :    0 : 20004                 /* void
  TB105   : TFOL :    9 : 20005 -20004           /* follower tube
  TB106   : TVO3 :    0 : 20006 -20005           /* void
  TB107   : TBPL :    9 : 20007                 /* bottom plug
  TB108   : TSP2 :    9 : 20008                 /* sp2
  TB109   : TVO4 :    0 : 20009                 /* void
  TB110   : TSPT :    9 : 20010 -20009           /* spacer tube
  TB111   : TVO5 :    0 : 20011 -20010           /* void
  TB112   : TTPL :    9 : 20012                 /* top plug
  TB113   : TCLA :    9 : 20013 -20002 -20003 -20006
                            -20007 -20008 -20011
                            -20012           /* clad
*
  TC101   : TB4C :   12 : 30001                 /* b4c
  TC102   : TVO1 :    0 : 30002 -30001           /* void
  TC103   : TSP1 :    9 : 30003                 /* sp1
  TC104   : TVO2 :    0 : 30004                 /* void
  TC105   : TFOL :    9 : 30005 -30004           /* follower tube
  TC106   : TVO3 :    0 : 30006 -30005           /* void
  TC107   : TBPL :    9 : 30007                 /* bottom plug
  TC108   : TSP2 :    9 : 30008                 /* sp2
  TC109   : TVO4 :    0 : 30009                 /* void
  TC110   : TSPT :    9 : 30010 -30009           /* spacer tube
  TC111   : TVO5 :    0 : 30011 -30010           /* void
  TC112   : TTPL :    9 : 30012                 /* top plug
  TC113   : TCLA :    9 : 30013 -30002 -30003 -30006
                            -30007 -30008 -30011
                            -30012           /* clad
*
  LAT1    : LAT1 :  -100 :  1000 -10000
                             -1016
                             -2016
                             -3016
                             -4016
                             -5016
                             -6016
                             -7016
                             -8016
                          -10013 -20013 -30013  /* U-ZrH
  LAT2    : LAT2 :  -200 :  2000 -10000 -30000
                            -500 -510 -520
                             -1016
                             -2016
                             -3016
                             -4016
                             -5016
                             -6016
                             -7016
                             -8016
                          -10013 -20013 -30013
                      -60110 -60120 -60130 -60140 -60150 -60160
                      -60210 -60220 -60230 -60240 -60250 -60260
                      -60310 -60320 -60330 -60340 -60350 -60360
                      -60410 -60420 -60430 -60440 -60450 -60460
                      -60510 -60520 -60530 -60540 -60550 -60560
                      -60610 -60620 -60630 -60640 -60650 -60660
                                           /* over U-ZrH
  LAT3    : LAT3 :  -300 :  3000 -10000
                             -1016
                             -2016
                             -3016
                             -4016
                             -5016
                             -6016
                             -7016
                             -8016
                          -10013 -20013 -30013
                      -60111 -60121 -60131 -60141 -60151 -60161
                      -60211 -60221 -60231 -60241 -60251 -60261
                      -60311 -60321 -60331 -60341 -60351 -60361
                      -60411 -60421 -60431 -60441 -60451 -60461
                      -60511 -60521 -60531 -60541 -60551 -60561
                      -60611 -60621 -60631 -60641 -60651 -60661
                      -60112 -60122 -60132 -60142 -60152 -60162
                      -60212 -60222 -60232 -60242 -60252 -60262
                      -60312 -60322 -60332 -60342 -60352 -60362
                      -60412 -60422 -60432 -60442 -60452 -60462
                      -60512 -60522 -60532 -60542 -60552 -60562
                      -60612 -60622 -60632 -60642 -60652 -60662
                                           /* under U-ZrH
*
* lattice 100
*
#CELL ID(1)  TYPE(HEXA)
  C101     :      : -999 :  -100
  C102     : MODR :    7 :   100  -14             /* moderator
  C103     : CLAD :    3 :    14  -13             /* cladding
  C104     : VOD1 :    0 :    13  -12             /* void
  C105     : FUEL :    2 :    12  -11             /* u-zrh
  C106     : VOD2 :    0 :    11  -10             /* void
  C107     : ZIRC :    1 :    10                 /* zr
#END CELL
*
#CELL ID(2)  TYPE(HEXA)
  C201     :      : -999 :  -100
  C202     : REFL :    8 :   100                 /* water reflector
#END CELL
*
#CELL ID(3)  TYPE(HEXA)
  C301     :      : -999 :  -100
  C302     : REFL :    8 :   100                 /* water reflector
#END CELL
*
#CELL ID(4)  TYPE(HEXA)
  C401     :      : -999 :  -100
  C402     : MODR :    7 :   100                 /* moderator
#END CELL
*
#CELL ID(5)  TYPE(HEXA)
  C501     :      : -999 :  -100
  C502     : REFL :    8 :   100                 /* water reflector
#END CELL
*
* lattice 200
*
#CELL ID(6)  TYPE(HEXA)
  C601     :      : -999 :  -200
  C602     : MODO :    7 :   210  -23             /* moderator
  C603     : REFL :    8 :    27  -23 -24 -25      /* water reflector
  C604     : REFL :    8 :   230  -25 -26          /* water reflector
  C605     : CLAO :    3 :    23  -21 -22          /* cladding
```

```
  C606     : VOIO :    0 :    21  -20             /* void
  C607     : GRAO :    6 :    20                 /* graphite
  C608     : PLUO :    4 :    22                 /* top plug
  C609     : CAPO :    4 :    24                 /* top c1
  C610     : CAPO :    4 :    25                 /* top c2
  C611     : CAPO :    4 :    26                 /* top c3
  C612     : GRIT :    9 :   220  -27             /* top grid
#END CELL
*
#CELL ID(7)  TYPE(HEXA)
  C701     :      : -999 :  -200
  C702     : REFL :    8 :   210                 /* water reflector
  C703     : REFL :    8 :   230                 /* water reflector
  C704     : GRIT :    9 :   220                 /* top grid
#END CELL
*
#CELL ID(8)  TYPE(HEXA)
  C801     :      : -999 :  -200
  C802     : REFL :    8 :   210                 /* water reflector
  C803     : REFL :    8 :    27                 /* water reflector
  C804     : REFL :    8 :   230                 /* water reflector
  C805     : GRIT :    9 :   220  -27             /* top grid
#END CELL
*
#CELL ID(9)  TYPE(HEXA)
  C901     :      : -999 :  -200
  C902     : REFL :    8 :   210                 /* water reflector
  C903     : REFL :    8 :    28                 /* water reflector
  C904     : REFL :    8 :   230                 /* water reflector
  C905     : GRIT :    9 :   220  -28             /* top grid
#END CELL
*
#CELL ID(10)  TYPE(HEXA)
  C1001    :      : -999 :  -200
  C1002    : REFL :    8 :   210                 /* water reflector
  C1003    : REFL :    8 :   230                 /* water reflector
  C1004    : GRIT :    9 :   220                 /* top grid
#END CELL
*
* lattice 300
*
#CELL ID(11)  TYPE(HEXA)
  C1101    :      : -999 :  -300
  C1102    : REFL :    8 :    40  -30 -31         /* water reflector
  C1103    : MODU :    7 :   320  -32 -33 -34     /* moderator
  C1104    : CLAU :    3 :    34  -35 -36         /* cladding
  C1105    : VOIU :    0 :    36  -37 -38         /* void
  C1106    : GRAU :    6 :    37                 /* graphite
  C1107    : MOLU :    5 :    38                 /* mo
  C1108    : PLUU :    4 :    35                 /* bottom plug
  C1109    : CAPU :    4 :    33                 /* bottom c1
  C1110    : CAPU :    4 :    32                 /* bottom c2
  C1111    : CAPU :    4 :    31                 /* bottom c3
  C1112    : CAPU :    4 :    30                 /* bottom c4
  C1113    : GRIB :    9 :   310  -39 -40         /* bottom grid
#END CELL
*
#CELL ID(12)  TYPE(HEXA)
  C1201    :      : -999 :  -300
  C1202    : REFL :    8 :   320                 /* water reflector
  C1203    : GRIB :    9 :   310                 /* bottom grid
#END CELL
*
#CELL ID(13)  TYPE(HEXA)
  C1301    :      : -999 :  -300
  C1302    : REFL :    8 :    39                 /* water reflector
  C1303    : REFL :    8 :    40                 /* water reflector
  C1304    : REFL :    8 :   320                 /* water reflector
  C1305    : GRIB :    9 :   310  -39 -40         /* bottom grid
#END CELL
*
#CELL ID(14)  TYPE(HEXA)
  C1401    :      : -999 :  -300
  C1402    : REFL :    8 :    41                 /* water reflector
  C1403    : REFL :    8 :   320                 /* water reflector
  C1404    : GRIB :    9 :   310  -41             /* bottom grid
#END CELL
*
#CELL ID(15)  TYPE(HEXA)
  C1501    :      : -999 :  -300
  C1502    : REFL :    8 :   320                 /* water reflector
  C1503    : GRIB :    9 :   310                 /* bottom grid
#END CELL
*
*
#TALLY REGION
  DEFINE @FUE1 (FUEL MODR CLAD ZIRC VOD1 VOD2 )
  DEFINE @FUE2 (FUEL CFUE )
  DEFINE @FUE3 (FUEL CFUE MODR CLAD ZIRC VOD1 VOD2 )
  DEFINE @NOCR (MODO CLAO GRAO PLUO CAPO EBTU GUTU
                MODU CLAU GRAU PLUU CAPU MOLU GRIT GRIB SHRD
                CZIR CSP1 CSPT CBPL CSP2 CB4C CSP3 CTPL
                CCLA
                TB4C TSP1 TFOL TBPL TSP2 TSPT TTPL TCLA     )
*
$END GEOMETRY
*
$TALLY
&
  LABEL( FUEL CELL NEUTRON FLUX 120 ENERGY GROUP )
  EVENT( TRACK )
  NEUTRON
  DIMENSION ( REGION  ENERGY)
  REGION( @FUE1 )
  IENERGY (  1   2   3   4   5   6   7   8   9  10
            11  12  13  14  15  16  17  18  19  20
            21  22  23  24  25  26  27  28  29  30
            31  32  33  34  35  36  37  38  39  40
            41  42  43  44  45  46  47  48  49  50
            51  52  53  54  55  56  57  58  59  60
            61  62  63  64  65  66  67  68  69  70
            71  72  73  74  75  76  77  78  79  80
            81  82  83  84  85  86  87  88  89  90
            91  92  93  94  95  96  97  98  99 100
           101 102 103 104 105 106 107 108 109 110
           111 112 113 114 115 116 117 118 119 120 )
&
  LABEL( FUEL CELL AND CFUE NEUTRON FLUX 120 ENERGY GROUP )
  EVENT( TRACK )
  NEUTRON
  DIMENSION ( REGION  ENERGY)
  REGION( @FUE3 )
  IENERGY (  1   2   3   4   5   6   7   8   9  10
            11  12  13  14  15  16  17  18  19  20
            21  22  23  24  25  26  27  28  29  30
            31  32  33  34  35  36  37  38  39  40
            41  42  43  44  45  46  47  48  49  50
            51  52  53  54  55  56  57  58  59  60
            61  62  63  64  65  66  67  68  69  70
```

```
          71  72  73  74  75  76  77  78  79  80
          81  82  83  84  85  86  87  88  89  90
          91  92  93  94  95  96  97  98  99 100
         101 102 103 104 105 106 107 108 109 110
         111 112 113 114 115 116 117 118 119 120 )
&
  LABEL( FUEL AND CFUE NEUTRON FLUX 120 ENERGY GROUP )
  EVENT( TRACK )
  NEUTRON
  DIMENSION ( REGION  ENERGY)
  REGION( @FUE2 )
  IENERGY (  1   2   3   4   5   6   7   8   9  10
          11  12  13  14  15  16  17  18  19  20
          21  22  23  24  25  26  27  28  29  30
          31  32  33  34  35  36  37  38  39  40
          41  42  43  44  45  46  47  48  49  50
          51  52  53  54  55  56  57  58  59  60
          61  62  63  64  65  66  67  68  69  70
          71  72  73  74  75  76  77  78  79  80
          81  82  83  84  85  86  87  88  89  90
          91  92  93  94  95  96  97  98  99 100
         101 102 103 104 105 106 107 108 109 110
         111 112 113 114 115 116 117 118 119 120 )
&
  LABEL( FUEL NEUTRON FLUX 120 ENERGY GROUP )
  EVENT( TRACK )
  NEUTRON
  DIMENSION ( REGION  ENERGY)
  REGION( FUEL )
  IENERGY (  1   2   3   4   5   6   7   8   9  10
          11  12  13  14  15  16  17  18  19  20
          21  22  23  24  25  26  27  28  29  30
          31  32  33  34  35  36  37  38  39  40
          41  42  43  44  45  46  47  48  49  50
          51  52  53  54  55  56  57  58  59  60
          61  62  63  64  65  66  67  68  69  70
          71  72  73  74  75  76  77  78  79  80
          81  82  83  84  85  86  87  88  89  90
          91  92  93  94  95  96  97  98  99 100
         101 102 103 104 105 106 107 108 109 110
         111 112 113 114 115 116 117 118 119 120 )
&
  LABEL( MODR NEUTRON FLUX 120 ENERGY GROUP )
  EVENT( TRACK )
  NEUTRON
  DIMENSION ( REGION  ENERGY)
  REGION( MODR )
  IENERGY (  1   2   3   4   5   6   7   8   9  10
          11  12  13  14  15  16  17  18  19  20
          21  22  23  24  25  26  27  28  29  30
          31  32  33  34  35  36  37  38  39  40
          41  42  43  44  45  46  47  48  49  50
          51  52  53  54  55  56  57  58  59  60
          61  62  63  64  65  66  67  68  69  70
          71  72  73  74  75  76  77  78  79  80
          81  82  83  84  85  86  87  88  89  90
          91  92  93  94  95  96  97  98  99 100
         101 102 103 104 105 106 107 108 109 110
         111 112 113 114 115 116 117 118 119 120 )
&
  LABEL( REFL NEUTRON FLUX 120 ENERGY GROUP )
  EVENT( TRACK )
  NEUTRON
  DIMENSION ( REGION  ENERGY)
  REGION( REFL )
  IENERGY (  1   2   3   4   5   6   7   8   9  10
          11  12  13  14  15  16  17  18  19  20
          21  22  23  24  25  26  27  28  29  30
          31  32  33  34  35  36  37  38  39  40
          41  42  43  44  45  46  47  48  49  50
          51  52  53  54  55  56  57  58  59  60
          61  62  63  64  65  66  67  68  69  70
          71  72  73  74  75  76  77  78  79  80
          81  82  83  84  85  86  87  88  89  90
          91  92  93  94  95  96  97  98  99 100
         101 102 103 104 105 106 107 108 109 110
         111 112 113 114 115 116 117 118 119 120 )
&
  LABEL( THE NUMBER OF NUFISSION PER SOURCE )
  EVENT( TRACK )
  NEUTRON
  DIMENSION ( REGION )
  REGION( @FUE1 )
  MACRO( NUFISSION )
&
  LABEL( THE NUMBER OF FISSION PER SOURCE )
  EVENT( TRACK )
  NEUTRON
  DIMENSION ( REGION )
  REGION( @FUE1 )
  MACRO( FISSION )
&
  LABEL( THE NUMBER OF NON-FISSION CAPTURE PER SOURCE )
  EVENT( TRACK )
  NEUTRON
  DIMENSION ( REGION )
  REGION( @FUE1 )
  MACRO( CAPTURE )
&
  LABEL( THE NUMBER OF NUFISSION PER SOURCE )
  EVENT( TRACK )
  NEUTRON
  DIMENSION ( REGION )
  REGION( @FUE2 )
  MACRO( NUFISSION )
&
  LABEL( THE NUMBER OF FISSION PER SOURCE )
  EVENT( TRACK )
  NEUTRON
  DIMENSION ( REGION )
  REGION( @FUE2 )
  MACRO( FISSION )
&
  LABEL( THE NUMBER OF NON-FISSION CAPTURE PER SOURCE )
  EVENT( TRACK )
  NEUTRON
  DIMENSION ( REGION )
  REGION( @FUE2 )
  MACRO( CAPTURE )
&
  LABEL( THE NUMBER OF NON-FISSION CAPTURE PER SOURCE )
  EVENT( TRACK )
  NEUTRON
  DIMENSION ( REGION )
  REGION( @FUE3 )
  MACRO( CAPTURE )
&
  LABEL( THE NUMBER OF NON-FISSION CAPTURE PER SOURCE )
  EVENT( TRACK )
  NEUTRON
  DIMENSION ( REGION )
  REGION( FUEL )
  MACRO( CAPTURE )
&
  LABEL( THE NUMBER OF NON-FISSION CAPTURE PER SOURCE )
  EVENT( TRACK )
  NEUTRON
  DIMENSION ( REGION )
  REGION( CFUE )
  MACRO( CAPTURE )
&
  LABEL( THE NUMBER OF NON-FISSION CAPTURE PER SOURCE )
  EVENT( TRACK )
  NEUTRON
  DIMENSION ( REGION )
  REGION( MODR )
  MACRO( CAPTURE )
&
  LABEL( THE NUMBER OF NON-FISSION CAPTURE PER SOURCE )
  EVENT( TRACK )
  NEUTRON
  DIMENSION ( REGION )
  REGION( CLAD )
  MACRO( CAPTURE )
&
  LABEL( THE NUMBER OF NON-FISSION CAPTURE PER SOURCE )
  EVENT( TRACK )
  NEUTRON
  DIMENSION ( REGION )
  REGION( ZIRC )
  MACRO( CAPTURE )
&
  LABEL( THE NUMBER OF NON-FISSION CAPTURE PER SOURCE )
  EVENT( TRACK )
  NEUTRON
  DIMENSION ( REGION )
  REGION( @NOCR )
  MACRO( CAPTURE )
&
  LABEL( THE NUMBER OF NON-FISSION CAPTURE PER SOURCE )
  EVENT( TRACK )
  NEUTRON
  DIMENSION ( REGION )
  REGION( REFL )
  MACRO( CAPTURE )
*
$END TALLY
*
*--------+---------+---------+---------+---------+---------+---------+--
* KINETICS PARAMETERS
*--------+---------+---------+---------+---------+---------+---------+--
$PERTURBATION
&
ID(1)
LABEL( KINETICS PARAMETERS )
BEFF
$END PERTURBATION
*
*--------+---------+---------+---------+---------+---------+---------+--
* SOURCE
*--------+---------+---------+---------+---------+---------+---------+--
$SOURCE
& RATIO( 1.0 )
  @( X Y ) = #DISC( 0.0 <0.5*DH2> );
  @Z      = #UNIFORM( <FZ1> <FZ2> );
  @E= #FISSION( U02350J50* 0.0253);
$END SOURCE
*
% NR =%NREG
WGTF( <NR>(1.0) )
/
```